

TRANSPORTATION RESEARCH  
**R E C O R D**

No. 1391

*Materials and Construction*

---

**Asphalt Cement and  
Asphalt/Polymer  
Blends**

*A peer-reviewed publication of the Transportation Research Board*

**TRANSPORTATION RESEARCH BOARD  
NATIONAL RESEARCH COUNCIL**

**NATIONAL ACADEMY PRESS  
WASHINGTON, D.C. 1993**

**Transportation Research Record 1391**

Price: \$21.00

**Subscriber Category**

IIIB materials and construction

**TRB Publications Staff**

*Director of Reports and Editorial Services:* Nancy A. Ackerman

*Senior Editor:* Naomi C. Kassabian

*Associate Editor:* Alison G. Tobias

*Assistant Editors:* Luanne Crayton, Norman Solomon,  
Susan E. G. Brown

*Graphics Specialist:* Terri Wayne

*Office Manager:* Phyllis D. Barber

*Senior Production Assistant:* Betty L. Hawkins

Printed in the United States of America

**Library of Congress Cataloging-in-Publication Data**

National Research Council. Transportation Research Board.

Asphalt cement and asphalt/polymer blends / Transportation  
Research Board, National Research Council.

p. cm.—(Transportation research record ISSN 0361-1981 ;  
no. 1391)

ISBN 0-309-05462-1

1. Asphalt cement. 2. Asphalt—Additives. 3. Polymers.  
4. Pavements, Asphalt—Testing. I. National Research  
Council (U.S.). Transportation Research Board. II. Series:  
Transportation research record ; 1391.

TE7.H5 no. 1391

[TE275]

388 s—dc20

[625.8'5]

93-30010  
CIP

**Sponsorship of Transportation Research Record 1391**

**GROUP 2—DESIGN AND CONSTRUCTION OF  
TRANSPORTATION FACILITIES**

*Chairman:* Charles T. Edson, Greenman Pederson

**Bituminous Section**

*Chairman:* Harold R. Paul, Louisiana Transportation Research  
Center

**Committee on Characteristics of Bituminous Materials**

*Chairman:* Leonard E. Wood, Purdue University

David A. Anderson, Chris A. Bell, S. W. Bishara, Joe W. Button,  
Brian H. Chollar, Claude Fevre, Norman W. Garrick, Eric E.  
Harm, Bobby J. Huff, Prithvi S. Kandhal, Thomas W. Kennedy,  
Gayle N. King, G. W. Maupin, Jr., Dean A. Maurer, Tinh  
Nguyen, R. D. Pavlovich, Charles F. Potts, Vytautas P.  
Puzinauskas, Peggy L. Simpson, Bernard A. Vallerga, John S.  
Youtcheff, Ludo Zanzotto

Frederick D. Hejl, Transportation Research Board staff

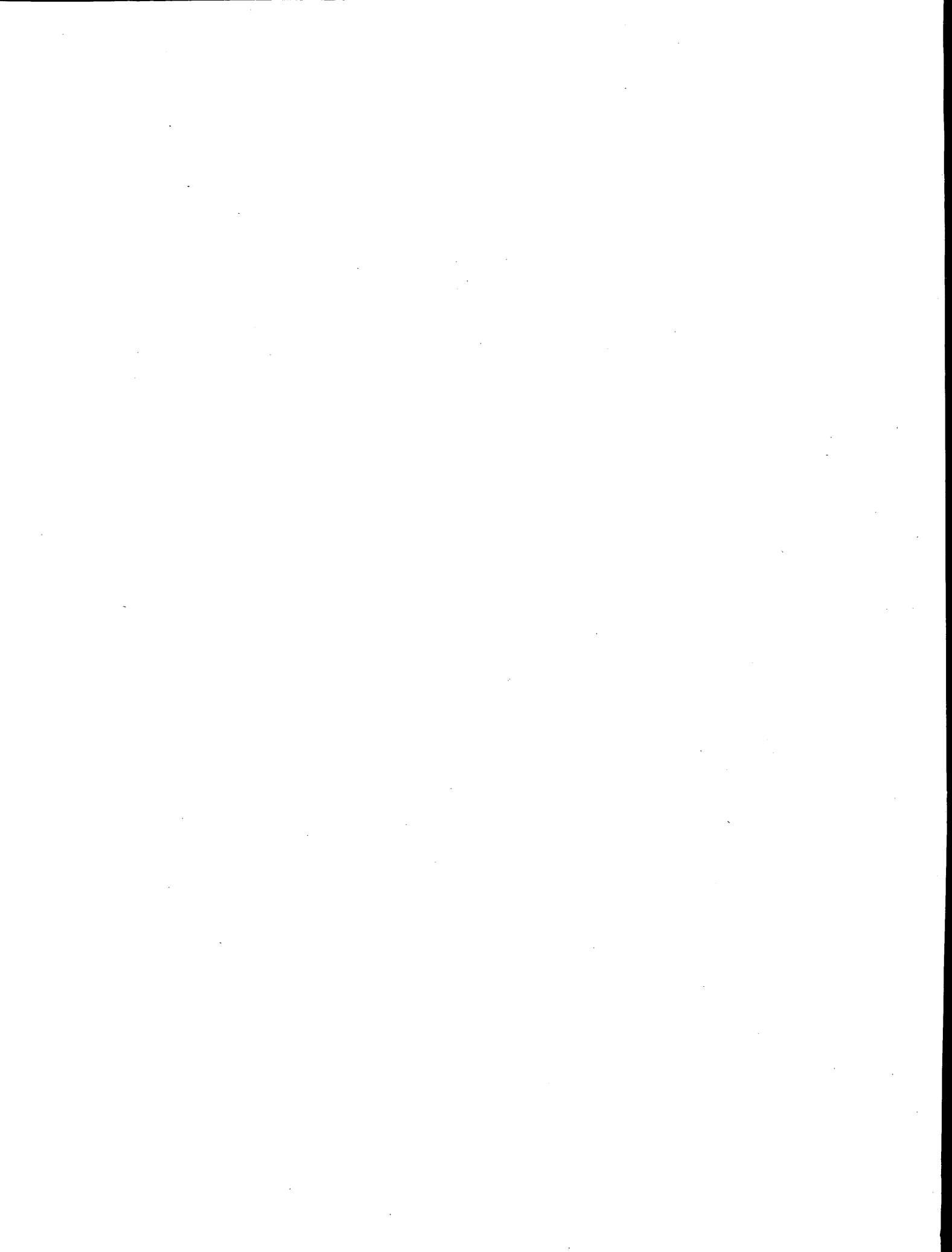
The organizational units, officers, and members are as of  
December 31, 1992.

# Transportation Research Record 1391

---

## Contents

<b>Foreword</b>	v
<b>Effects of Physicochemical Factors on Asphalt Oxidation Kinetics</b> <i>J. Claine Petersen, Jan F. Branthaver, Raymond E. Robertson, P. Michael Harnsberger, John J. Duvall, and E. Keith Ensley</i>	1
<b>Evaluation and Development of a Pressure Aging Vessel for Asphalt Cement</b> <i>Joe W. Button, Manoj Jawle, Vidyasagar Jagadam, and Dallas N. Little</i>	11
<b>New Apparatus and Procedure for the Extraction and Recovery of Asphalt Binder from Pavement Mixtures</b> <i>B. L. Burr, C. J. Glover, R. R. Davison, and J. A. Bullin</i>	20
<b>Comparing Field and Laboratory Aging of Bitumens on a Kinetic Basis</b> <i>A. F. Verhasselt and F. S. Choquet</i>	30
<b>Some Aspects of the Effect of Asphalt Chemical Composition on Material Behavior and Pavement Performance</b> <i>Ilan Ishai, Yaw A. Tuffour, and Joseph Cras</i>	39
<b>Preparation and Characterization of Asphalt-Modified Polyethylene Blends</b> <i>William H. Daly, Zhaoyao Qui (Chiu), and Ioan Negulescu</i>	56

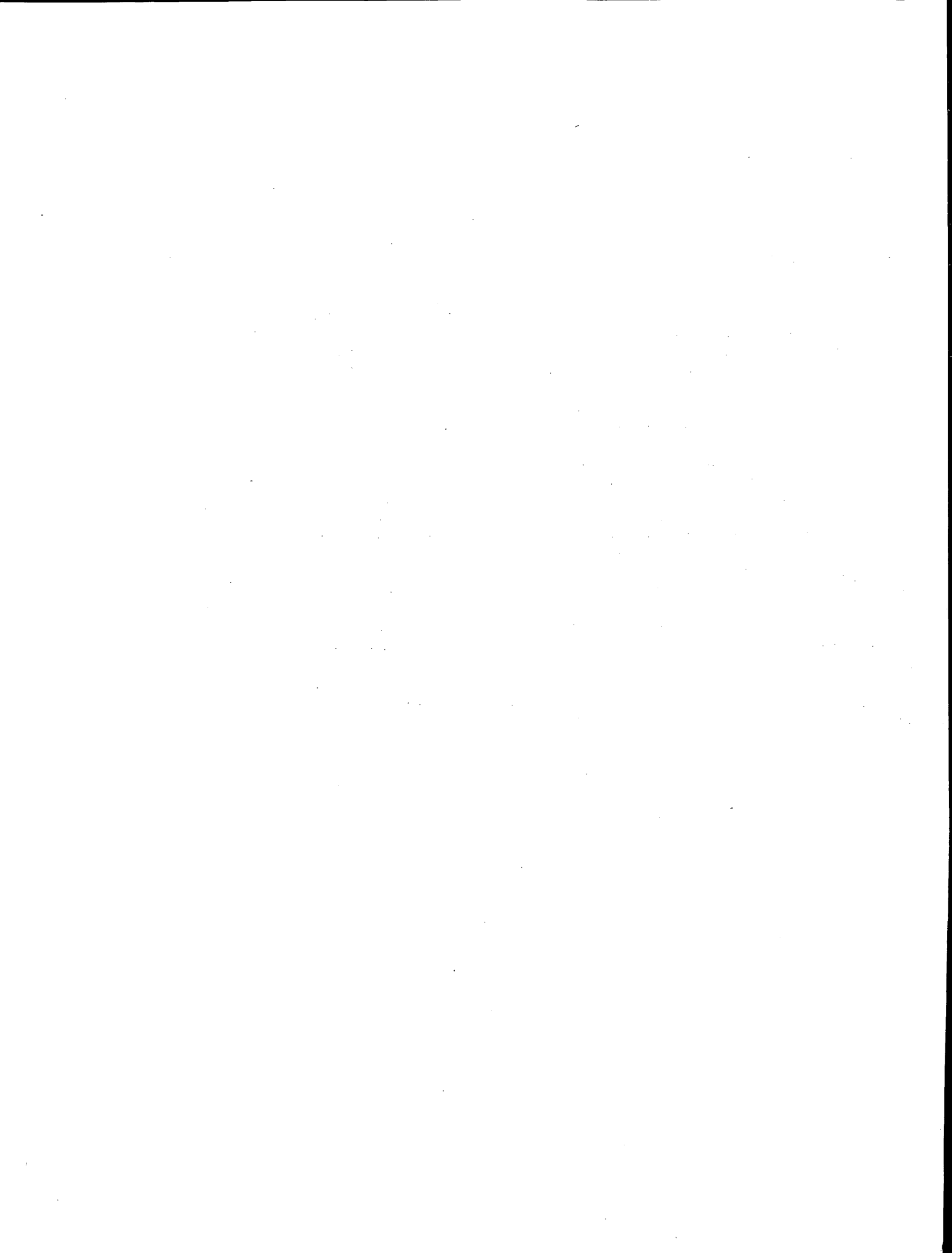


# Foreword

The papers in this Record, dealing with various facets of asphalts and asphalt additives, should be of interest to state and local construction, design, materials, and research engineers as well as contractors and material producers.

Petersen et al. report on an investigation on the kinetics of asphalt oxidation to better understand the mechanisms of age hardening. They present a new microstructural model of the age hardening of asphalt cement that proposes that the kinetics of aging is largely governed by physicochemical factors related to the state of dispersion of the molecular microstructure. Button et al. present the results of a study to evaluate a pressure aging vessel (PAV) for asphalt cement, with the specific objectives of examining the safety of the procedure and the effects of aging temperature, film thickness on aging, vertical location within the PAV, and proximity of aging asphalt to other asphalts. After the study was completed, the Strategic Highway Research Program PAV conditioning protocol was modified by increasing the temperature and decreasing the time of aging to accommodate the needs of state departments of transportation for an aging test requiring no more than 24 hours. Burr et al. report on the development of a new apparatus and procedure for extracting asphalt binder from hot-mix and pavement samples. The authors claim that this new procedure provides recovered asphalt with physical properties that are much closer to the true physical properties of the binder as it existed in the hot-mix or pavement.

Verhasselt and Choquet discuss a laboratory aging device and procedure developed at the Belgian Road Research Centre for predicting field aging. The procedure uses an overall kinetic approach to aging that agrees relatively well with findings and observations on actual field aging. Ishai et al. report on some aspects of the effect of asphalt chemical composition on the properties and performance of some fresh asphalt binders, as well as of plant- and field-aged samples, and the way in which long-term aging may be affected by changes in material composition. Daly et al. discuss the preparation and characterization of asphalt-modified polyethylene blends in a research effort to develop a simple method to estimate the compatibility of polymer additives with asphalt.



# Effects of Physicochemical Factors on Asphalt Oxidation Kinetics

J. CLAINE PETERSEN, JAN F. BRANTHAVER, RAYMOND E. ROBERTSON,  
P. MICHAEL HARNSBERGER, JOHN J. DUVALL, AND E. KEITH ENSLEY

Oxidative aging of asphalt is a primary cause of asphalt hardening in pavements, thus contributing to various forms of pavement cracking. Although the changes in asphalt physical properties on oxidative aging are primarily the result of the formation of oxygen-containing functional groups in the asphalt, the sensitivity of an asphalt to these oxidation products varies widely with asphalt source (composition). An understanding of the kinetics of oxidation in the pavement temperature range is confounded by both the complex composition of asphalt and its thermally reversible microstructure. To better understand the mechanisms of age hardening, the kinetics of asphalt oxidation were investigated from the pavement temperature range [60°C (140°F)] through the higher temperature range of commonly used accelerated laboratory tests [130°C (266°F)]. It was found that asphalts with different component compatibilities may exhibit similar age hardening kinetics at the low end of the pavement temperature range, but quite different kinetics at the high end of the range. This is because the aging kinetics become highly dependent on how temperature affects the molecular microstructure. A new microstructural model of the age hardening of asphalt cement is presented that proposes that the kinetics of aging in the pavement temperature range is largely governed by physicochemical factors related to the state of dispersion of the molecular microstructure rather than the inherent reactivity of the molecular components with oxygen. The model is supported by results of past and present research.

The oxidative hardening of asphalt contributes significantly to the embrittlement of asphalt pavements. This hardening is attributed primarily to the introduction of polar, oxygen-containing chemical functionality that increases interactions among asphalt molecules. Much work has been done in identifying the polar, strongly associating functional groups in asphalt, either naturally present or formed on oxidation, and characterizing their association forces (1). The sensitivity of an asphalt to the oxidation products varies with asphalt source. These and related phenomena are discussed elsewhere in a detailed review (1). A new model for asphalt oxidation has been proposed (2,3) suggesting that physicochemical factors dominate the kinetics of oxidative age hardening of most asphalts. This model proposes that potentially reactive polar asphalt molecules associate to form microstructure. This molecular association immobilizes the inherently reactive components, thus reducing their ability to react with atmospheric oxygen.

Because molecular association of polar asphalt components plays a major role in determining aging characteristics (2,3), and because it is well known that molecular association is reversible and highly temperature sensitive, it becomes obvious that the kinetics of aging as a function of temperature must be examined to understand the age hardening characteristics of asphalt. The importance of such a study is underlined by the results of the field aging study of Kemp and Predeohl (4), in which pavement mixtures were aged in different climates. Although void content of a mixture is well known to influence pavement hardening, the California study showed that age hardening was much more dependent on climate temperature than void content. Thus, an understanding of the age-hardening kinetics as a function of temperature is important to the design of a realistic aging test. Aging indexes calculated from single-point viscosity measurements at one test temperature provide little or no information regarding the overall kinetics and limited information about the expected aging of asphalts in pavements.

The research results and data interpretation in this paper further define the physicochemical aging model and provide additional insight into the compositional factors governing the age hardening of asphalts at pavement temperatures. In addition, they provide kinetic information useful for the design of a realistic aging test.

## MODEL OF ASPHALT OXIDATION KINETICS

The earlier work on the microstructural aging model (2,3) provided evidence that physicochemical factors are primarily responsible for (a) the lack of correspondence among asphalts between the concentration of oxidation products and viscosity increase on aging, and (b) the differences between low- and high-temperature age-hardening kinetics. This is illustrated in Figure 1 by a refinement of the earlier aging model. For simplicity, the four asphalt generic fractions are used in the illustration. This illustration is not intended to depict the exact spatial arrangement of molecules of the generic fractions because this is unknown, but is presented only for the purpose of illustrating the principles involved. The molecular polarity and inherent reactivity of the fractions with oxygen have been shown (1) to be asphaltenes > polar aromatics > aromatics > saturates. In some asphalts, over 85 percent of the easily oxidizable hydrocarbon moieties may reside in the asphaltene and polar aromatic fractions (3). In highly dispersed asphalts, the polar molecules are "solvated," thus they retain consid-

J. Claine Peterson, 1316 Jennifer Court, Loveland, Colo. 80537. Jan F. Branthaver, Raymond E. Robertson, P. Michael Harnsberger, John J. Duvall, and E. Keith Ensley, Western Research Institute, P.O. Box 3395, Laramie, Wyo. 82071.

erable molecular mobility. On the other hand, the more polar molecules in a highly associated asphalt interact to form microstructure that significantly reduces molecular mobility. The assumption that molecular immobility decreases reactivity with oxygen is not without support. For example, the asphaltene fraction, although highly reactive in solution, is virtually inert to air oxidation at ambient temperature in its dry, powdered state.

Because the inherently reactive polar components (represented in Figure 1 by asphaltenes and polar aromatics) of a highly dispersed asphalt are highly mobilized at both high and low temperatures, the age-hardening kinetics are similar throughout a wide temperature range. The age-hardening kinetics of a highly associated asphalt, on the other hand, are highly temperature dependent. At low temperatures, the inherently reactive molecules are highly immobilized from association, which physically inhibits their oxidation. When the oxidation temperature is increased, the reactive polar molecules are mobilized by dissociation of microstructure, making more of them available for oxidation. The proposed model is supported by numerous examples in this paper.

#### EFFECTS OF TEMPERATURE AND ASPHALT COMPONENT COMPATIBILITY ON AGE-HARDENING KINETICS

Two laboratory aging tests were selected for the study of age-hardening kinetics. For the low temperature range, the pressure oxygen vessel (POV) technique developed by Lee (5) was selected. This method uses a 3.18 mm- ( $\frac{1}{8}$  in.-) thick asphalt film in a thin film oven test (TFOT) pan exposed to oxygen at 2.07 MPa (300 psi). Pure oxygen and elevated pressure accelerates the rate of oxidative aging. The aging test selected to evaluate aging at higher temperatures was the thin

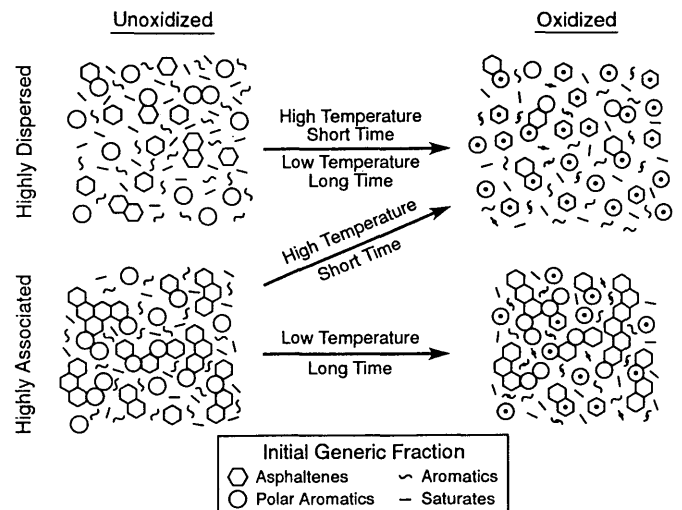


FIGURE 1 Model of Asphalt Oxidative Aging.

film accelerated aging test (TFAAT) (6). This test uses a 160- $\mu\text{m}$  (0.0063-in.) film of asphalt deposited on the inside of a rolling thin film oven (RTFO) bottle that is aged in an RTFO. The bottle contains a capillary opening to restrict volatile loss to an amount similar to that of pavement service. The asphalts studied were the eight Strategic Highway Research Program (SHRP) core asphalts. In the SHRP core asphalts, the uses of both oxygen and air in the pressure vessel were evaluated.

In the pressure air vessel (PAV) test to simulate pavement aging, the asphalt is first aged using the TFO test to simulate asphalt changes that occur in the hot mixture plant. The viscosity-time plots for PAV aging of the SHRP core asphalts at 60°C (140°F), together with viscosity changes during TFO aging, are shown in Figure 2. Changes upon TFO aging varied

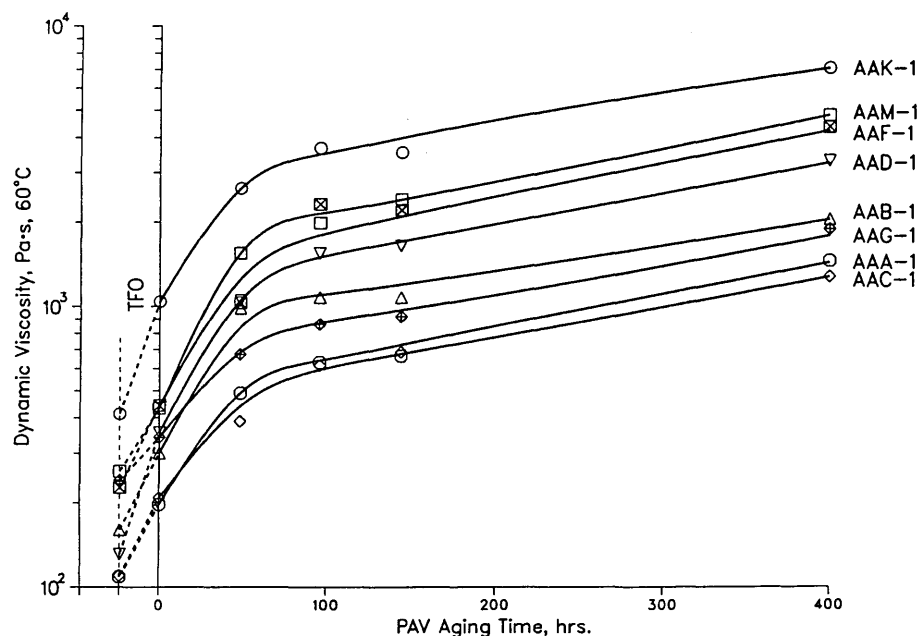


FIGURE 2 Kinetic aging plot of SHRP asphalts using PAV method at 2.07 MPa, 60°C.

considerably among asphalts; however, the PAV kinetic aging for the eight asphalts at 60°C (140°F) are surprisingly similar. All plots are distinctly parabolic, exhibiting a rapid viscosity increase during about the first 50 to 100 hr of aging followed by a rate decrease leading to a "steady state" viscosity increase in the plateau region beyond about 150 hr.

Prior TFO aging of the SHRP asphalts produced higher viscosity asphalts exhibiting the same subsequent POV aging kinetics as the original asphalt. This is illustrated in Figure 3

using asphalt AAD-1 aged at 60°C (140°F) in the POV. To better understand TFO aging, consider the weight versus viscosity changes during TFO aging of the SHRP asphalts at 163°C (325°F) as illustrated in Figure 4. Two factors dominate during TFO aging: (a) volatile loss producing a weight loss, and (b) oxidation producing a weight gain. The actual weight change is the net result of these two factors. If volatile loss dominates, the asphalt is found located on the right side of the zero weight change line; if oxidation dominates, it is on

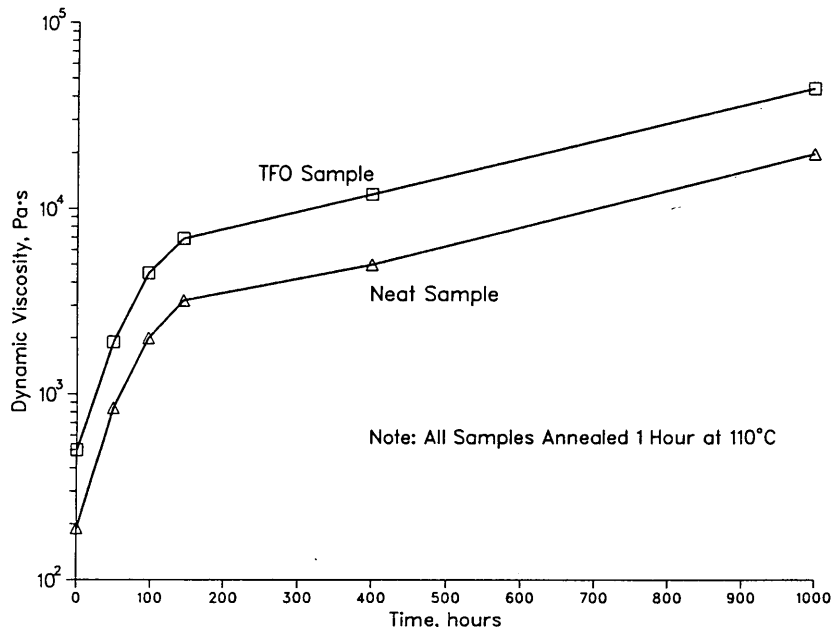


FIGURE 3 POV aging of asphalt AAD-1 at 60°C with and without prior TFO aging.

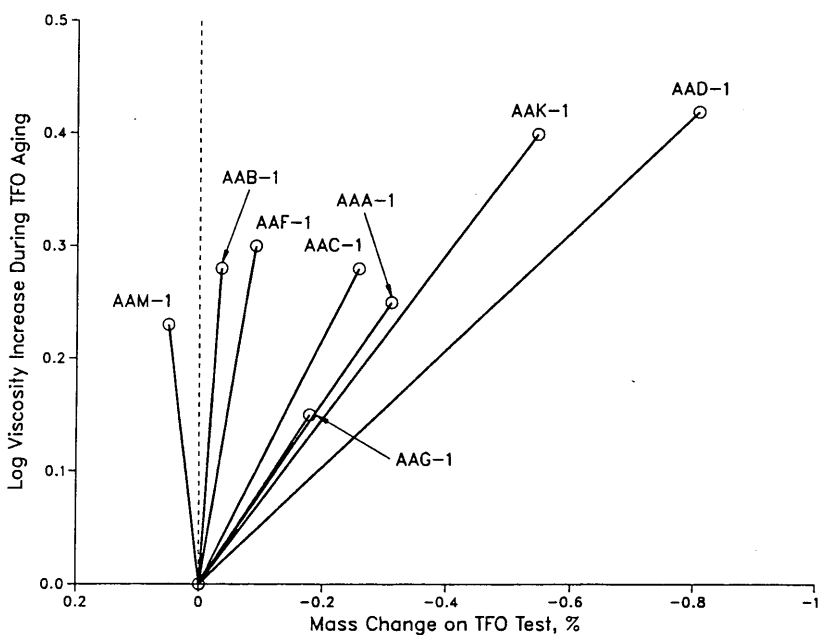


FIGURE 4 Mass change versus log viscosity increase during TFO aging.

the left. For asphalts AAD-1 and AAK-1, weight loss appears to dominate in increasing viscosity. On the other hand, for asphalts AAM-1, AAB-1, and AAF-1, changes from volatile loss are virtually offset by oxidative weight gain, indicating that oxidation contributes significantly to the viscosity increase.

More understanding of the TFO aging mechanism can be gleaned from Figure 5. The increase in viscosity with increasing carbonyl oxidation products during POV aging of AAD-1 with and without prior TFO aging is shown in this figure. The data points were obtained by analyzing a collection of samples of AAD-1 aged as a function of time at 60°C (140°F) for up to 1,000 hr. The data fit is within the expected precision of the experimental techniques. An excellent correlation exists between viscosity increase and carbonyl oxidation products formed. The relationship between carbonyl oxidation products [greater than 95 percent are ketones (1)] and viscosity increase has been previously reported (7,8) and will be discussed later in this paper. Of particular significance with regard to TFO aging, the data in Figure 5 imply that at any point in time on the POV kinetic plot (see Figure 3), the TFO aged asphalt has the same carbonyl content as the asphalt with no prior TFO aging. Thus, TFO aging apparently did not significantly alter the compositional factors responsible for the shape of the kinetic aging curve. This is not surprising because the volatiles lost are primarily nonpolar hydrocarbons. Similar shaped kinetic curves for the asphalt at different viscosities (Figure 3) also indicate that the shapes of the kinetic curves were not significantly influenced by viscosity increase during POV aging. The lack of significant ketone formation during TFO aging probably results from two factors: (a) the thick asphalt film that inhibits diffusion, and (b) the scavenging of oxygen by the highly reactive sulfides to form sulfoxides as air diffuses through the asphalt. At the TFO test temperature, the sulfoxides are thermally unstable (9,10) and subsequently decompose; thus few are found in the TFO re-

sidue. The sulfoxide decomposition products (retention of oxygen) may possibly be largely responsible for the oxidation component of the weight change during TFO aging (see Figure 4).

Data in Figure 5 also strongly suggest that carbonyl compounds (ketones) formed during oxidative aging may be involved in the viscosity increase. To more fully understand the kinetics of asphalt aging as affected by temperature and composition, it was necessary to bridge the gap in the kinetic data between the low-temperature pressure vessel data and past data obtained at rather high temperatures. This was done using the TFAAT, which is fast and was designed to eliminate the confounding effects of volatile loss at higher temperatures. It was decided to first determine if the age hardening kinetics for both the pressure vessel and TFAAT aging methods were similar. Data confirming the similarity are shown in Figure 6 for POV and PAV aging at 60°C (140°F) and TFAAT aging at 65°C (149°F). The TFAAT aging was conducted at 65°C (149°F) because of equipment limitations.

The kinetic data in Figure 6 for asphalts AAG-1 and AAK-1 are quite similar regardless of which test method was used. The plateau region for the POV aging curve has a steeper slope than that for PAV aging, undoubtedly because of a greater oxygen concentration. Asphalts AAG-1 and AAD-1 were chosen for test method comparisons because they represent extremes in asphalt component compatibility (2,3), AAG-1 having a highly dispersed polar phase and AAD-1 a highly associated polar phase. Data in Figure 6 show that a 60°C (140°F) aging test would rank asphalts AAD-1 and AAG-1 as having similar age-hardening characteristics. However, such a conclusion was found not valid for these two asphalts aged at higher temperatures (2,3). This will become apparent from the higher-temperature kinetic data that follow.

Kinetic data for the TFAAT aging of the SHRP asphalts at 85°C (185°F), 113°C (235°F), and 130°C (266°F) are shown

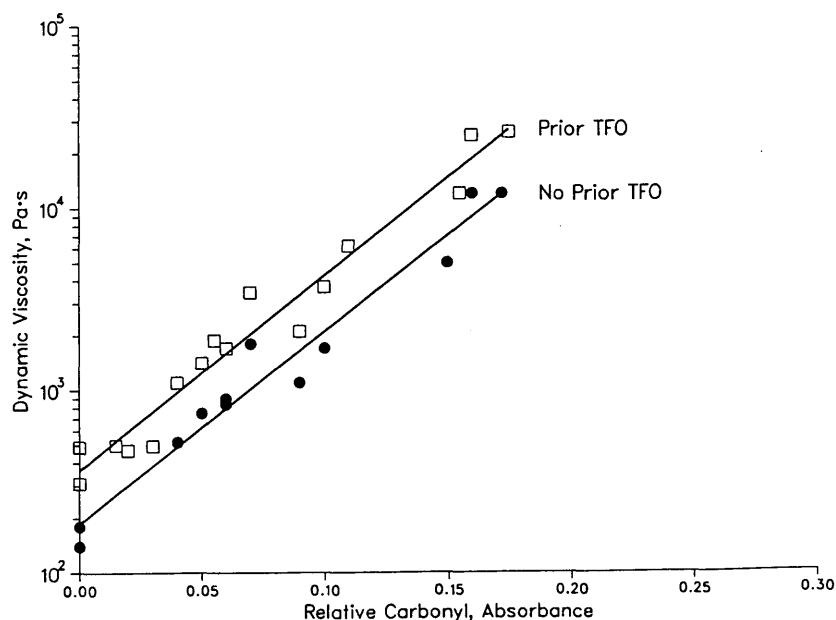
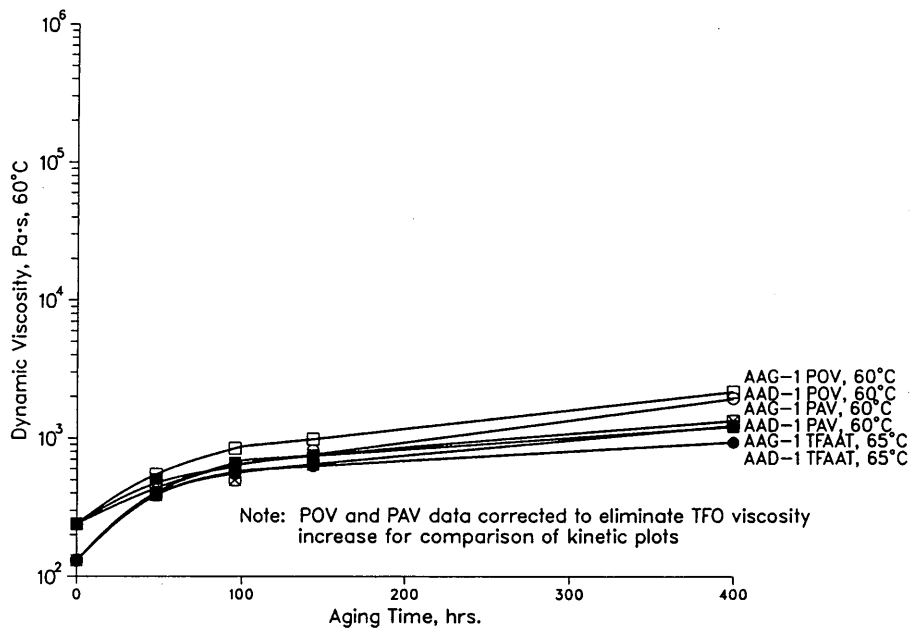


FIGURE 5 Relationship of viscosity change with carbonyl (ketone) formation on POV oxidation of asphalt AAD-1 with and without prior TFO oxidation.



**FIGURE 6** Comparison of low-temperature aging kinetics of asphalts AAD-1 and AAG-1 using POV, PAV, and TFAAT methods.

in Figures 7, 8, and 9, respectively. As seen in Figure 7, the kinetic plots at 85°C (185°F) show a greater rate of viscosity increase than at 60°C (140°F) (see Figure 6). Further, the similarity of kinetic data beyond the inflection point found for all asphalts aged at 60°C (140°F) (Figure 2) is no longer apparent. For example, kinetic plots for asphalts AAD-1 and AAG-1, which were similar at 60°C (140°F), now show disparity. The disparity among asphalts becomes even greater (Figure 8) at 113°C (235°F). Also, the time needed to reach

the inflection point of the kinetic curve (e.g., AAG-1) has decreased from about 100–200 hr (at 60°C) to 20–40 hr (at 113°C). Any single point aging test conducted, for example at 113°C (235°F) for 24 hr, would rank the asphalts and their differences quite differently than a test conducted for, say, 120 hr at the lower temperature. Finally, at 130°C (266°F) (Figure 9), large differences in the kinetic data are apparent. As judged by AAG-1, the inflection point now appears after about 5 hr of aging. For asphalts AAG-1 and AAD-1, whose

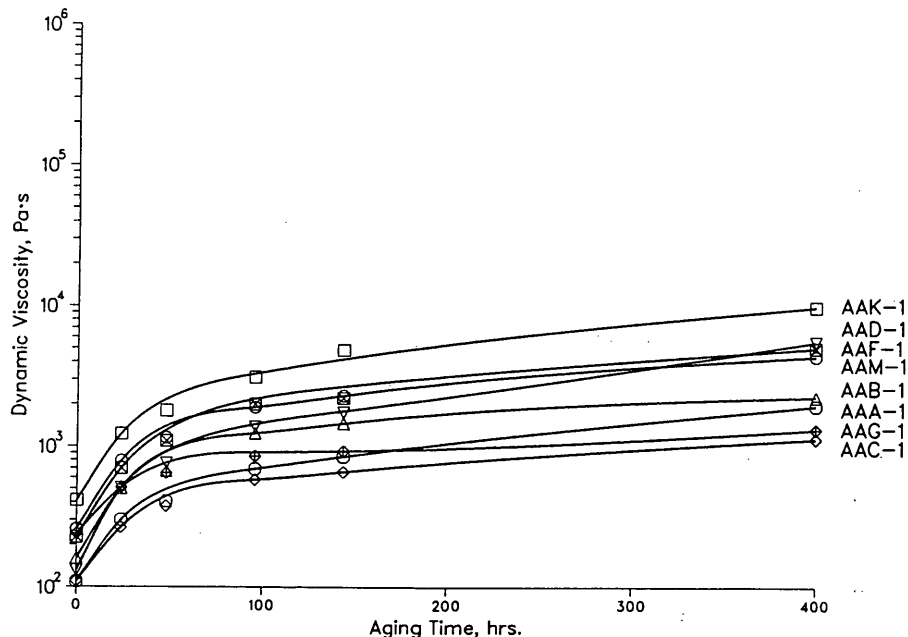


**FIGURE 7** Aging kinetics of SHRP core asphalts using TFAAT method at 85°C.

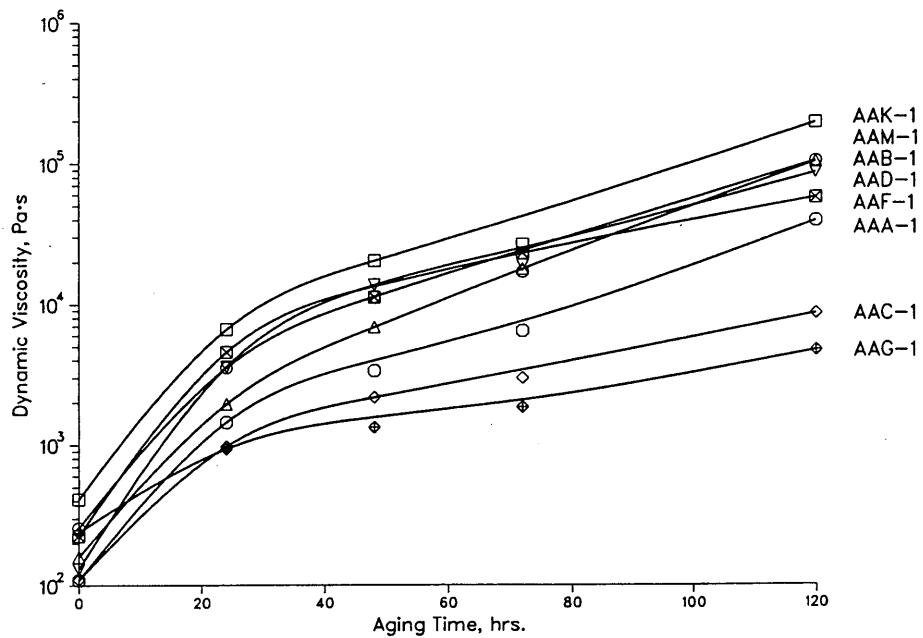


FIGURE 8 Aging kinetics of SHRP core asphalts using TFAAT method at 113°C.

plots were similar at 60°C (140°F), the plots are significantly different from each other, with AAD-1 showing a much greater age-hardening rate at 130°C (266°F) than AAG-1.

It is instructive for the further evaluation of age-hardening kinetics to examine the kinetics of the formation of the dominant oxidation products. The kinetics of ketone and sulfoxide formation during 113°C (235°F) TFAAT aging are shown in Figure 10 for asphalt AAG-1. Sulfoxides form rapidly during the first 5 hr followed by the familiar pseudo-steady-state concentration as their rate of formation and rate of subsequent thermal decomposition become equal (9,10). The rate of ke-

tone formation, also initially rapid, reaches a plateau in about 5 hr, after which the rate of formation remains constant.

That asphalt AAG-1 is a highly dispersed asphalt and AAD-1 is a highly associated asphalt is evidenced by the reduced specific viscosity data in Figure 11. Reduced specific viscosity,  $\langle \eta \rangle$ , as here applied to asphalts, is defined as follows (11).

$$\langle \eta \rangle = \frac{\eta_s - \eta_o}{\eta_o c} \quad (1)$$

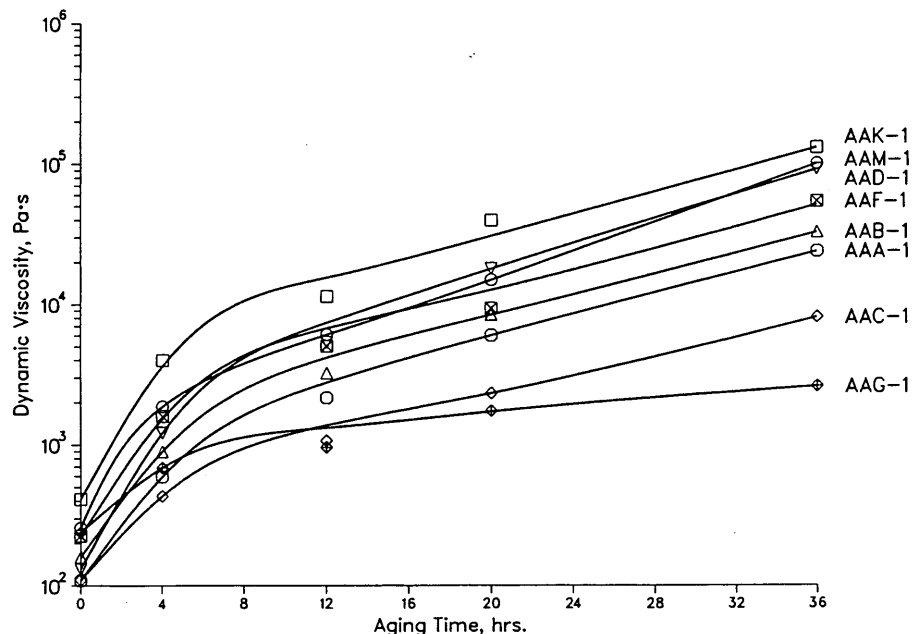


FIGURE 9 Aging kinetics of SHRP core asphalts using TFAAT method at 130°C.

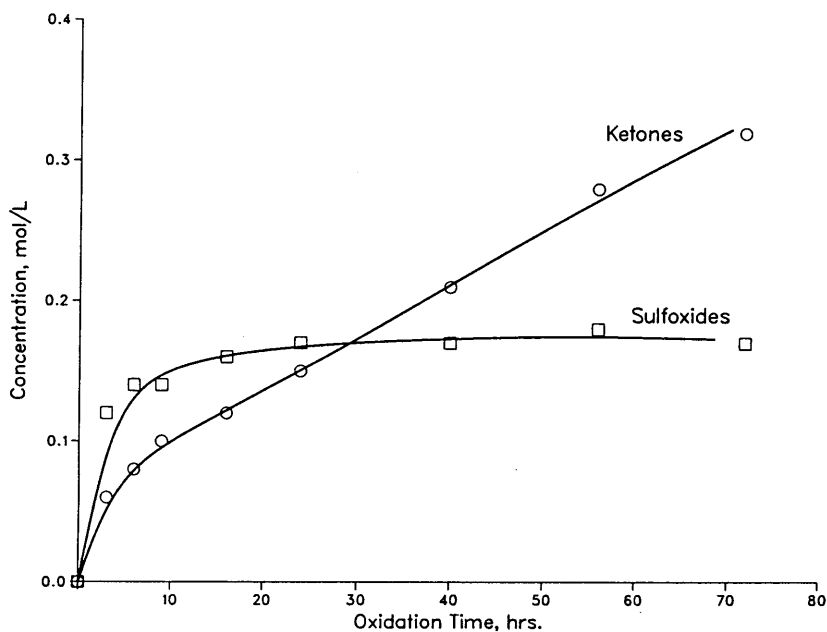


FIGURE 10 Chemical kinetic data for TFAAT oxidation of asphalt AAG-1 at 113°C.

where

- $\eta_o$  = viscosity of the maltenes (solvent),
- $\eta_s$  = viscosity of a maltene-asphaltene mixture, and
- $c$  = concentration of asphaltenes (solute) in maltenes in gms/100 gms.

Viscosity measurements were made at 45°C (113°F) on maltene fractions of asphalts AAG-1 and AAD-1, which contained asphaltene concentrations below and above their nat-

ural abundance levels. Data on TFAAT-aged asphalts were obtained from asphalts aged for 72 hr at 113°C (235°F). This aging procedure produces an oxidation level significantly greater than POV and PAV aging (compare Figures 6 and 8). Reduced specific viscosities of the mixtures were then calculated. This technique is advantageous because it allows the asphaltene association to be studied in its natural environment in the absence of solvent. Because the  $\langle \eta \rangle$  is related directly to the apparent molecular weight of the solute (asphaltenes) in

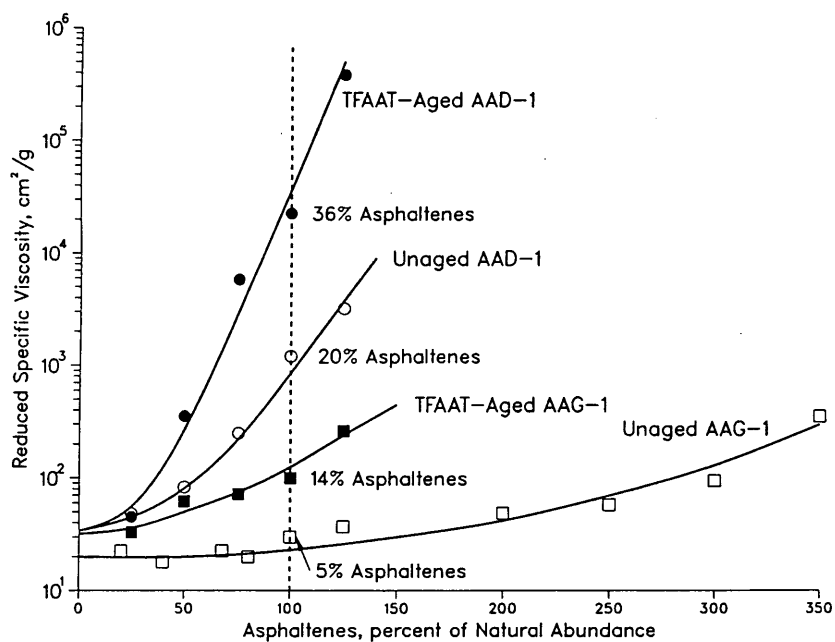


FIGURE 11 Reduced specific viscosity measurements at 45°C for asphalts AAD-1 and AAG-1 before and after TFAAT aging at 113°C, 72 hr.

the solvent (maltenes), the relative tendency for the asphaltenes to associate and form microstructure is directly observable. If the  $\langle \eta \rangle$  remains constant as asphaltene content is increased, this is evidence that the asphaltenes are soluble and are highly dispersed in the maltenes phase. If the  $\langle \eta \rangle$  increases with increasing asphaltene concentration, this shows that the size of the asphaltene agglomerates is increasing through molecular association. At zero concentration, the asphaltenes are at their smallest divisible size at 45°C (113°F).

Interpretation of the data in Figure 11 shows that the asphaltenes in asphalt AAG-1 are solubilized, dispersed, and highly mobile. Even the asphaltenes in the TFAAT-aged AAG-1 are quite well dispersed. The data for asphalt AAD-1 show that the asphaltenes are much less compatible with their maltenes phase, even in the unoxidized sample, at much less than their natural abundance concentration. With increasing asphaltene concentration, the asphaltene microstructure of AAD-1 increases rapidly in size, thus immobilizing reactive components (2,3). It is also seen that oxidation [at 113°C (235°F)] has a much greater effect on microstructure formation in AAD-1 than in AAG-1.

On the basis of the data presented thus far, it is appropriate to discuss the age-hardening kinetic data with regard to the aging model proposed in Figure 1. This will be done using the kinetic data in Figure 12 for the two asphalts with representative component compatibility extremes, asphalts AAG-1 and AAD-1. The time scale for the lower temperature aging [60°C (140°F)] was compressed to offset the increase in reaction rate at the high temperature [113°C (235°F)]. Because the most reactive components of asphalt AAG-1 are mobilized even at low temperatures, the kinetics of age hardening are similar at both low and high temperatures when the time scales are shifted to overlap the data. This behavior is illustrated in the top half of Figure 1. This result reveals important

information on the oxidation mechanism. It implies that the sharp decrease in the rate of age hardening near the inflection point of the kinetic curve for low temperature oxidation does not result from depletion of asphalt components reactive only at low temperatures. The rapid rate of viscosity increase during the initial period of AAG-1 aging is tentatively attributed to the reaction of a small population of more reactive hydrocarbon components and possibly to the formation of sulfoxides. Data in Figure 10 for the formation of sulfoxides and ketones support this view.

Kinetic data in Figure 12 for the low- and high-temperature aging of asphalt AAD-1 are quite different from one another. At 60°C (140°F), the kinetic data for AAD-1 are similar to those of AAG-1; however, at 113°C (235°F), AAD-1 shows a much greater increase in age hardening during the initial stages of oxidation and a more rapid rate of increase in the plateau region than at 60°C (140°F). This is interpreted as follows. During low temperature oxidation, the reaction rate decreases because a large part of the inherently reactive molecules are immobilized as depicted in the lower half of Figure 1. However, at higher temperatures, there is less microstructure, making greater amounts of reactive components available for reaction (arrow to the upper right corner of Figure 1). Also, as more reactive molecules become available at higher temperatures, more of the small, reactive hydrocarbon population in AAD-1 is made available, producing a significantly greater initial increase in viscosity during oxidation at 113°C (235°F) than at 60°C (140°F). Finally, evidence that the age-hardening kinetics for AAD-1 are different at high and low temperatures is provided by the inability to superimpose their kinetic plots by shifting the time scales as was done with AAG-1.

Because high oxygen or air pressure [2.07 MPa (300 psi)] is used in pressure vessel aging, it is important to know how oxidation proceeds through the sample thickness during ag-

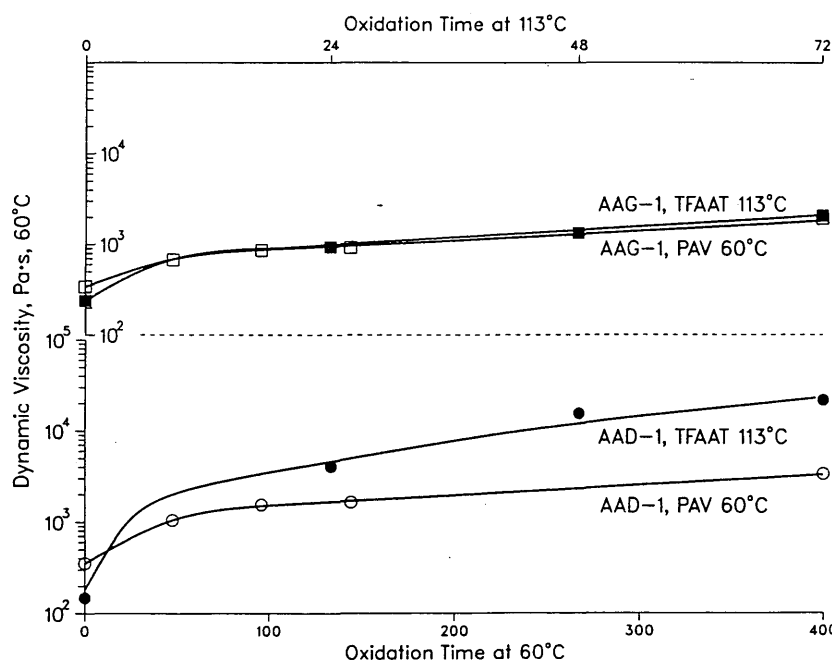


**FIGURE 12 Effects of temperature on aging characteristics of asphalts AAD-1 and AAG-1.**

ing. Lee (5) found that at 66°C (150°F) the viscosity through the sample thickness [3.18 mm ( $\frac{1}{8}$  in)] approached a uniform value after about 250 hr at 200 kPa (29 psig) oxygen pressure and after about 50 hr at 847 kPa (132 psig). It was found that, after 96 hr in oxygen and 144 hr in air at 2.07 MPa (300 psi), the viscosity and the concentrations of carbonyls and sulf-oxides were identical at both the top and bottom of the sample. Two important deductions can be made from these data. First, when the POV test is run near 60°C (140°F) at 2.07 MPa (300 psi), the oxidation should be nearly uniform throughout the sample thickness in much less than 50 hr, thus the oxidation should not be diffusion controlled after a short period of initial aging. Second, because more than 50 hr are needed to reach the plateau region of the kinetic aging plot during 2.07 MPa (300 psi) aging (Figure 3), it is highly unlikely that diffusion alone can account for the shape of the kinetic curve during the first 150 hr. This latter observation supports the previous proposition that the shape of the front end of the kinetic curve is largely controlled by reaction of a small population of highly reactive asphalt components.

#### EFFECTS OF OXIDATION REACTIONS ON AGE-HARDENING KINETICS

The relationship between carbonyls formed on oxidation and viscosity increase is shown in Figure 13. The data points include PAV aging at 60°C (140°F) for 48, 96, 144, and 400 hr; TFAAT aging at 85°C (185°F) for 24, 48, 96, 144, and 400 hr; TFAAT aging at 113°C (235°F) for 24, 48, 72, and 144 hr; and TFAAT aging at 130°C (266°F) for 4, 12, 20, and 36 hr. The correlation for each individual asphalt is good. These

data include the entire temperature range of concern from 60°C (140°F) to 130°C (266°F), and the data imply that the mechanism of hydrocarbon oxidation of asphalts is essentially the same from the pavement temperature range through the temperature range of common laboratory tests. Because both PAV and TFAAT data fit the same plot, evidence is provided that the hydrocarbon oxidation mechanism is the same for both atmospheric pressure and pressure vessel aging.

The different sensitivity of the asphalts to the oxidation products is evident from the data in Figure 13. More carbonyls are formed in asphalt AAG-1 than in any of the other asphalts; however, it is much less sensitive to the oxidation products, undoubtedly because of its high degree of dispersion. The highly structured asphalt, AAK-1, is highly sensitive to oxidation, suggesting that the oxidation products formed, rather than being solubilized, participate in strong association interactions.

#### IMPORTANT CONSIDERATIONS FOR A PRESSURE VESSEL AGING TEST

Several technical recommendations for test method development seem justified from this study. First, because of the high sensitivity of highly associated asphalts to age harden with increasing temperature, it is recommended that any single-point aging test be conducted as near as practical to the actual maximum pavement temperature. Second, the test aging time should be sufficient to move the measurement point beyond the inflection point of the kinetic plot. Finally, aging indexes that include viscosity changes that occurred during prior TFO testing are not necessarily reflective of the changes that actually take place during pavement service.

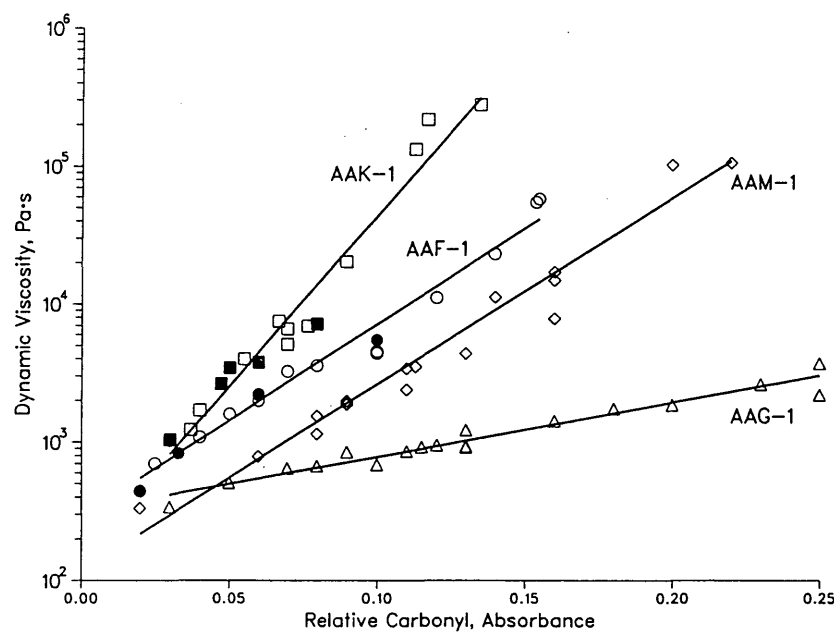


**FIGURE 13** Relationship between carbonyls formed and dynamic viscosity increase using PAV (solid points) and TFAAT (open points) data.

## CONCLUSIONS

The following conclusions are based on the data and interpretations presented in this paper.

1. The age-hardening kinetics at pavement temperatures of all but the most highly dispersed asphalts are dominated by the immobilization of polar, reactive asphalt molecules through microstructure formation.
2. The sensitivity of an asphalt to viscosity increase on oxidation is strongly influenced by its component compatibility. The more highly structured an asphalt, the more sensitive it is to viscosity increase with increasing temperature of oxidation.
3. TFO aging increases the viscosity of an asphalt but does not significantly affect its POV age-hardening kinetics.
4. The viscosity increase on oxidation correlates with the rate of oxidation of asphalt hydrocarbon moieties, however the viscosity sensitivity to the oxidation varies greatly among asphalts.
5. The hydrocarbon oxidation chemistry is similar for both ambient and pressure vessel aging of asphalts, and is also similar throughout the temperature range of 60°C (140°F) to 130°C (266°F).

In light of these conclusions, it seems advisable that the sensitivity of an asphalt to viscosity increase as a function of maximum pavement temperature should be carefully evaluated when selecting asphalts for use in different climates.

## ACKNOWLEDGMENTS

Financial support by the Strategic Highway Research Program for the work reported herein is gratefully acknowledged. The principal author is grateful to his former employer, Western Research Institute, and former coworkers of WRI for assistance and review during the preparation of this manuscript.

## REFERENCES

1. J. C. Petersen. Chemical Composition of Asphalt As Related to Asphalt Durability—State of the Art. In *Transportation Research Record 999*, TRB, National Research Council, Washington, D.C., 1984, pp. 13–30.

2. J. C. Petersen. Effects of Physicochemical Factors on Asphalt Aging. In *Serviceability and Durability of Construction Materials Vol. 1*. In *Proc., First Materials Engineering Congress*, American Society of Civil Engineers, New York, N.Y., Aug. 13–15, 1990, pp. 244–253.
3. J. C. Petersen. Asphalt Oxidation—An Overview Including a New Model for Oxidation Proposing That Physicochemical Factors Dominate the Oxidation Kinetics. *Fuel Science and Technology International*, Vol. 11, 1993, pp. 57–87.
4. G. R. Kemp and N. H. Predeohl. A Comparison of Field and Laboratory Environments on Asphalt Durability. In *Proc., Association of Asphalt Paving Technologists*, Vol. 50, 1981, pp. 492–531.
5. D. Lee. Development of a Laboratory Durability Test for Asphalts. In *Highway Research Record 231*, HRB, National Research Council, Washington, D.C., 1968, pp. 34–49.
6. J. C. Petersen. A Thin Film Accelerated Aging Test for Evaluating Asphalt Oxidation. In *Proc., Association of Asphalt Paving Technologists*, Vol. 58, 1989, pp. 220–237.
7. J. Epps, J. C. Petersen, T. W. Kennedy, D. A. Anderson, and R. Haas. Chemistry, Rheology, and Engineering Properties of Manganese-Treated Asphalts and Asphalt Mixtures. In *Transportation Research Record 1096*, TRB, National Research Council, Washington, D.C., 1986, pp. 106–119.
8. C. K. Lau, K. M. Lunsford, C. J. Glover, R. R. Davidson, and J. A. Bullin. Reaction Rates and Hardening Susceptibilities as Determined from Pressure Oxygen Vessel Aging of Asphalts. In *Transportation Research Record 1342*, TRB, National Research Council, Washington, D.C., 1992, pp. 50–57.
9. J. C. Petersen. Oxidation of Sulfur Compounds in Petroleum Residues: Reactivity-Structural Relationships and Reaction Kinetics. In *Confab 82 on Fossil Fuel Chemistry and Energy*, Saratoga, Wyo., July 20–23, 1982.
10. J. C. Petersen, S. M. Dorrence, M. Nazir, H. Plancher, and F. A. Barbour. Oxidation of Sulfur Compounds in Petroleum Residues: Reactivity-Structural Relationships. *Preprints, Division of Petroleum Chemistry*, Vol. 26 (4), American Chemical Society, 1981, pp. 898–906.
11. K. H. Altgelt and O. L. Harle. The Effect of Asphaltenes on Asphalt Viscosity. *I and EC Product Research and Development*, Vol. 14, 1975, pp. 240–246.

---

*The contents of this report reflect the views of the authors, who are solely responsible for the facts and accuracy of the data presented. The contents do not necessarily reflect the official view or policies of the Strategic Highway Research Program (SHRP) or SHRP's sponsors. The results reported here are not necessarily in agreement with the results of other SHRP research activities. They are reported to stimulate review and discussion within the research community. This report does not constitute a standard, specification, or regulation. Mention of specific brands of material does not imply endorsement by SHRP or Western Research Institute.*

# Evaluation and Development of a Pressure Aging Vessel for Asphalt Cement

JOE W. BUTTON, MANOJ JAWLE, VIDYASAGAR JAGADAM,  
AND DALLAS N. LITTLE

This study evaluates a pressure aging vessel (PAV) for asphalt cement, with the specific objectives of examining the safety of the procedure and the effects of aging temperature, film thickness on aging, vertical location within the PAV, and proximity of aging asphalt to other asphalts. Four Strategic Highway Research Program (SHRP) core asphalts (AAC-1, AAD-1, AAF-1, and AAG-1) were used in this study. An interlaboratory test program to establish the variability associated with the PAV conditioning procedure was conducted. The study indicated that the PAV operated at  $71^{\circ}\text{C}$  ( $160^{\circ}\text{F}$ ),  $2.07 \times 10^6$  pascals (300 psi) air pressure for 144 hr, effectively simulates 2 to 10 years of pavement aging depending on the method used to measure hardening, air voids in the paving mixture, average ambient temperature, and other factors. Degree of oxidative hardening of asphalt increases with increase in temperature. For a given temperature and time of exposure, degree of hardening increases with decrease in asphalt film thickness. The vertical location of asphalt in the PAV and proximity to other asphalts had no effect on the extent of hardening. Different asphalts exhibited different rates of hardening at the same conditions of temperature and time. After this work was essentially completed, the SHRP PAV conditioning protocol was modified by increasing the temperature and decreasing the time of aging. This was done to accommodate the needs of state departments of transportation for an aging test requiring no more than 24 hr.

Research efforts to develop simple, practical, and reliable procedures to simulate aging of asphalt go back to the beginning of this century. The objective of a long-term aging test for asphalt cement is to realistically simulate hardening that occurs during mixing, construction, and service of asphalt pavements. Acceleration of the oxidation reaction has been achieved using several techniques, which include (a) increased temperature, (b) decreased asphalt film thickness, (c) increased air flow, (d) increased pressure, (e) increased oxygen concentration, and (f) various combinations of these factors.

The rate of reactivity of oxygen with asphalts in pavements has been observed to depend significantly on the temperature level, which led to the various types of oven aging tests that exist today. The idea of thin film aging was first introduced to simulate the aging during plant mixing operations. Because of simplicity, low cost, and the short time required to harden asphalts, oven aging was selected by a large number of researchers to simulate long-term aging as well.

To simulate long-term aging in the shortest period of time, a number of studies were conducted to find the best technique

for increasing oxygen accessibility, accelerating its reaction, and limiting volatilization of the asphalt. Increasing the temperature, reducing the film thickness, rotating the asphalt in horizontal or tilted pans or bottles, and adjusting the amount of air flow in the oven have all been used. Temperature levels have been varied between  $60^{\circ}\text{C}$  ( $140^{\circ}\text{F}$ ) and  $163^{\circ}\text{C}$  ( $325^{\circ}\text{F}$ ), time of aging varied between a few hours and a few days, and the film thickness varied between a few microns and several millimeters. As a result, a large number of procedures have been developed, some of which reasonably successfully simulate field aging.

At higher temperatures light constituents of asphalt evaporate, producing unrealistic changes in the chemistry of the oxidation reactions when compared with field-aged asphalts. In addition, the high molecular constituents are believed to dehydrogenate and a large percentage of oxygen consumed is discharged in the form of water vapor and other gases, which does not occur at normal service temperatures.

An alternative selected for application in this project was to use pressure as the main accelerating factor and lower the temperature to the level at which volatilization and dehydrogenation do not result in significant alteration of the oxidation process from that experienced in the field. The aging temperature selected was near the maximum expected pavement surface temperature. Because paving asphalts are subjected to significant oxidation and thus hardening during mixing in the plant, it appeared desirable to simulate this step in the laboratory. Therefore, all asphalts were subjected to thin film oven (TFO) aging before they were exposed to the PAV.

This report is an abridged version of the original research report prepared for SHRP as partial fulfillment of project A-002a (1).

## OBJECTIVES

A study was performed at the Texas Transportation Institute as part of a larger study headed by the Western Research Institute (WRI) in Laramie, Wyoming, to develop a procedure using oxygen or air under pressure at realistic pavement temperatures to simulate long-term field aging of asphalt cement and associated equipment. The overall objective of this project was to evaluate a PAV for asphalt cement, modify the equipment design and procedure as necessary to optimize suitability for routine use by an asphalt specifying agency, and develop a standardizable test protocol for accelerated aging

of asphalt cement. Specific objectives included determining the effects of aging temperature, asphalt film thickness, simultaneously aging asphalts of different grades or from different sources, and location of asphalt within the PAV. The study also examined the effect of oxidative aging on rheological properties of asphalts using test methods normally specified by state highway agencies and evaluating the repeatability and sources of variability in the test.

## SCOPE OF WORK

The effects of PAV conditioning were determined from measurements of penetration and viscosity before and after the conditioning. The method is designed to predict the approximate change in properties of asphalt during the first few years of service in an asphalt concrete pavement as indicated by standard viscosity and penetration measurements. Four SHRP "core" asphalts with a wide range of aging characteristics were chosen for use in the evaluation. An interlaboratory test program (round-robin) was performed using 10 laboratories for estimating the reproducibility and repeatability of the procedure.

The initial PAV aging procedure, developed for SHRP by WRI, was a slight modification of that developed by Lee (2). In order to accelerate oxidative aging yet maintain kinetic effects similar to those in a pavement, the use of pure oxygen was specified. The pressure of the reaction vessel was specified to be  $2.07 \times 10^6$  pascals (300 psi) but the temperature was maintained at  $60^\circ\text{C}$  ( $140^\circ\text{F}$ ), average maximum pavement surface temperature, for a period of 144 hr.

Early in the study, safety of the test was a concern and, after investigation, oxygen was replaced with air. During the course of the work, the recommended PAV conditioning temperature was raised by SHRP from  $60^\circ\text{C}$  ( $104^\circ\text{F}$ ) to  $71^\circ\text{C}$  ( $160^\circ\text{F}$ ). The PAV aging period remained unchanged. Most of the work reported herein was conducted at the latter temperature. The prototype test procedure and equipment design received from WRI was thoroughly evaluated.

## DESCRIPTION OF EXPERIMENT

### Design of Apparatus

In the early stages of the study, the asphalt aging procedure required pure oxygen to be pressurized to  $2.07 \times 10^6$  pascals (300 psi). Three prototype pressure aging vessels were fabricated of stainless steel to accommodate the test program. These were designed to withstand pressures of up to  $6.2 \times 10^7$  pascals (9000 psi) in case of a deflagration of the asphalt-oxygen mixture.

After careful consideration of the hazards associated with pressurized oxygen in the presence of a hydrocarbon fuel like asphalt, a study was conducted by WRI to assess the effect of oxygen concentration on the oxidation reaction of asphalt. It was found that oxygen concentration (between 20 and 100 percent) had relatively little effect on the rate of reaction; therefore, the decision was made to use pressurized air (which contains 20 percent oxygen) in the procedure. The operating

parameters were initially  $60^\circ\text{C}$  ( $140^\circ\text{F}$ ) and  $2.07 \times 10^6$  pascals pressure. After significant testing had been completed, it was recommended by WRI that the aging temperature be raised to  $71^\circ\text{C}$  ( $160^\circ\text{F}$ ) to increase the rate of reaction and thus simulate a longer in-service aging period.

### Test Procedures

The response variables measured for each specimen before and after aging consisted of the following:

Penetration at  $25^\circ\text{C}$ , dmm – ASTM D 5: Test Method for Penetration of Bituminous Materials ( $77^\circ\text{F}$ ), and  
Viscosity at  $60^\circ\text{C}$ , Pa·s – ASTM D 2171: Viscosity of Asphalts by Vacuum Capillary Viscometer ( $140^\circ\text{F}$ )

Penetration and viscosity of (a) original asphalt, (b) TFO, and (c) TFO + PAV-aged asphalt were measured to estimate the relative age-hardening potential of the material.

### *Original Unaged Specimens*

Asphalt cement specimens were prepared in accordance with the SHRP Materials Reference Library protocol for handling and use of asphalt cements. Physical properties (penetration and viscosity) of original asphalts were measured.

### *TFO-Aged Specimens*

The first step in aging the asphalt specimens was to expose the specimens to the TFO test to simulate hardening in an asphalt plant. This was performed in accordance with ASTM D 1754. The asphalt properties were then measured using those same tests performed on the unaged specimens.

### *TFO Plus PAV-Aged Specimens*

In all cases, PAV aging of asphalts was preceded by TFO aging. The pans of TFO-aged asphalts were placed in the PAV and aged according to the protocol developed. After removing the asphalts from the PAV, changes in their physical properties were measured using the same tests performed on the unaged and TFO-aged specimens.

### Experimental Design

Two separate experimental programs were conducted to accomplish the goals of the work: (a) PAV Test Development and (b) Interlaboratory Test Program (Round-Robin).

### *PAV Test Development*

Development of the PAV test encompassed items such as equipment design, variability of the aged asphalts, control of independent variables, written procedures, and personnel

safety. The experimental design for evaluating and developing the PAV test included the following controlled variables and levels:

Oxidation level: 2 levels (zero and 144 hours);  
 Asphalt type: 4 levels/tests (selected SHRP core asphalts);  
 Different asphalts in PAV simultaneously: 2 levels (yes, no);  
 Film thickness: 3 levels 1.6 mm, 3.2 mm, and 6.4 mm or ( $\frac{1}{16}$  in.,  $\frac{1}{8}$  in., and  $\frac{1}{4}$  in.);  
 Location in PAV: 3 levels (top, middle, bottom); and  
 Aging temperature: 4 levels 54°C, 60°C, 71°C, and 77°C (or 130°F, 140°F, 160°F and 170°F).

Because the recommended test temperatures changed during the course of the work, it was necessary to conduct the experiment on a partial factorial basis. Penetration and viscosity were selected as response variables because they give a reasonable assessment of oxidative hardening of asphalts, and most state highway agencies have these capabilities.

### *Interlaboratory Test Program*

An interlaboratory test program was conducted to establish accuracy and precision associated with the PAV conditioning procedure. The experimental design included the following controlled variables and levels:

Number of laboratories: 10 levels;  
 Asphalt type: three levels per test; and  
 Number of specimens: three samples of each asphalt in the PAV simultaneously.

### **Asphalts Tested**

In this project, four SHRP core asphalts of different grades and from different sources were chosen. Asphalts AAC-1, AAD-1, AAF-1, and AAG-1 were obtained from the SHRP Materials Reference Library in Austin, Texas (Table 1; data supplied by SHRP Contract A001).

TABLE 1 Properties of asphalts chosen for project

Asphalt Grade	AC-5	AC-3	AC-20	AR-4000
MRL Code	AAC-1	AAD-1	AAF-1	AAG-1
<b>Original Asphalt</b>				
Viscosity 60°C (140°F), poise 135°C (275°F), Cst	419 179	1055 309	1872 243	1862 327
Penetration, 0.1 mm 25°C or 77°F, 100 g, 5 sec 4°C or 39.2°F, 100 g, 5 sec	133 7	135 9	55 0	53 2
Ductility, cm 4°C or 39.2°, 1 cm/min	137.0	150+	7.6	0.0
Softening Point(R&B), °C (°F)	43 (109)	48 (118)	50 (122)	49 (120)
Component Analysis, % Asphaltenes (n-heptane) Polar Aromatics Naphthalene Aromatics Saturates	11.0 37.4 37.1 12.9	23.0 41.3 25.1 8.6	14.1 38.3 37.7 9.6	5.8 51.2 32.5 8.5
Elemental Analysis Nitrogen, % Sulfur, % Vanadium, ppm Nickel, ppm	0.42 2.74 71 40	0.90 8.60 293 145	0.23 4.52 68 27	1.10 2.00 32 71
<b>Thin Film Oven Residue</b>				
Mass Change, percent	-0.2590	-0.8102	-0.0921	-0.1799
Viscosity 60°C (140°F), poise 135°C (275°F), Cst	1014 239	3420 511	4579 472	3253 304
Viscosity Ratio (60°C or 140°F)	2.42	3.24	2.45	1.75

Three complete repetitions of the PAV aging procedures were conducted with three of these four asphalts to determine the inherent variability of the aging procedure. These three asphalts were then used in the round-robin testing program to further analyze variability for the aging protocol.

## RESULTS OF LABORATORY INVESTIGATION AND DISCUSSION

A laboratory testing program was conducted to evaluate the PAV procedure and equipment, to assess any hazards associated with the process, and to determine the allowable variation in such items as aging temperature or thickness of the asphalt film. The laboratory investigation is described in the following subsections.

### Safety Investigation

As pure oxygen was used in the first artificial asphalt aging procedure, significant effort was expended to study the associated hazards. A hydrocarbon fuel like asphalt in the presence of pressurized pure oxygen presents a serious potential hazard, particularly in relatively large quantities as desired in the proposed procedure. Furthermore, extreme caution would be necessary when designing, fabricating, and operating such a vessel.

Disastrous explosions were reported when "liquid" oxygen contacted asphalt and pressure was applied on the reacted product (3), because of the formation of peroxides. As a part of this study, tests performed by WRI to determine if the use of gaseous oxygen under these conditions would form peroxides revealed no peroxide formation.

Chemical and engineering principles and thermodynamics were applied to determine whether detonation or deflagration would be likely to occur should a spark enter a PAV fully

charged with asphalt and gaseous pure oxygen. Deflagration appeared most probable (3,4). Recommendations were made regarding the design of the vessel, construction materials, rapid pressure relief systems, and venting of gases or flaming liquids in case of deflagration. The PAV was hydraulically tested to withstand pressures twice the normal operating pressure. Operation behind a safety barrier such as a concrete wall or bunker was recommended.

Interviews with state highway agency and industry personnel indicated a reluctance to routinely operate test equipment with the hazards previously described. Further work at WRI indicated that replacement of oxygen with air in the PAV made little difference in the extent of oxidation of asphalts. Therefore, based on these findings, the decision was made to forego the use of pure oxygen in the PAV and use dry air instead.

### Effect of Aging Temperature

In order to determine the effect of PAV aging temperature, PAV tests were performed at 54°C, 60°C, 71°C, and 77°C (130°F, 140°F, 160°F and 170°F). Pressure and aging time remained the same for all tests:  $2.07 \times 10^6$  (300 psi) air pressure and 144 hr. Fifty grams of asphalt were used for all tests as prescribed by ASTM D 1754. The effects of aging temperature are depicted in Figures 1 and 2.

It should be noted that the relative degree of hardening of asphalts varies at different aging temperatures in the PAV; that is, two asphalts may age similarly at one temperature but age differently at another temperature. This phenomenon is demonstrated by the difference in slopes of the lines in Figures 1 and 2. These findings agree with previous work by Lau et al. (5). This fact is significant because the relative results of an aging test will be dependent on the temperature at which the test is conducted. It may be necessary, therefore, to age asphalts at different temperatures to obtain an accurate and complete assessment of susceptibility to oxidation.

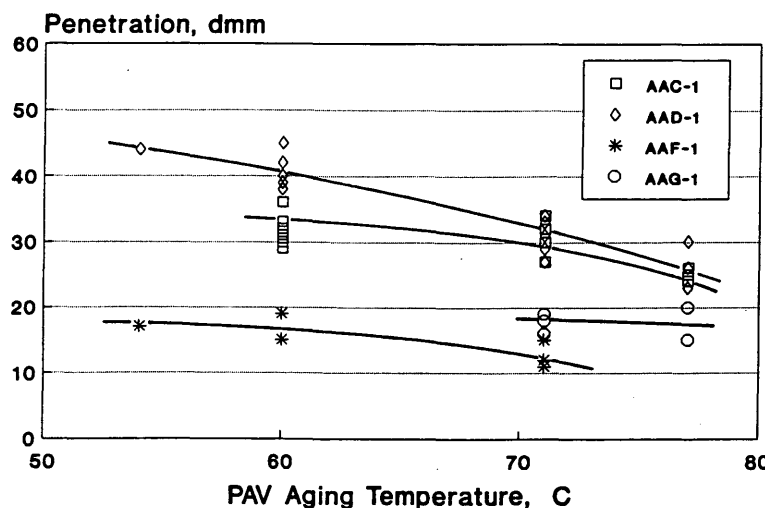
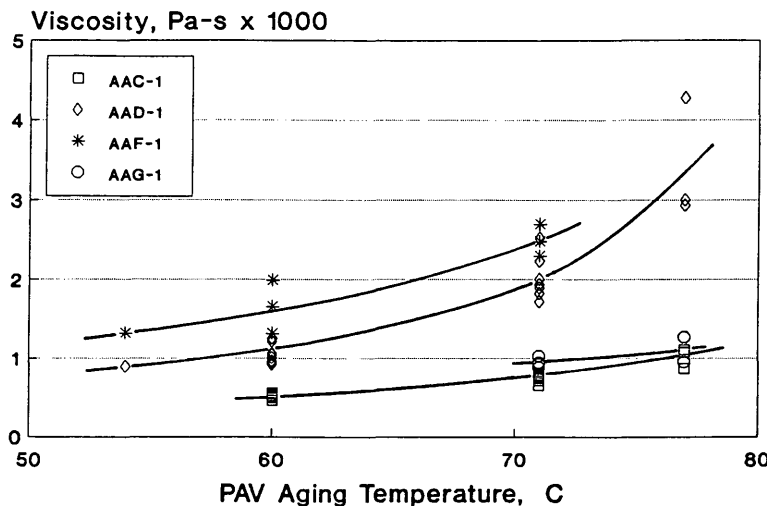


FIGURE 1 Penetration at 25°C of TFO/PAV-aged asphalts as a function of PAV temperature.



**FIGURE 2** Viscosity at 60°C of TFO/PAV-aged asphalt as a function of PAV temperature.

#### Effect of Film Thickness on Aging

Tests were conducted to examine the effect of asphalt film thickness on aging in the TFO/PAV. The three film thicknesses chosen for this test were 1.6 mm, 3.2 mm, and 6.4 mm ( $\frac{1}{16}$  in.,  $\frac{1}{8}$  in. and  $\frac{1}{4}$  in.). Normally, 50 gm of asphalt per TFO pan was used throughout this aging study, which gives an asphalt layer thickness of approximately 3.2 mm ( $\frac{1}{8}$  in.) in the TFO pan. In this portion of the study, one-half this amount (25 gm) and twice this amount (100 gm) were used. The pressure aging vessel (PAV) was operated at  $2.07 \times 10^6$  (300 psi) air at 71°C for 144 hr. Penetration at 25°C and viscosity at 60°C were measured before and after aging. Each test included two replicates (3 separate specimens per replicate) for each of the three film thicknesses.

An almost linear relationship between asphalt film thickness and age hardening over the range of film thickness tested and at the 71°C aging temperature is shown, on the average, in Figures 3 and 4, and this relationship is asphalt dependent.

#### Effect of Vertical Location Within PAV

The objective of these tests was to determine if there is any effect of vertical location on a specimen within the PAV. An experiment was designed to determine if gases or vapors will stratify within the static PAV to form an oxygen-deficient atmosphere near the top or bottom that would ostensibly reduce oxidative aging in that vicinity. The PAVs used in this study would accommodate up to 10 TFO pans stacked ver-

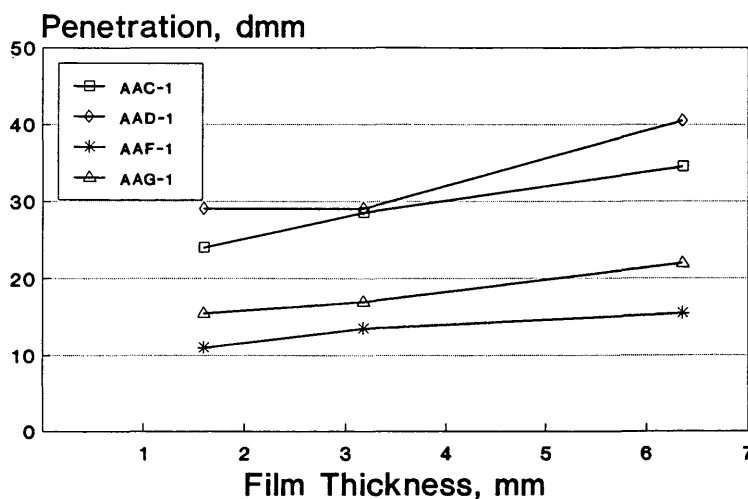


**FIGURE 3** Penetration at 25°C after TFO/PAV as a function of asphalt film thickness.

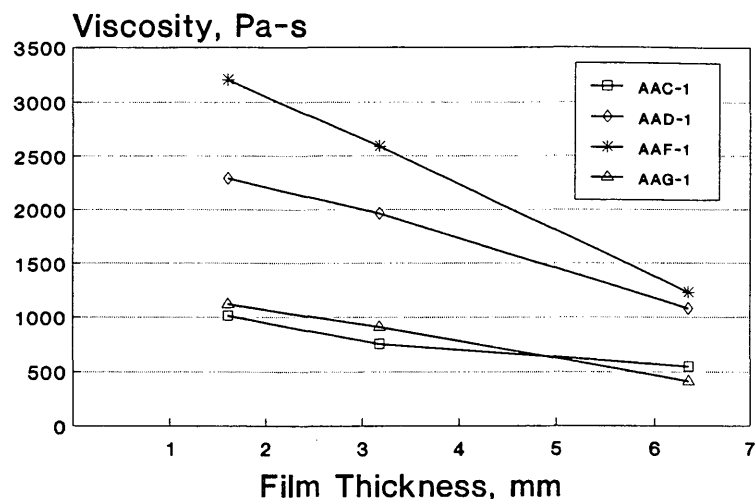


**FIGURE 4** Viscosity at 60°C after TFO/PAV as a function of asphalt film thickness.

tically with about 5 mm of space between them. Pans of asphalt were placed in the upper, middle, and lower positions of the pan rack and aged as usual in the PAV. Tests were conducted at 54°C, 60°C, and 71°C (130°F, 140°F, and 160°F).

None of the tests indicated that differential aging occurred with respect to the vertical position in the PAV.

#### Effect of Proximity to Other Asphalts

The objective of this experiment was to determine the effect of simultaneous aging of asphalts from different sources. Tests were performed to determine whether or not hydrocarbon vapors are released from the asphalt that has been previously exposed to TFO test procedure during PAV aging at 60°C and 71°C. TFO pans filled with a known weight of dried silica gel were placed in the bottom and top pans in the PAV during separate aging tests with three identical asphalts and with three different asphalts aged simultaneously. Asphalts AAC-1, AAD-1, and AAF-1 were used. After completion of the normal aging procedure, the silica gel was removed and weighed. The silica gel was then desorbed using cyclohexane and the extracted solution was subjected to the fourier transform infrared analyzer (FTIR) and gravimetric analysis to determine whether hydrocarbons were present and, if so, to identify them as fully as possible. No asphalt components were detected in the silica gel extracts.

On the basis of this evidence, the assumption was made that no commingling would occur when asphalts from different sources or of different grades are aged simultaneously in the PAV at 71°C. It should be pointed out that only three asphalts were tested in this manner but one of them (AAD-1) was selected because of its relatively high volatile loss in the TFO test (see Table 1). Before the silica gel experiment was conceived, a series of aging tests had been initiated to determine whether commingling occurs when two or more chemically and physically different asphalts are aged simultaneously at 60°C or 71°C in a PAV. Penetration at 25°C and viscosity at 60°C were used in the evaluation. The results show that the range of values for asphalts aged individually are

about the same as the range of those aged with other asphalts in the PAV, thus substantiating the silica gel experiment.

#### Other Findings

When conditioning asphalts in a standard thin film oven equipped with exposed heating elements at the bottom and a rotating shelf containing large pie-shaped ventilation slots, it was found that the extent of aging depended on the location of the asphalt pan on the TFO shelf. If the pan was placed over a slot, thus exposing a portion of the bottom of the pan directly to the radiation from the heating element, much more hardening of the asphalt occurred. After realizing this phenomenon fairly early in the study, all subsequent work was performed with the asphalt pans located between the slots so that no part of the pan was exposed directly to the heating element and to permit the ventilation slots to function as designed. Random placement of pans on the TFO shelf during the test will result in wide variation of aging between pans. This problem is being addressed by ASTM. Pan placement on the shelf should be specified. Heating coils should be covered to shield radiant heat from the asphalt pan.

Because of the rapid evaporation of the hot water, a system was devised using a float valve to automatically replace the lost water so as to prevent overheating of the water-heating elements. In addition, hollow plastic balls 19 mm ( $\frac{3}{4}$  in.) in diameter that float on the water bath were used quite successfully to reduce evaporation and heat loss.

Kandhal (6) measured penetration at 25°C, viscosity at 60°C, ductility at 15°C (59°F), and 5 cm/min of asphalts extracted from pavements at various times during their service lives, and compared the results with the onset of cracking. He produced plots of these values as a function of time for up to 140 months. Asphalts AAF-1 and AAG-1 have original physical properties similar to the asphalts used in his study. When penetration and ductility of these asphalts after conditioning in the PAV operated at 71°C are compared with the plots produced by Kandhal, it appears that the PAV simulates in-place pavement aging greater than 140 months. However,

when viscosity of these asphalts after PAV aging at 71°C is compared with his data, the PAV appears to simulate only about 20 to 40 months of pavement aging.

When penetration and viscosity data from the TFO/PAV tests are compared with field aging data published by Lee (7), they appear to represent about 70 months (extrapolated beyond 50 months of recorded data) of aging in the field.

### Additional Comments

Although not considered in this study, other related work has indicated that the TFO test is unsuitable for use with many polymer-modified asphalts. A hard crust will often form on the surface of TFO-aged modified asphalt, thus rendering it unsuitable for further testing. For these types of materials, it may be necessary to use the rolling thin film oven test (ASTM D 2872).

Since the completion of this study, the SHRP PAV conditioning protocol has again been changed. The aging temperature was increased to 100°C (212°F) and the aging time was decreased to 20 hr. A forced-air oven instead of a water bath is required to control the aging temperature of the PAV. The primary reason for these changes was to reduce the time requirements from 6 days to 1 day to accommodate the needs of the state highway agencies. These changes in the test protocol will, of course, significantly reduce the value of the test results reported herein.

## INTERLABORATORY TEST PROGRAM

### General

On the basis of the foregoing work, a written procedure for the TFO/PAV asphalt conditioning process was prepared. The written protocol and equipment were subjected to an interlaboratory test program, or round-robin, to examine the variability in the properties of artificially aged asphalts.

The following ten agencies participated in the round-robin test program:

- Alabama Department of Transportation (Ala)
- Arkansas Department of Transportation (Ark)
- Colorado Department of Transportation (Col)
- Florida Department of Transportation (Fla)
- Georgia Department of Transportation (Geo)
- Louisiana Department of Transportation (La)
- Mississippi Department of Transportation (Mis)
- Oklahoma Department of Transportation (Ok)
- Southwestern Laboratories (SwL)
- Texas Department of Transportation (Tx)

Round-robin participants received training at their respective laboratories by a representative of the research team and were provided with a written test protocol. The round-robin participants performed the tests on replicate sets of the three asphalts. The tests were conducted using the PAV operated at 71°C (160°F) and  $2.07 \times 10^6$  pascals (300 psi) air pressure for 144 hr. Penetration and viscosity data were recorded.

### Statistical Analysis

The overall mean values at each level of aging are plotted in Figures 5 and 6 to illustrate the different effects of aging on the three asphalts.

A two-factor analysis of variance (ANOVA) model with interaction was performed on the data from the various laboratories. The two factors were asphalt type (AAC-1, AAD-1 and AAG-1) and treatment (original asphalt, after TFO, and after TFO/PAV).

For the penetration data, there was a significant interaction between asphalt and treatment, meaning that the three asphalts did not respond the same for each treatment level. In order to better understand this difference in response, two analyses were conducted. The first was to compare asphalts

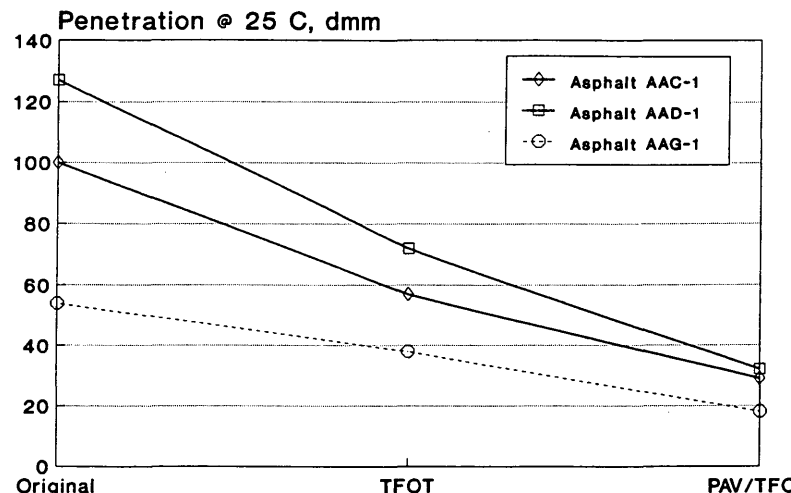


**FIGURE 5** Penetration data from round-robin tests showing sensitivity of asphalts to artificial aging.

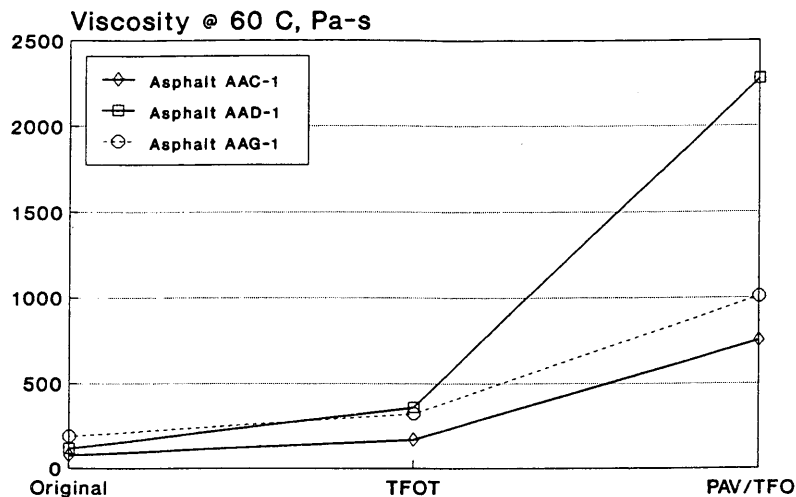


**FIGURE 6** Viscosity data from round-robin tests showing sensitivity of asphalts to artificial aging.

for each treatment and the second was to compare treatments for each asphalt.

For the original asphalt, the after TFO, and the after TFO/PAV groups, there was a significant difference in the average penetration among the three asphalts, with AAD-1 being significantly greater than AAC-1, which was significantly greater than AAG-1, according to Duncan's multiple range test at the 5 percent level of significance. Similarly, for each asphalt, there was a significant difference among mean penetrations for each group, with penetration decreasing from the original to the after TFO/PAV.

An interlaboratory analysis was performed to determine if there were significant differences among penetrations measured by the different laboratories. For both the original and after TFO groups, there were no significant differences among the laboratory results for any of the three asphalts. However, after TFO/PAV, there were significant differences for all three asphalts.

For AAC-1, there is no practical difference among the laboratories. For AAD-1, Ok gave significantly higher penetration values than the other states. For AAG-1, Ark had significantly higher penetration values and Lou and Col had significantly lower penetration values than the other states.

The viscosity data yielded similar results. Analysis over all states indicated that there was a significant asphalt-treatment interaction and that mean viscosity significantly increased from original to after TFO/PAV for all three asphalts. Also, there was a significant difference among asphalts within any treatment level (i.e., mean viscosity was different in the original sample for all three asphalts and this difference remained both after TFO and after TFO/PAV).

The interlaboratory analysis for viscosity was similar to the penetration results in that the only significant difference in viscosity among laboratories occurred after TFO/PAV. There were no differences in laboratories in the original or after TFO. However, after TFO/PAV, there was a significant difference among laboratories for all three asphalts.

For AAC-1 and AAG-1, Fla gave significantly higher viscosity than the other states, and for AAG-1, Ok, Lou, and

SwL gave significantly lower viscosities. AAD-1 did not show any distinct differences among the laboratory readings.

#### Precision

Precision of penetration and viscosity test results following TFO/PAV conditioning was computed based in the round-robin test. Criteria for judging acceptability of penetration and viscosity of an asphalt after conditioning in the TFO/PAV are provided in the following two subsections.

#### Penetration

The single operator coefficient of variation was 5.97 percent (1S percent). Thus results of two properly conducted tests by the same operator on similar material should not differ by more than 16.88 percent (D2S percent).

The multilaboratory coefficient of variation was 10.90 percent (1S percent). Thus results of two properly conducted tests from two different laboratories on similar material should not differ by more than 30.82 percent (D2S percent).

#### Viscosity

The single operator coefficient of variation was 7.09 percent (1S percent). Thus results of two properly conducted tests by the same operator on similar material should not differ by more than 20.05 percent (D2S percent).

The multilaboratory coefficient of variation was 13.79 percent (1S percent). Thus results of two properly conducted tests from two different laboratories on similar material should not differ by more than 39.0 percent (D2S percent).

The following data for the associated ASTM tests show that most of the variability obtained in the TFO/PAV conditioning procedure originates in the thin film oven test.

	<i>Single Operator Precision</i>	<i>Multiple Laboratory Precision</i>
Penetration, ASTM D5	1	4
Viscosity, ASTM D2171	7	10
TFOT, ASTM D1754 (for viscosity)	9	33

## FINAL DESIGN OF EQUIPMENT

After a thorough evaluation of the PAV written procedure and the prototype equipment fabricated as a part of this study, a final equipment design was developed (1). This final design was formulated to accommodate commercial production and routine operations in a laboratory. All effort was given to furnish a design that is functional yet convenient, safe, and economical.

## CONCLUSIONS

1. Degree of asphalt hardening caused by oxidation increases as aging temperature in the PAV increases from 54°C to 71°C (130°F to 160°F).
2. At a given aging temperature and aging time period, degree of hardening caused by oxidation increases as asphalt film thickness decreases from 6.4 mm to 1.6 mm ( $\frac{1}{4}$  in. to  $\frac{1}{16}$  in.).
3. For the asphalts tested in this study, vertical location of the asphalt in the PAV has no effect on degree of hardening at an aging temperature of 71°C (160°F).
4. For the asphalts tested and the conditions used in this study, aging asphalts simultaneously in the PAV has no effect on the extent of hardening.
5. Different asphalts exhibit different rates of hardening at the same conditions of temperature and time.
6. The relative degree of hardening of asphalts varies at different aging temperatures in the PAV; that is, two asphalts may age similarly at one temperature but age differently at another temperature.

7. On the basis of comparisons of data obtained in this study with field data obtained in other studies, it generally appears that the PAV operating conditions of 71°C (160°F), 2.07  $\times$  10<sup>6</sup> pascals (300 psi), and 144 hr will simulate 2 to 10 years of aging in a pavement, depending on the method used to measure hardening, air voids in the paving mixture, average ambient temperature, and other factors.

8. On the basis of testing by 10 laboratories of three asphalts in an interlaboratory test series, precision of the TFO plus PAV tests were as follows:

	<i>Single Operator</i>	<i>Multi-Laboratory</i>
Penetration	17	31
Viscosity	20	39

## REFERENCES

1. J. W. Button, M. Jawle, D. N. Little. *Evaluation and Development of a Pressure Aging Vessel for Asphalt Cement*. Texas Transportation Institute, Texas A&M University, June 1992.
2. D. Y. Lee. Development of a Laboratory Durability Test for Asphalts. In *History Research Record 231*. HRB, National Research Council, Washington, D.C., 1968, pp. 34–49.
3. L. H. Dimpfl. *Asphalt Tank Explosions, Fire Protection Manual for Hydrocarbon Processing Plants*. Chevron Research Company, Vol. 1, 1985.
4. G. E. Moffett, M. D. Pedley, N. Schmidt, R. E. Williams, D. Hirsch, and F. J. Benz. *Ignition of Nonmetallic Materials by Impact of High-Pressure Gaseous Oxygen, Flammability and Sensitivity of Materials in Oxygen-Enriched Atmospheres*. ASTM STP 986, American Society for Testing and Materials, 1988.
5. C. K. Lau, K. M. Lunsford, C. J. Glover, R. R. Davison, and J. A. Bullin. *Reaction Rates and Hardening Susceptibilities as Determined from POV Aging of Asphalts* (in publication). TRB, National Research Council, Washington, D.C., Jan. 1992.
6. P. S. Kandhal. *Low-Temperature Ductility in Relation to a Pavement Performance, Low-Temperature Properties of Bituminous Materials and Compacted Bituminous Paving Mixtures* (C. R. Marek, ed.). ASTM STP 628, American Society for Testing and Materials, 1977, pp. 95–106.
7. D. Y. Lee. Asphalt Durability Correlation in Iowa. In *Highway Research Record 468*, HRB, National Research Council, Washington, D.C., 1973, pp. 43–60.

# New Apparatus and Procedure for the Extraction and Recovery of Asphalt Binder from Pavement Mixtures

B. L. BURR, C. J. GLOVER, R. R. DAVISON, AND J. A. BULLIN

A new apparatus and procedure for the purpose of extracting asphalt binder from hot-mix and pavement samples has been developed. This procedure is the culmination of previous reports on solvents for the extraction of asphalt, the aging of asphalt in solution, and the removal of solvent from asphalt. The apparatus consists of a rotary drum for the purpose of efficient and thorough contacting of the aggregate-binder sample with the solvent, followed by filtration and then solvent removal using a Roto-vap procedure. Intralaboratory tests of the procedure on a variety of samples indicate that the precision associated with one standard deviation is about 6 percent for extracted asphalt viscosities. This compares with interlaboratory precision of about 30 percent for previous methods according to the AASHTO Materials Reference Laboratory proficiency sample program. Additionally, this new procedure provides recovered asphalt that has physical properties, such as viscosity, that are much closer to the "true" physical properties of the binder as it existed in the pavement. This is essential if tests performed on the binder are to have any meaning with respect to pavement performance.

Although properly measuring chemical and physical properties of asphalt in hot mix or pavement samples requires accurate extraction and recovery procedures, currently used methods show poor precision and unknown accuracy. This can be seen in American Association of State Highway and Transportation Officials' (AASHTO) interlaboratory proficiency tests in which various laboratories analyze pavement specimens provided by AASHTO for several properties, including asphalt content and viscosity. Shown in Figure 1 is the scatter in extracted asphalt viscosities of two different but similar asphalt mixtures of unknown origin (samples 27 and 28 in this test) determined by 62 different laboratories. Points inside the box lie within one standard deviation of the mean and the diagonal line represents perfect intralaboratory reproducibility. The standard deviations of viscosities in these tests have ranged from 25 to 42 percent during the years 1986 to 1991. Unfortunately, the extraction methods were not specified and vary considerably between laboratories (1). Nevertheless, it is obvious that even self-consistency is difficult for laboratories to achieve using current methods and that interlaboratory differences can be great. It is likely that the error in extracted asphalt properties stems from the following problems:

1. Asphalt is not completely or consistently extracted from the aggregate;
2. Residual solvent is left in the asphalt after recovery; and
3. Reaction of asphalt while in solution, sometimes called solvent aging, can alter properties during both extraction and recovery.

After studying these error sources for the past three years, we have designed and tested a new asphalt extraction and recovery method for the Strategic Highway Research Program (SHRP) that addresses these problems. Tests to date indicate that the SHRP method is more precise and accurate than any standard method. However, incorporation of certain aspects of our new method can greatly improve the performance of one existing method to the point of being comparable.

To describe briefly the SHRP procedure, the extraction is performed in a rotating drum in which the solvent and pavement sample are thoroughly contacted. The extract is vacuum filtered through a woven polypropylene filter assembly on one end of the drum. The filtrate then goes through a tighter filter to remove most of the aggregate fines before being transferred to a rotary evaporator where the solvent is vacuum distilled. In order to adequately extract strongly adsorbed asphalt, several solvent washes are required. Before final solvent removal, all remaining fines are centrifuged. (Undoubtedly, both absorption and adsorption phenomena are, or may be, important. Throughout this paper we refer to adsorption but recognize that adsorption/absorption is more correct.) Recovery of the asphalt is performed according the protocol described by Burr et al. (2).

The purpose of this paper is to present in detail the SHRP extraction and recovery method and to compare it with modifications of two commonly used procedures with respect to both precision and accuracy.

## HISTORY OF METHODS

Extraction and recovery have been practiced in some form since the turn of the century. In 1903, as discussed by Abson (3), Dow extracted with carbon disulfide ( $CS_2$ ) and recovered using simple distillation. Bateman and Delp (4) centrifuge-extracted with  $CS_2$  and removed the solvent by vacuum distillation. Soxhlet type reflux extractions using  $CS_2$  were common

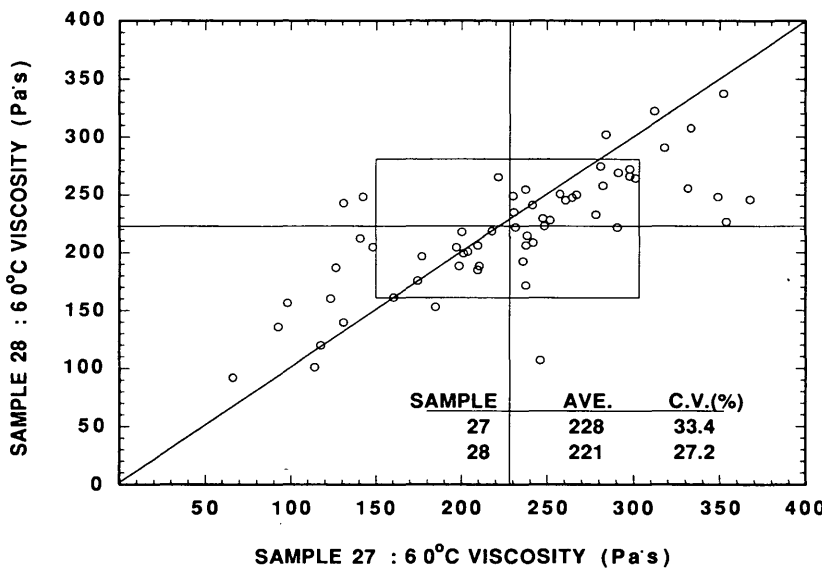


**FIGURE 1** Results from the AASHTO Materials Reference Laboratory Proficiency Sample Program. Samples 27 and 28 are replicates.

in this early period. Several other methods were developed through 1930, but none gained lasting acceptance (3,5).

#### Extraction Methods

Today centrifuge and reflux extraction methods (usually in the form of ASTM D-2172, methods *A* and *B* respectively) are used almost exclusively. Vacuum extraction (6) and sonication methods (7,8) also have been used, but infrequently. The centrifuge method was developed in the 1920s (4,5) and eventually adopted by ASTM as D-2172A (6) in 1963. The reflux extraction method was in existence before 1949 and there were reservations about its use in obtaining asphalt for property analysis (5). ASTM warns that the reflux method D-2172B should not be used if asphalt properties are to be measured. Despite the warnings, use of reflux extractions is far more prevalent in the literature than other methods (2). In this paper, Methods *A* and *B* refer specifically to ASTM D-2172 *A* and *B*.

Incomplete extraction and solvent aging are two problems to consider when selecting an extraction method. Reflux methods expose the asphalt to solvent at elevated temperatures for long periods of time. This has been shown to cause considerable hardening caused by reactions that the asphalt undergoes when it is in a dissolved state. The reactions occur at room temperature, but have higher rates at reflux temperatures (9,10). In general, reaction rates increase exponentially with temperature and are constant over time, so it is desirable to minimize these variables to limit any reactions that might occur. Asphalt concentration in solution and type of solvent can be other important variables, but it is not yet clear what effect, if any, these have on this system.

The extraction methods' means of contacting the samples, choice of extraction solvents, and aggregate adsorptivity determine how much of the asphalt is extracted. Method *A* typically leaves 2 to 4 percent of the asphalt on the aggregate

when trichloroethylene (TCE) is the extraction solvent. Method *B*, which seems to have poor solvent contacting, leaves much more asphalt unextracted (11). Modification of Method *A* by adding 15 percent ethanol to the TCE in later washes and mixing thoroughly during each wash removes about half of the strongly adsorbed material that method *A* leaves behind (11).

The choice of extraction solvent is important in determining how much of the asphalt is extracted by a given method. TCE with 15 percent ethanol and pyridine are the most powerful solvents for extracting asphalts. Toluene with 15 percent ethanol, although not as powerful as the other two, is good and has safety advantages that make it more attractive (11).

#### Solvent Removal Methods

Typically, removal of solvent is performed by the Abson method, ASTM D-1856 (6) or by rotary evaporation (12,13). These two methods share equal popularity (2).

Both methods have been plagued with the problem of incomplete solvent removal because the prescribed distillation times and temperatures do not guarantee complete solvent removal. Even low solvent concentrations in asphalt (about 0.2 percent) are enough to cause significant physical property errors. Gel permeation chromatography (GPC) has been used to detect small amounts of residual TCE and toluene. Both recovery methods were calibrated using this direct TCE detection to determine appropriate recovery conditions for different sample masses and viscosities (2).

#### EXPERIMENTAL PROCEDURES

The intent of this study is to evaluate the performance of the SHRP extraction and recovery method, and compare it with

current extraction methods, modified to achieve improved recovery. A suitable solvent removal method had been developed earlier (2), and it was used after all extractions in this study with only minor variations in some cases. This was so that all extraction methods could be judged fairly, instead of tainting the results of one method by using an inadequate recovery method.

## Extraction Methods

### SHRP Method

The SHRP extraction and recovery apparatus is shown in Figure 2. The extractor drum, made of 15.2-cm (6-in.) Sch. 80 aluminum pipe and 1.27-cm (½-in.) aluminum discs, has a filter arrangement consisting of a 10-mesh steel screen followed by about 2.54 cm (1 in.) of glass wool packing, an 8-µm polypropylene monofilament filter (Filter-All, Inc. #13118, from Magnolia, Texas), and another 10-mesh steel screen for filter support. The drum is also fitted with four baffles to improve mixing. The fine filter is composed of two 33-cm (13-in.) aluminum discs containing about 1.27 cm (½ in.) of liquid space followed by a 1- to 2-µm polypropylene monofilament filter (Filter-All, Inc. #13107) and a 10-mesh steel screen filter support.

To begin an extraction, 1 kg of pavement sample and 600 mL of toluene (or TCE) are charged to the extractor drum. The drum is attached as shown to the 30 rpm, 49.7 W (½ hp) shaded pole gear motor and turned for 5 min. Next, the drum is connected above the first filtrate flask, about 39.9

kPa vacuum is applied (61.3 kPa pressure, absolute), and the extract is filtered. This filtrate is further put through the fine filter to remove as many small aggregate particles as possible. Unfortunately the coarse filter by itself passes too many fines to the recovery step, and a 1 to 2 µm filter plugs when it is used as the drum filter.

The filtrate from the fine filter is transferred to the rotary evaporator's 1000 mL recovery flask, which contains several 3-mm glass boiling beads. The rotary evaporator is a Buchii RE-111, and a common kitchen fryer is used as an oil bath. The bath temperature is held at 100°C and pressure is lowered to 12.0 kPa absolute. The recovery flask is lowered into the oil bath and the solvent is distilled until the condensate rate is down to about one drop every 15 seconds when the flask is raised from the oil bath. The condensate flask is emptied into a container where the solvent is used for subsequent washes.

The oil bath temperature and recovery pressure were chosen to obtain a relatively low distillation temperature without overwhelming the condenser. Having the boiling temperature low limits the rate of solvent aging during the recovery step. The relatively low bath temperature helps reduce unstable boiling in the recovery flask.

While the solvent is distilling, the extractor drum is charged with 400-mL solvent and turned for 15 min. The mixing, filtering, and distilling sequence is repeated for this second wash.

The third wash follows similarly, except that the mixing time is 30 min. After distilling the third wash, the recovery flask is removed and set aside. This flask contains about 90 percent of the asphalt in the sample, and removing it from the recovery conditions helps prevent solvent aging. Another recovery flask is attached to the rotary evaporator for the remaining washes. For the fourth and subsequent washes, toluene (or TCE) with 15 percent ethanol is used. The mix times are 30 min each. When the extract flowing through the transfer tube attains a light brown color, the extraction is completed. This usually takes a total of seven washes, or about 3000 mL of solvent contacting the sample.

Before final recovery, the asphalt in both flasks is mixed into solution and poured into two 250-mL centrifuge jars. The last remaining aggregate fines are centrifuged for 25 min at 3,600 rpm. After centrifuging, the solution is decanted into a 1000-mL recovery flask with boiling beads.

For the final recovery, the bath is heated to 171°C. The recovery flask is attached to the rotary evaporator, pressure is set at 8.0 kPa absolute, the flask is lowered into the bath, and solvent is distilled. When the condensate rate falls to less than one drop every 30 sec, a nitrogen ( $N_2$ ) purge tube is inserted through the condenser and down to the asphalt surface. The  $N_2$  is bubbled at 1000 mL/min through the asphalt for 30 min to complete the extraction and recovery.

This solvent-removal scheme will be called "the two-flask method." A similar scheme that involves continuously recovering the extracts but uses only one recovery flask will be called "the single-flask method."

### Modified Method A

A modified method A procedure also was performed. The instructions in ASTM D-2172A (6) were followed except that

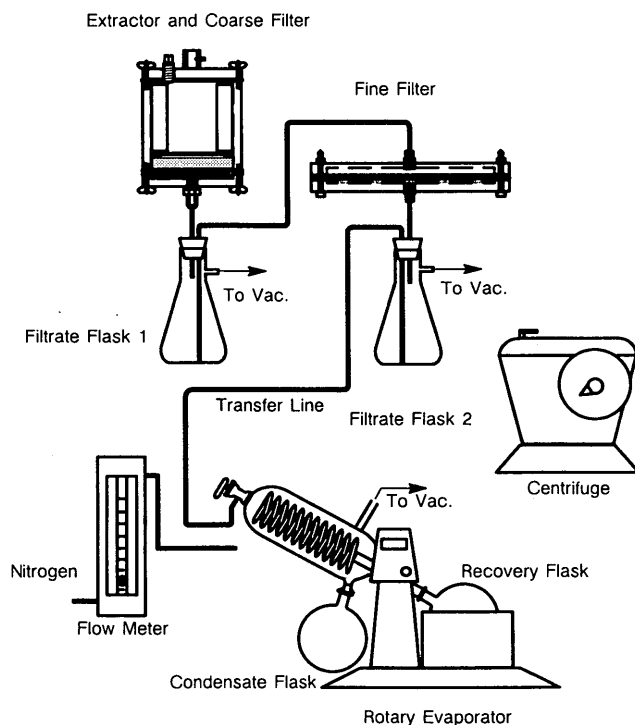


**FIGURE 2** Schematic representation of SHRP extraction and recovery apparatus.

toluene was substituted for TCE in some cases, ethanol (EtOH) was added to the solvent in late washes, and more solvent wash was used than is called for in the standard procedure. After the fourth wash, solvent with 15 percent ethanol was used. The filtrates from all washes were collected in a 4-L bottle until the extraction was completed. The extract was recovered using the rotary evaporator as previously described except that it is not continuous and only one recovery flask was needed. The term "batch method" will be used to describe this type of recovery.

The standard method leaves the number of solvent washes to the user's discretion by stating that the extraction should proceed until the filtrate obtains an arbitrary light straw color. In order to compare Method A and the SHRP method on an equal basis, we extracted with 11 washes (about 3000 mL)—considerably more than are used by most experimenters. Consequently, it should be understood that our Modified Method A data may not be comparable with those of other laboratories that do not use ethanol addition and employ only six solvent washes, for instance.

#### *Method B*

The Method B extractions followed ASTM D-2172B (6) except that solvent was varied in some of our experiments. The extract was recovered using the batch method. In Method B, about 100 g of the asphalt mixture are placed in two cone-shaped filters, one above the other in a cylindrical glass container. About 500 ml of solvent is added to the bottom of the container and heated to boiling on a hot plate. Vapors rise to the top of the container to a condenser. The reflux falls through the sample, extracts asphalt, and flows through the filter and back into the solvent pool. Most of the asphalt is extracted and resides in the pool after several hours of refluxing. It is an inexpensive and labor-saving method and is preferred by most asphalt laboratories. However, it alters the asphalt during extraction caused by solvent aging and its use is discouraged by ASTM if the extracted asphalt is to be studied.

#### **Viscosity Measurements**

In this study, some viscosities are measured using Cannon-Manning vacuum capillary viscometers at 60°C according to ASTM D-2171 (6). Some samples were very hard, so it became more practical to use a Carri-Med CSL controlled stress rheometer (CSL) at 60°C and 90°C. The data from the two temperatures were shifted using the principle of time-temperature superposition (14) to provide zero-shear viscosities at 60°C. Though the two methods provide similar information, the data are not comparable and are not combined.

#### **Residual Solvent Analysis**

GPC analyses were performed on an IBM Model LC-9533 high-pressure liquid chromatograph (HPLC). A 100- $\mu$ L sample of 5-mass percent asphalt in tetrahydrofuran (THF) was injected into the carrier solvent, THF, flowing at 1 mL/min through two Polymer Laboratories (PL) columns containing PL gel of

50 nm (500 $\text{\AA}$ ) (Column 1) and 5 nm (50 $\text{\AA}$ ) (Column 2) pore sizes. The details of operation are described by Donaldson et al. (15). Solvent detection by GPC requires that the column be able to handle high sample loadings (about 5 mg of asphalt) and have a small pore size (5 nm, 50 $\text{\AA}$ ). This is because of problems with peak interference from dissolved water and nitrogen. All extracted asphalts were analyzed by GPC to ensure that solvent was completely removed.

#### **Samples**

To properly test the extraction methods, it was necessary to obtain a variety of road pavements containing hard asphalt. This is preferable to generating laboratory cores that do not have enough strongly adsorbed material to properly challenge the methods. Unfortunately, there were no large, uniform quantities of road-aged material of known origin available. Nevertheless, the following samples were obtained:

1. About 23 kg (50 lbm) of pavement found in a pile near the intersection of Texas Highway 21 and US-77 (Tex 21/77) near Giddings, Texas. The pavement had limestone aggregate and asphalt having a 60°C vacuum capillary viscosity of about 2.5 kPa·s (25 kPoise).
2. About 45 kg (100 lbm) of pavement from a pile being readied for recycling at Young Brothers Construction in Bryan, Texas. The aggregate was river gravel but the asphalt's viscosity was about 90 kPa·s (900 kPoise) at 60°C using the CSL.
3. Two hot mixes used in the round robin tests of the SHRP method. The aggregates were limestone and the asphalts were Exxon AC-20 and a polymer modified Coastal AC-10.

Several rolling thin-film oven (RTFO)-aged asphalts were also studied for their susceptibility to solvent aging under various recovery conditions. These asphalts were SHRP-AAK1, -AAD1, -AAF1, Exxon AC-20, and Coastal AC-20.

## **RESULTS AND DISCUSSION**

It is important to recognize that one serious obstacle dictates the way experiments for evaluating extraction methods are designed. This is the fact that one of the goals is to develop a method that does not alter the asphalts' properties. However, there is no way to know the properties of a pavement asphalt before extraction because these properties change when it is mixed with aggregate. Consequently, simulations with tank asphalts under extraction or recovery conditions are often performed. Comparisons of asphalt properties after extraction from pavements subjected to different conditions are also good ways to measure effects of these conditions. However, since the "correct" result is never known, intuitive knowledge of which condition is least damaging is required before a proper analysis can be made.

#### **Optimum Recovery Scheme**

Before evaluating the extraction procedure, it was first necessary to determine how much solvent hardening should be

expected in the recovery step. An earlier study indicated that tank asphalts, when dissolved and immediately recovered, hardened from 10 to 40 percent (10). In those tests, the asphalts were mixed to 7 percent by mass in toluene with 15 percent ethanol and recovered in a rotary evaporator.

It was suspected that some of the hardening might be caused by loss of asphalt volatiles during the final recovery step. All pavement samples, though, have been through a hot-mix process that is likely to drive off most volatile material. To get asphalts that had not been solvent aged and lacked volatiles, several tank asphalts were aged in the RTFO according to ASTM D-2872. These imitation pavement asphalts could be used in simulations to measure recovery solvent aging.

Three recovery schemes were proposed for the SHRP method. The first was the single flask method in which the extracts are transferred to the recovery flask immediately after filtration and the solvent is removed. Any asphalt extracted before a given wash is exposed to conditions of the recovery of that wash. Because about 90 percent of the asphalt is extracted in the first three washes, most of the asphalt spends a great deal of time in the recovery flask at elevated temperature exposed to some solvent. The two-flask method solves this problem by having the first recovery flask removed after the third wash is recovered and replaced by a new recovery flask. The batch method is essentially the recovery method suggested by ASTM's proposed Roto-vap procedure (12), but applied to the new extraction process. The extracts are stored in a container until all washes are performed. Then the entire quantity of extract is recovered in the rotary evaporator.

To simulate hardening in the two-flask method, 54 g of RTFO-aged tank asphalt were mixed with 450 mL of toluene in the recovery flask. The toluene was distilled at 100°C and 12 kPa absolute. Two more 450 mL aliquots of toluene were added and distilled before the flask was removed and set aside at room temperature. Another flask containing 6 g of the asphalt was attached to the rotary evaporator. Four 450 mL aliquots of toluene with 15 percent ethanol were added and distilled. The asphalts from both flasks were dissolved in toluene with ethanol and the solvent was completely distilled. The viscosity of the asphalt after the simulation was divided by the viscosity of the RTFO-aged asphalt to give a hardening index. The single-flask simulation used the same sequence of asphalt and solvent additions but there was no replacement of the recovery flask with a second one.

The batch method was simulated by adding asphalt to 450 mL toluene aliquots over 30-min intervals and storing them in one 4-L bottle at room temperature. The first aliquot is mixed with 45 g of asphalt, the second with 9 g, and the third with 6 g. Five 500-mL aliquots of toluene with 15 percent (vol/vol) ethanol are added to the bottle in the next 150 min. The solution is then removed using the rotary evaporator.

Hardening indexes for five asphalts subjected to each of the recovery simulations are shown in Table 1. The batch method appears to be the most severe. The two-flask method gave the lowest hardening indexes for all asphalts except for Coastal AC-20. However, several of the asphalts are not susceptible to solvent aging, so method differences, if they exist, are within viscosity measurement error. As expected, SHRP-AAK1 and -AAD1 were quite susceptible to solvent aging. They are both highly sensitive to oven aging and solvent aging (10). Viscosity ratios less than, but near 1, represent viscometer errors rather than solvent "softening" of asphalt.

Differences between the two-flask and single-flask methods are slight. However, it makes sense that the two-flask method is less severe and the data indicate this. The two-flask method is no more time consuming than the single flask method. Therefore, the two-flask method was chosen as the recovery scheme for the SHRP method.

#### Precision of the SHRP Method

Once a suitable recovery scheme was established, repeatability tests of the SHRP method were performed to obtain precision estimates. Several different pavement samples were extracted. The 60°C viscosities for the extracted asphalts from each pavement are shown in Table 2. GPC chromatograms taken on each of the samples showed that there was no solvent contamination.

In order to combine data from materials of differing viscosities, a normally distributed variable, percent difference (Table 2), was made that represents the percent deviation of the viscosity of the sample from the mean viscosity of that particular material. For example, the average viscosity for Tex 21/77 is 2.57 kPa·s (25,700 poise) and the value of the first trial of that pavement is 2.505 kPa·s (25,050 poise). The

TABLE 1 Comparison of tendencies of different recovery methods to solvent age asphalts

Sample	Method		
	Two Flask	Single Flask	Batch
SHRP-AAK1 (Trial 1)	1.08	1.20	1.30
SHRP-AAK1 (Trial 2)	1.11	1.13	1.13
SHRP-AAF1	.96	1.08	1.07
SHRP-AAD1	1.08	1.15	1.10
Exxon AC-20	.98	.98	1.07
Coastal AC-20	1.02	.99	1.07
Method Average	1.04	1.09	1.12

NOTE: Numbers shown are viscosity ratios.

**TABLE 2 Reproducibility of SHRP extraction and recovery method (toluene, toluene/ethanol)**

Sample	60°C Viscosity After Extraction (kPa·s)	%Difference
SHRP #1	0.9903	4.27
	0.9092	-4.27
SHRP #2	0.4780	-10.90
	0.5945	10.80
	0.5370	0.10
Tex 21/77	2.505	-2.53
	2.621	1.98
	2.358	-8.25
	2.765	7.59
	2.599	1.13
Young Brothers	95	-4.40
	90	-1.10
	88	-3.30

Coefficient of Variance (C.V.) = 6.1%

Upper 90% Confidence Limit on C.V. = 9.2%

Lower 90% Confidence Limit on C.V. = 4.6%

percent difference for that trial is then

$$\text{Percent difference} = (2.505 - 2.570)/2.570 \times 100 \text{ percent}$$

$$= -2.53 \text{ percent} \quad (1)$$

The percent differences give information about how precise the method is regardless of the sample, as long as there are multiple measurements on that sample. The standard deviation of the percent difference values is an estimate of the coefficient of variance (CV), which is reported in the AASHTO proficiency tests. The estimate of CV for these data is 6.1 percent and there is a 90 percent chance that the true CV lies between 4.6 percent and 9.2 percent. Typical values for CV in recent AASHTO proficiency tests are between 25 and 42 percent. This means that, within our laboratory, the precision in the SHRP method associated with one standard deviation is about 6 percent whereas it is at least 25 percent for several laboratories using the current assortment of extraction and recovery methods. Of course, additional tests, such as the AASHTO proficiency tests, will be required to assess the interlaboratory CV.

### Comparison of Extraction Methods

Replicate extractions and recoveries of Tex 21/77 and Young Brothers pavements were performed using the SHRP method, Modified Method A, and Modified Method B. The extractions exactly followed the procedures discussed previously. Toluene was the solvent for the Method B extractions of the Young Brothers pavement and toluene/15 percent EtOH was used to extract the Tex 21/77 samples. Viscosities of the extracted asphalts are listed in Table 3. Aggregates from several of the extractions were collected and soaked in 400 mL of TCE/15 percent EtOH. After four days, the solvent was filtered from the aggregate samples. The asphalt concentrations in the fil-

trates were measured by evaporation. The amount of strongly adsorbed material recovered from each extracted aggregate was determined and the percentage of the total asphalt that this material represents is shown in Table 3. The asphalt content of the Tex 21/77 pavement was found to be 8.3 percent and that for the Young Brothers pavement was 5.1 percent. The viscosities of the recovered asphalt and the total volume of solvent that contacted the aggregate (for the SHRP and Modified Method A tests) are also shown in Table 3. The viscosities are compared in Figures 3 and 4.

The results show that the SHRP method and Modified Method A yield similar average viscosities and have comparable precision. However, the Method B (using TCE) and Modified Method B (using toluene or toluene/ethanol) extractions result in lower viscosities in all cases and generally are less reproducible. This is despite solvent aging, which is more severe in reflux methods and has only hardened asphalts in previous tests. The amount of strongly adsorbed material left on the aggregate after extraction seems to depend heavily on the asphalt-aggregate system. The Tex 21/77 mixture contained limestone aggregate, which is more absorptive than the river gravel aggregate found in the Young Brothers pavement. The amount of strongly adsorbed asphalt varied significantly between methods on the more absorptive Tex 21/77 mixture but was relatively constant on the Young Brothers samples. This suggests that good solvent-aggregate contacting is only important when extracting from absorptive aggregates. The Tex 21/77 samples extracted by Modified Method B yielded very low viscosity asphalts and left large amounts of unextracted material on the aggregate. Modified Method B probably has poor extraction efficiency because the ethanol in the toluene/15 percent EtOH mixture concentrated itself in the vapor phase of the reflux extraction. This caused the condensate, which actually contacts the pavement, to have a higher than optimal ethanol concentration. It is possible that the unextracted material has a very high viscosity. Then its ab-

**TABLE 3 Comparison of extraction methods**

Sample	Method	Viscosity - 60°C (kPa·s)	Unextracted Asphalt (% of Total)	Total Solvent Used (mL)
Tex 21/77	SHRP: Toluene, Toluene/ETOH	2.51 2.62 2.36 2.77 2.60  Average	1.4 1.0 1.0 0.6 -  2.57	2575 3915 2910 3800 3100  3260
	Modified Method A: Toluene, Toluene/ETOH	2.83 3.03 2.71  Average	5.2 3.8 -  2.86	3085 2985 3230  3100
	Modified Method B: Toluene/ETOH	0.541 0.655 1.335  Average	11.4 11.7 -  0.844	N/A N/A N/A  N/A
Young Bros. Pavement	SHRP: Toluene, Toluene/ETOH	95.0 90.3 88.2  Average	1.66 1.34 1.26  1.42	3000 3000 3000  3000
	SHRP: TCE, TCE/ETOH	95.4 115.0 114.0  Average	1.48 1.21 1.37  1.35	3000 3000 3000  3000
	Modified Method A: Toluene, Toluene/ETOH	93.7 90.6 91.8  Average	1.60 2.04 2.00  1.88	3000 3000 3000  3000
	Modified Method B: Toluene	65.6 62.2  Average	1.37 1.16  1.27	N/A N/A  N/A
	Method B: TCE	67.4 80.4  Average	1.75 1.80  1.78	N/A N/A  N/A

- indicates data not determined

sence would result in low viscosities for the extracted asphalt. However, information presented in the next paragraphs shows that this is probably not an adequate explanation.

There were still differences in viscosities of asphalts extracted using different methods or solvents for the Young Brothers material, even though the amount of asphalt extracted seemed to be constant. The Method *B* and Modified Method *B* extractions of this mixture used TCE or toluene, with no ethanol, and thus no ethanol-rich solvent contacted the aggregate. This, in combination with Young Brother's aggregate being less absorptive, resulted in strongly adsorbed asphalt levels that were comparable with other methods. However, the extracted asphalts had very low viscosities, just as in the Tex 21/77 samples. This indicates that strongly ad-

sorbed material may not be responsible for the low viscosities. Extracted asphalt viscosities varied directly with the power of the contacting solvent, increasing from toluene to toluene/15 percent EtOH to TCE/15 percent EtOH. It appears that, in general, the more rigorous solvent and contacting conditions yield higher viscosity asphalts. The one exception is that Modified Method *A*-extracted Tex 21/77 asphalt has a 10 percent higher viscosity than the SHRP-extracted sample. Possibly, this asphalt is more susceptible to solvent aging and recovery by the batch method would make it slightly harder than the SHRP method's two-flask recovery. Nonetheless, our strongly adsorbed asphalt data do not adequately explain the differences in asphalt viscosities, especially the low viscosities in the Method *B* samples.

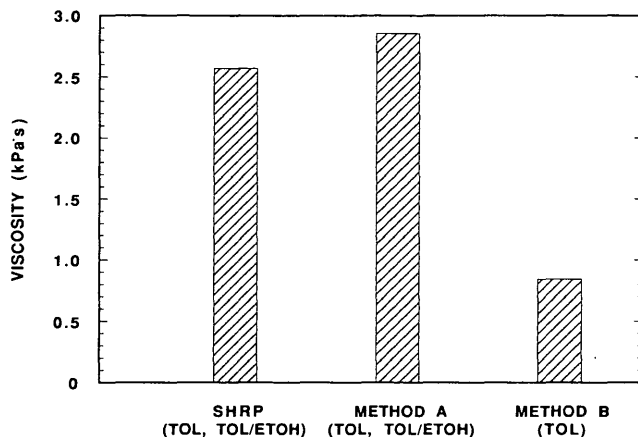


**FIGURE 3** Average viscosities of asphalt binder extracted from Tex 21/77 samples using various extraction methods.

#### Extraction Efficiency of the Methods

Several questions remain concerning the strongly adsorbed material and its effect on the bulk asphalt. It is likely that no practical method will ever remove all of the strongly adsorbed components. Thus it is important to know how many washes are required to attain a certain level of extraction and how much bulk properties might change if the unextracted material were present.

The volume and asphalt concentration in each wash was measured for four SHRP extractions and two Modified Method A extractions of Tex 21/77. The solvents lose their ability to extract additional asphalt as the extraction proceeds (see Figure 5). The first wash always removes a high percentage of the total asphalt, but the extractability drops quickly. The last washes are only extracting small amounts of the total asphalt that was originally on the sample. This indicates that the solvent is not close to being saturated. However, it is still not clear if the strongly adsorbed material has difficulty diffusing

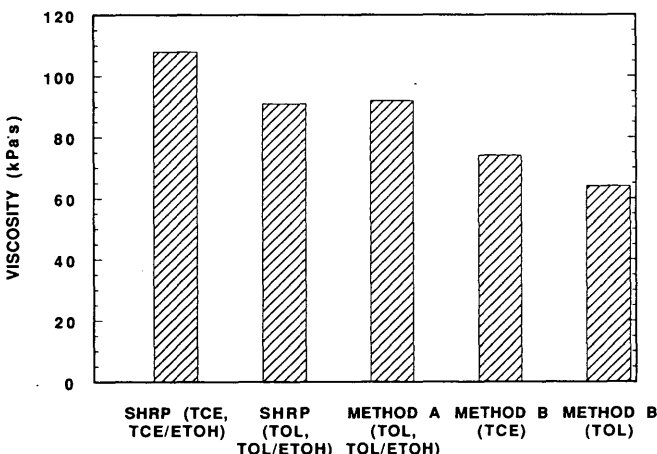


**FIGURE 4** Average viscosities of asphalt binder extracted from Young Brothers samples using various extraction methods.

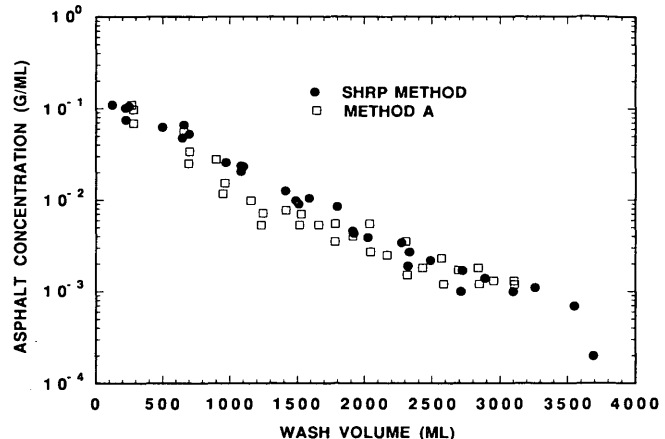


**FIGURE 5** Concentration of asphalt in extraction filtrate as a function of cumulative wash volume for SHRP and Modified Method A procedures.

through the aggregate pore structure, or if an adsorption-desorption equilibrium is limiting the amount of asphalt that is extracted. The two methods seem comparable in their asphalt-removal patterns even though, at around 3000 mL, the SHRP Method has removed all but 1 percent of the asphalt and Modified Method A has left about 4.5 percent on the aggregate.

Several SHRP extractions of the Tex 21/77 pavement were extracted using different numbers of washes. Variation of the 60°C viscosity of the extracted asphalt as additional material is extracted is shown in Figure 6. The material extracted in the later washes does not seem to increase greatly the total viscosity of the asphalt. It was originally suspected that the material near the aggregate was very hard because of possible interactions with the aggregate during hot mixing and road aging. This may well be, but the amount of this material is so small that it cannot contribute much to the overall properties of the extracted asphalt. Further studies may involve determining whether it is necessary to achieve complete ex-

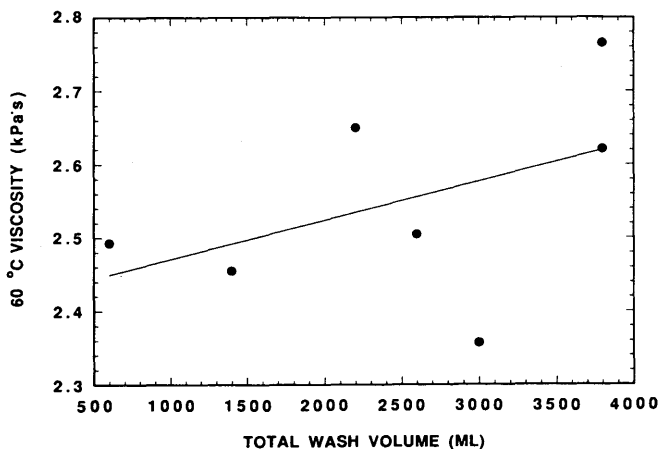


**FIGURE 6** Viscosity of the recovered asphalt binder as affected by total wash volume of solvent used in extraction process for SHRP Method (Tex 21/77 pavement).

traction if representative asphalt can be obtained in the early washes.

While working to remove the last traces of asphalt from the aggregate, it is worth considering that material that is so strongly adsorbed or associated with the aggregate may not be contributing to asphalt "binder" properties. If this material is caught in aggregate pores, or is adsorbed, it cannot be performing any of the mechanical functions of a binder. It may be important in adhesion or water-stripping phenomena, but those effects could not be measured if the strongly adsorbed material were mixed with the bulk asphalt.

## SUMMARY

An integrated asphalt extraction and recovery procedure, the SHRP method, has been developed and tested. It improves on previous methods by accomplishing complete solvent removal, limiting solvent aging, and extracting more of the strongly adsorbed material from the aggregate. Reproducibility tests indicate that the method is precise to about 7 percent for one standard deviation for a single operator. Additional tests are required to determine interlaboratory precision. Tests for solvent aging in the recovery method show that little hardening occurs during recovery for the SHRP method.

ASTM Methods *A* and *B*, modified using toluene and toluene/15 percent EtOH as solvents, were also tested for comparison. Extracted asphalt viscosities for Modified Method *A* were about 10 percent higher than those for the SHRP method on the Tex 21/77 pavement and were similar on the Young Brothers' samples. Modified Method *A* also left about 5 percent of the total asphalt on the aggregate after extraction of the Tex 21/77 samples, whereas the SHRP method removed all but the last 1 percent. The differences in the viscosities of the methods may be caused by differences in extraction efficiency, or solvent hardening in Modified Method *A* because it employs a more severe recovery scheme. However, differences between the SHRP method and Method *A*, with the modifications we have described, are negligible.

Method *B* and Modified Method *B* consistently yielded lower viscosities than the other methods and were less precise. From past experience, one might expect Method *B*-extracted asphalts to have higher viscosities because of solvent aging and lower viscosities caused by incomplete extraction of asphalt. Neither one of these phenomena adequately describes the behavior of the Method *B*-extracted samples. However, Method *B* does have an inherent problem in that it maintains the asphalt in a dissolved state for several hours at high temperature. This is likely to promote reactions that can distort properties. Also, ethanol additions to the extraction solvent in Modified Method *B* extractions are not advised because it is difficult to control the ethanol content in the reflux that contacts the aggregate.

Comparisons of viscosities of asphalts extracted using different methods showed that viscosities varied directly with solvent strength, contacting efficiency, and volume of solvent used in the extraction. The viscosities were not, however, related to the amount of strongly adsorbed material that we could recover from the aggregate after extraction.

Because the real properties of a pavement asphalt are indeterminate and a method that removes all of the asphalt from the aggregate would be impractical, the specification of proper extraction methods and operating conditions will be somewhat arbitrary. Both the SHRP and Method *A* (with modifications in procedure) equipment are suitable for such extraction methods. The adoption of the Roto-vap method using the proper recovery conditions would guarantee complete solvent removal and improve the accuracy and precision of extraction methods. Also, periodic checks of residual solvent contamination in recovered asphalts by using GPC analysis is advised.

At the moment, the SHRP and Modified Method *A* procedures will provide researchers with better asphalt samples that are free of contaminants, represent all of the asphalt in the mixture, and have properties that are nearly unaltered during extraction. Still, there are problems with the methods because they require considerable operator attention and too much laboratory space. Further work addressing these problems is needed before the methods will be appreciated by a large portion of the practitioners.

## ACKNOWLEDGMENTS

Support for this work by the Texas Department of Transportation, in cooperation with the U.S. Department of Transportation, the Federal Highway Administration, the Strategic Highway Research Program, and the Advanced Technology Program, is gratefully acknowledged. Helpful discussions with Don O'Connor and Darren Hazlett, and the technical contributions of Penny Bartnicki and Stephen Smiley are greatly appreciated.

The Carri-Med Controlled Stress (CSL) Rheometer was manufactured by Carri-Med, Ltd., Dorking, Surrey, England, and distributed in North America by Carri-Med Americas, Inc., Twinsburg, Ohio.

## REFERENCES

1. *AASHTO Materials Reference Laboratory Report for Bituminous Concrete Proficiency Samples*. Reports from 1987, 1988, 1989 tests. National Bureau of Standards, Gaithersburg, Md.
2. B. L. Burr, R. R. Davison, C. J. Glover, and J. A. Bullin. Solvent Removal from Asphalt. In *Transportation Research Record 1269*, TRB, National Research Council, Washington, D.C., 1990, pp. 1-8.
3. G. Abson. Method and Apparatus for the Recovery of Asphalt. In *Proc., ASTM II*, 1933, pp. 704-714.
4. J. H. Bateman, and C. Delp. The Recovery and Examination of the Asphalt in Asphaltic Paving Mixtures. In *Proc. ASTM II*, 1927, pp. 465-479.
5. D. C. Broome. *The Testing of Bituminous Mixtures*. 2nd ed., Edward Arnold & Co., London, England, 1949, pp. 271-301.
6. *1981 Annual Book of ASTM Standards, Part 15*. American Society for Testing and Materials, Philadelphia, Penn., 1981.
7. M. A. Plummer and C. C. Zimmerman. Asphalt Quality and Yield Predictions from Crude Oil Analyses. In *Proc. Association of Asphalt Paving Technologists*, Vol. 53, 1984, pp. 138-159.
8. P. W. Jennings. *Use of HPLC to Determine the Effects of Various Additives and Fillers on the Characteristics of Asphalts*. Report FHWA/MT/82/001, 1982, pp. 197.
9. G. Abson and C. Burton. The Use of Chlorinated Solvents in

- the Abson Recovery Method. In *Proc. Association of Asphalt Paving Technologists*, Vol. 29, 1960, pp. 246–252.
- 10. B. L. Burr, R. R. Davison, H. B. Jemison, C. J. Glover, and J. A. Bullin. Asphalt Hardening in Extraction Solvents. In *Transportation Research Record 1323*, TRB, National Research Council, Washington, D.C., 1991, pp. 70–76.
  - 11. C. A. Cipione, R. R. Davison, B. L. Burr, C. J. Glover and J. A. Bullin. Evaluation of Solvents for the Extraction of Residual Asphalt from Aggregates. In *Transportation Research Record 1323*, TRB, National Research Council, Washington, D.C., 1991, pp. 47–52.
  - 12. Standard Test Method for Recovery of Asphalt from Solution Using the Roto-vapor Apparatus. Proposed ASTM Method, Draft 2, March 21, 1988.
  - 13. H. L. Davis. Progress Report: AR Grading System Subcommittee to Investigate ASTM D 1856-75, Abson Recovery Test Method. In *Proc., Pacific Coast User-Producer Conference*, 1983.
  - 14. J. D. Ferry. *Viscoelastic Properties of Polymers*, 3rd ed., Wiley & Sons, New York, N.Y., 1980.
  - 15. G. R. Donaldson, J. A. Bullin, R. R. Davison, C. J. Glover, and M. W. Hlavinka. The Use of Toluene as a Carrier Solvent for Gel-Permeation Chromatography Analyses of Asphalt. *Journal of Liquid Chromatography*, Vol. 11, 1988, pp. 749–765.

---

The contents of the report reflect the views of the authors, who are responsible for the facts and the accuracy of the data presented herein. The contents do not necessarily reflect the official views or policies of the Federal Highway Administration, the Texas Department of Transportation, or the Strategic Highway Research Program. This report does not constitute a standard, specification, or regulation, and it is not intended for construction, bidding, or permit purposes.

# Comparing Field and Laboratory Aging of Bitumens on a Kinetic Basis

A. F. VERHASSELT AND F. S. CHOQUET

Studying accelerated bitumen aging in the laboratory on a kinetic basis leads to evaluating the activation energy of oxidation reactions from developments in certain characteristics such as asphaltene content, penetration, and ring-and-ball softening point. In Belgium, temperatures 5 mm deep in bituminous road pavements have been measured and recorded for several years, thus making it possible to draw a frequency distribution curve of those temperatures. From this distribution and the activation energy evaluated in the laboratory, it has been established that the annual value of kinetic mean temperature lies around 19.5°C for field aging. Using measurements of bitumen characteristics published in the literature, and referring to the original condition as well as the conditions at the time of opening to traffic and at various stages of aging, the reaction constants can be estimated for the road pavements under consideration. This approach enables the estimated constants to be related to the specific climatic environments of the various countries or regions concerned.

From the point of view of chemical constitution and composition, the aging of bitumens results mainly from oxidation reactions affecting certain functionalities in the more or less complex fabrics of molecules that constitute their structure.

During its life, any bitumen or other bituminous binder is subject to two types of aging:

1. A rapid aging in manufacture and laying (coating, mixing, compaction, cooling). The effects of this aging in construction are well simulated by standard aging tests such as a thin film oven test (TFOT) and a rolling thin film oven test (RTFOT) (ASTM D2872-88) or by the DIN 52016 test.

2. A slow aging in the climatic environment in service (field aging), which is composed of all the changes occurring in the bitumen during its life on site.

The laws governing the aging process still remain to be discovered. Most of the usual aging tests do not make it possible to predict field aging because they are conducted at too high a temperature and on too small a quantity of bitumen, which reduces the possibilities for technological and physico-chemical measurements on the aged sample. To accurately monitor the progress of aging with exposure time, the relevant measurements must be made on a single sample of sufficient mass (e.g., 500 to 600 g).

A laboratory aging device has been designed and tried at the Belgian Road Research Centre (BRRC). With this device, it has been possible to develop an overall kinetic approach to

aging that agrees relatively well with findings and observations with respect to actual field aging.

## BITUMEN AGING IN SERVICE

The progress of in-service aging depends on a number of factors, including

1. Susceptibility of the binder to aging (i.e., the ease or difficulty with which it can be oxidized). An oxidized bitumen will obviously be less susceptible to aging. It is being tried to assess this property from accelerated tests conducted mainly at temperatures above 100°C, the extrapolation of which to ambient temperatures is unreliable.

2. Porosity of the bituminous pavement, as characterized by the percentage of voids. A dense pavement ages almost exclusively at the surface.

3. Temperature: oxidation reactions are stimulated by an increase in exposure temperature.

4. Sun radiation: the ultraviolet component of it affects only a very thin layer of the binder at the surface of the pavement, whereas the infrared (IR) part increases the mean temperature in the pavement as they are absorbed.

5. The nature of the aggregates—a difficult factor to demonstrate.

6. Other factors such as moisture, precipitation, aggregate porosity (preferential adsorption of certain bitumen components), and deicing salts.

When considering these factors, it will be obvious that accurate simulation of field aging in the laboratory is a utopian objective. The situation can, however, be simplified by starting from the rather realistic assumption that, all other factors remaining equal, the aging process observed in the field will depend mainly on the binder's susceptibility to oxidation. Accelerated aging tests in the laboratory should, therefore, aim at evaluating the reaction constants in the asphalt concrete at service temperature, using a kinetic approach to binder aging (1).

## KINETIC DEVELOPMENT

### Some Concepts in Chemical Reaction Kinetics

Taking classical kinetic theory and the concept of extent of reaction,  $\alpha$ , as a basis, and using the one-dimensional diffusion

model (2) for solid-state reactions (exponent = 2 in following equation), it is possible to clarify the process of bitumen aging in time. The mathematics involved are explained in Verhasselt (1), Brown and Galwey (2), Verhasselt and Choquet (3), and Choquet and Verhasselt (4).

By randomly selecting a reaction indicator  $S$ , the general equation representing the development of aging can be written as follows:

$$a^2 = \left[ \frac{S_t - S_o}{S_f - S_o} \right]^2 = \left( \frac{DS_t}{DS_x} \right)^2 = kt \quad (1)$$

where

$\alpha$  = extent of reaction,

$S_o$  = value of the indicator being considered at time  $t = 0$ ,

$S_t$  = value of the indicator being considered at time  $t$ ,

$S_f$  = value of the indicator being considered at time  $t = t_{final}$ , and

$k$  = reaction or rate constant (at the test temperature).

As term  $DS_x$  is hardly accessible by experiment and represents a constant for the bitumen being considered, this equation can be transformed into two others that are markedly more practical:

$$(S_t - S_o)^2 = DS_t^2 \\ = Kt \quad (2)$$

By transformation this equation becomes

$$S_t = S_o + K^{1/2} \cdot t^{1/2} \quad (3)$$

Using these two equations, it is possible to determine the overall reaction constant,  $K$ , from experimental data as far as the tests have been conducted at an exposure temperature no higher than 100°C on an original bitumen (i.e., still virtually unaffected by oxidation) (1).

The following indicators have proved to be suitable for the kinetic study:

1. Asphaltenes' content (insoluble in hot n-heptane), A7;
2. Ring-and-ball (R&B) softening temperature; and
3. The reciprocal of penetration, 1/penetration.

The logarithms of viscosity at 60°C and 135°C could also be suitable as indicators in the suggested kinetic approach.

### Generalization of This Theoretical Approach

When a bitumen in the laboratory has already been subject to some aging before the beginning of the test, this aging corresponds with a time of reaction,  $t_o$ , at the test temperature. Likewise, in a pavement that starts its service life, the bitumen has already undergone an aging process, for example, in construction. Equation 3 can, consequently, be rewritten as follows:

$$(S_t - S_o)^2 = DS_t^2 = K(t_o + t) = Kt_o + Kt \quad (4)$$

where  $t_o$  is the actual reaction time defined as the sum of the exposure time chosen for the test or the field time of service in the road and the fictitious time,  $t_o$ .

Where  $S_o$  is known, Equation 4 can be applied directly to the experimental results and the value of  $t_o$  can be estimated from the ordinate at the origin ( $= Kt_o$ ). If, in addition, the initial value of  $S$  (i.e.,  $S_i$ ) is known, a second (generally less reliable) estimation of  $t_o$  will be possible:

$$(S_i - S_o)^2 = Kt_o \quad (5)$$

By transformation, Equation 4 becomes

$$S_t = S_o + K^{1/2} (t_o + t)^{1/2} \quad (6)$$

in which the estimated value of  $t_o$  is entered for the regression calculation.

It is also possible, by successive approximation, to find the value of  $t_o$  that leads to the best degree of correlation for Equation 6 applied to the experimental results.

In practice, however, the values of  $S_o$  and  $t_o$  are generally unknown. In such cases, processing data by means of Equation 6 often results in unrealistic estimates of  $S_o$  and/or  $t_o$ , and hence of  $K$ , because of experimental errors. This difficulty can be met to some degree by estimating  $S_o$  from information and specifications contained in standard tender specifications.

### KINETIC MEAN TEMPERATURE ON SITE

One of the important factors in the kinetic approach to aging is temperature (1). Accelerated laboratory tests make it possible to determine the overall reaction constant,  $K$ , for various indicators at several exposure temperatures and, hence, to evaluate the activation energy of the aging reactions (1,3). To transfer this approach to in-service road conditions, use must be made of the concept of kinetic mean temperature.

On site, a road pavement does not remain at constant temperature throughout the year. It is subject to variations in temperature according to the surrounding climatic conditions, the most important of which are air temperature and sun radiation. (C. De Backer, unpublished data, BRRC) and De Backer (5). As is the case for all other exposed layers on earth, temperature and its variations depend on the depth of measurement and the nature of the material (C. De Backer, unpublished data, BRRC). In Belgium, the temperature of an asphalt pavement ranges from -10 to +50°C and from -5 to +40°C at the surface (-0.5 cm) and at a depth of 4-5 cm, respectively (5).

Equal times of exposure to various temperatures will obviously contribute in different ways to the aging of the binder. For example, 24 hr at 0°C will have a markedly smaller aging effect than 24 hr at 40°C (smaller by a factor of about 16, as the rate of aging almost doubles with a 10°C increase in temperature). In fact, the exact value of this factor depends on the activation energy of the aging reactions, because it is this energy that determines the value of the (overall) reaction

constant and hence the reaction rate at the temperature under consideration.

Because of the variations in field temperature, the total in-service aging of a binder will be the sum of a series of partial aging processes, the contributions of which depend on the time of exposure to a given temperature. To be fully correct, the assessment of field aging must therefore be made by integrating these contributions on the basis of the histogram of the distribution of temperatures over the period being examined.

Another approach that is more practical and more centered on predicting binder aging in service consists of estimating the kinetic mean temperature of the pavement annually under the local climatic conditions of the region or country where the road is situated. This requires the availability of statistical data on temperatures at various depths in, but mainly at the surface of, asphalt pavements.

Some ground in this field has already been covered in Belgium (5,6):

1. Data on temperature at different depths in various asphalt pavements are available in addition to a set of meteorological data relating to air temperature, minimum and maximum temperature, amplitude of daily variation, sun radiation, and so on. They are the result of several years of measurements of BRRC and systematic measurements by the Royal Belgian Meteorological Institute (7);

2. From these measured data, a mean curve of temperature distribution (per 5°C interval) at different depths in asphalt concrete has been established, especially for temperatures at the surface (-0.5 cm), which are the most relevant to road binder aging (Figure 1, Curve 1);

3. Using the data on mean air temperature, the amplitude of variation in air temperature, and total sun radiation on a horizontal surface, it has been possible to reproduce with a good approximation the mean curve of temperature distribution at the surface of asphalt concrete (5). This predictive method can be transferred to other countries and other climates (6).

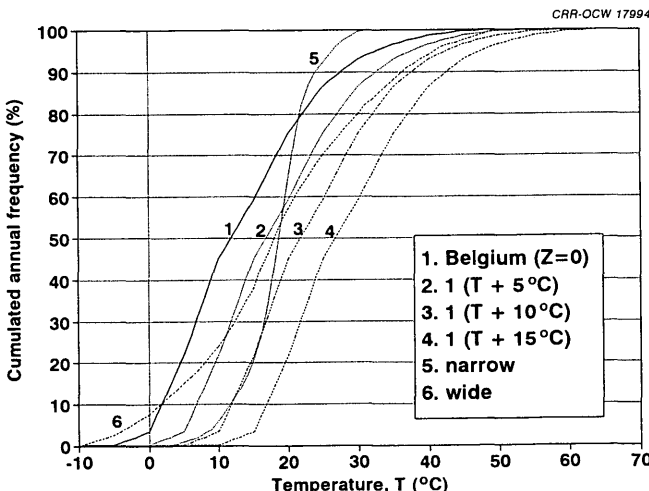


**FIGURE 1 Examples of annual distribution curves of temperature (1. relates to the surface of asphalt pavements in the Brussels region).**

To estimate the annual value of kinetic mean temperature at the surface of asphalt pavements in Belgium (more precisely in the region of Brussels), the following procedure was used:

- Starting from the mean distribution curve already described (Figure 1, Curve 1), the fraction of time per year,  $f_i$ , during which the binder is exposed to temperatures between  $T_{i-1}$  and  $T_i$  is determined. The temperature interval used being 1°C, a linear interpolation is made for each 5°C interval on the curve between the frequency values corresponding to the limits of the 5°C temperature interval being considered (Figure 1);

- The following sum is calculated:

$$SCR = \sum f_i \exp[-E/R(T_i - 0.5)]$$

where

$E$  is the activation energy of the reaction,

$R$  is the perfect gas constant, and

( $T_i - 0.5$ ) the absolute temperature corresponding to the middle of the temperature interval under consideration (in °K).

Given the activation energies found in the accelerated aging tests at temperatures below 100°C,  $E/R$  is taken to be 9,000 (1,3);

- The value of temperature  $T_k$ , which leads to the same  $SCR$  value, represents the annual kinetic mean temperature of the country or region concerned:

$$T_k(\text{°K}) = -E/R \ln(SCR)$$

or, in °C:

$$T_k(\text{°C}) = T_k(\text{°K}) - 273.2$$

By way of example, the arithmetic mean temperature and the annual value of kinetic mean temperature for the temperature distributions represented in Figure 1, assuming an  $E/R$  of 9,000, are respectively:

- 13.2 and 19.55°C (Curve 1),
- 18.2 and 24.35°C (Curve 2),
- 23.2 and 29.1°C (Curve 3),
- 28.2 and 33.95°C (Curve 4),
- 18.2 and 19.4°C (Curve 5, narrow distribution), and
- 18.2 and 26.25°C (Curve 6, wide distribution).

The kinetic mean temperature 0.5 cm deep in bituminous pavements in Belgium is thus 19.5°C.

The divergence between arithmetic mean temperature and kinetic mean temperature increases with the width of the distribution curve (curves 5, 3 and 6) and remains more or less constant when the curve has been subjected to a simple translation (curves 1 to 4).

The mean temperature at the surface (13.2°C) is higher than the annual mean air temperature in Belgium, which is about 10°C. This difference is due mainly to the absorption of sun radiation by the pavement.

## LABORATORY TESTS: EXPERIMENTAL APPROACH

### Accelerated Aging Test Device

The description and performance potential of this device are given in Verhasselt and Verhasselt and Choquet (1,3). It will be noted that a thermocouple fixed inside the cylinder measures and controls the test temperature with an accuracy of  $\pm 0.5^\circ\text{C}$ .

The load of binder per aging test is 500 g and samples of 20 to 25 g are taken at each exposure time to measure technological characteristics and determine generic composition. It is thus possible to monitor binder characteristics with age and to develop a kinetic approach to the phenomenon, as set out earlier in this paper and others (1,3).

### Bitumens Investigated and Interpretation

Three straight-run bitumens of penetration grade 80/100 were aged in the laboratory at temperatures ranging from 70 to  $100^\circ\text{C}$  (1). Their initial physicochemical characteristics are given in Table 1. From the developments in the values of

these characteristics recorded during aging, highly significant relations have been established, more particularly among

R&B and A7,  
1/penetration and A7,  
1/penetration and R&B, and  
IR absorbance at  $1700 \text{ cm}^{-1}$  and A7 or R&B.

Examples are presented and discussed by Verhasselt and Choquet (3).

Reviewed in Table 2 for the three indicators considered are the  $S_o$  values adopted and the  $K_T$  constants calculated as follows from the results obtained under normal test conditions (1 rpm under a flow of oxygen) (1):

1. Equations 2 and 3 are applied while determining the exponent that agrees best with the experimental results. Generally, exponent 2 is most suitable;

2. Using Equation 3,  $S_o$  is evaluated for the different test temperatures. The mean value of  $S_o$  is then calculated and this will be used in the subsequent calculations if it is compatible with the  $S_o$  of the bitumen before aging. If such is not the case, the  $S_o$  of the unaged bitumen is adopted;

TABLE 1 Main characteristics of the investigated bitumens

		Bitumen		
Technological and physicochemical characteristics		472	481	577
Pen 25°C, 100 g, 5sec	(mm/10)	92	89	87
R&B Temperature	(°C)	47.0	46.0	46.5
Viscosity at 135°C	(Pa.s)	0.308	0.336	-
Density	(g/cm <sup>3</sup> )	1.012	1.019	1.020
Neutralization Value (Method I.P. 213/82-BS)	(%)	0.3	3.3	-
		Bitumen		
Generic composition (% by mass)		472	481	577
Asphaltenes content (A7)		10.7	9.4	9.2
Saturates		20.8	20.2	14.4
Cyclics (nonpolar aromatics)		43.7	44.5	43.3
Resins (polar aromatics)	R1	-	15.4	21.8
	R2	-	10.3	11.4
	R1 + R2	24.9	25.7	33.2

- : missing data

TABLE 2 Initial value  $S_o$  and mean overall reaction constant  $K_T$  according to equations 2 and 3

T°C	A7 (% <sup>2</sup> .h <sup>-1</sup> )			R&B (°C <sup>2</sup> .h <sup>-1</sup> )			1/pen [10 <sup>6</sup> (10/mm) <sup>2</sup> .h <sup>-1</sup> ]		
	472	481	577	472	481	577	472	481	577
70	0.0556	0.0408	0.0524	0.380	0.327	0.291	0.823	0.894	0.681
80	0.105	0.1095	-	0.847	0.673	-	1.73	1.78	-
82.5	-	-	0.112	-	-	0.634	-	-	1.82
90	0.196	-	-	1.59	-	-	4.34	-	-
95	-	-	0.346	-	-	1.425	-	-	5.17
100	0.357	0.473	-	2.35	3.22	-	6.38	10.1	-
$S_o$ :	10.4	9.4	9.1	46.8	46	46.8	92	89	90

- : not investigated

3. The overall reaction constant,  $K$ , is calculated using Equation 2 on the one hand and Equation 3 on the other. The mean of the two constants thus calculated is taken as the  $K_T$  constant for the exposure temperature and indicator being considered;

4. The  $K_T$  constants obtained are used as real reaction constants  $k_T$  and entered in an Arrhenius equation in order to evaluate the activation energy of the reaction.

To pass from the laboratory to the field, where there is no rotation of the bitumen nor flow of oxygen, the effects of the experimental parameters have been determined when changing over from oxygen to air and when extrapolating the rotation rate to the zero value (1):

1. On average, the "gas" correction factor,  $G$  (i.e., the ratio between the reaction constants,  $K_{\text{air}}/K_{O_2}$ ) is 0.570 (with individual values ranging from 0.484, to 0.617);

2. Accelerating the rotation of the container from 1 to 5 or to 10 rpm causes the reaction constant to increase by an average factor of 1.57 (1.44 to 1.72 individually) or 2.18 (1.63 to 2.66 individually), respectively.

From this it can be concluded that the total correction factor for tests conducted under the "standard" conditions (1 rpm and oxygen flow) is 0.502.

## LABORATORY/FIELD COMPARISON

### Extrapolation to Field Conditions

In Table 3, among other things, the values of the overall reaction constants extrapolated to the field conditions pre-

vailing in the region of Brussels are given: surface of the pavement, static binder, and annual value of kinetic mean temperature 19.5°C. For the three bitumens considered, the differences in overall reaction constants may reach almost 40 percent.

Measurements of air temperature and pavement surface temperature (i.e., at a depth of 0.5 cm) carried out in the region of Brussels over a long period of time have yielded mean values of 10°C and 13.2°C, respectively. From these statistics, a kinetic mean temperature of 19.5°C can be calculated, as previously explained. A 10°C translation of Curve 1 in Figure 1 results in Curve 3, which would correspond more or less with a mean air temperature of about 20°C and a kinetic mean temperature of 29.1°C.

It is shown in Table 3 how the values of the overall reaction constants for the three selected indicators are affected by an increase in kinetic mean temperature from 19.5°C to 29.1°C. The  $K_T$  values are almost tripled. The value of 29.1°C for kinetic mean temperature would roughly correspond to the situation in states and provinces such as Ontario, Pennsylvania, and Texas.

In Table 4, mean air temperatures are associated with kinetic mean temperatures. The latter are presumed values as they have been calculated from data on mean air temperature in the state or region being considered and the existing relation between this temperature and the period of sunshine (generally these two parameters increase concurrently, thus causing the temperature in the road to rise).

In Figure 2 are simulated the developments in R&B temperature that would be observed on site with two Belgian bitumens (472 and 577) if they were exposed to exactly the same conditions of aging (also in construction). The difference in development is clearly visible. For example, an R&B temperature of 65°C would be reached in 10 or 26 years for

TABLE 3 Overall reaction constant on site at two kinetic mean temperatures for three Belgian penetration 80/100 bitumens (laboratory-to-field extrapolation)

K on site		
	$T_k = 19.5^\circ\text{C}$ (Brussels)	$T_k = 29.1^\circ\text{C}^*$
A7 ( $\%^2 \cdot \text{h}^{-1}$ )	1.7 to $2.7 \times 10^{-4}$	4.9 to $7.1 \times 10^{-4}$
R&B ( $^\circ\text{C}^2 \cdot \text{h}^{-1}$ )	1.2 to $2.1 \times 10^{-3}$	3.3 to $5.4 \times 10^{-3}$
1/pen [ $(10/\text{mm})^2 \cdot \text{h}^{-1}$ ]	3.2 to $4.7 \times 10^{-9}$	9 to $12 \times 10^{-9}$

\* This would roughly correspond with the situation in Ontario, Pennsylvania and Texas.

TABLE 4 Annual values of mean air temperature and kinetic mean temperature

State or region	Annual mean air temperature ( $^\circ\text{C}$ )	Annual kinetic mean temperature* ( $^\circ\text{C}$ )
Brussels	10	19.5
Alberta	0	(≤ 10)
Saskatchewan	3	(≤ 13)
Iowa	10.1 - 10.4	(≈ 20)
Delaware	13	(≥ 22)
Ontario	18	(> 27)
Pennsylvania	18	(> 27)
Texas	(13) 17 - 23	(> 29)
Arizona	20.5 - 21.4	(> 30)

\* ( ) = presumed value (see text).

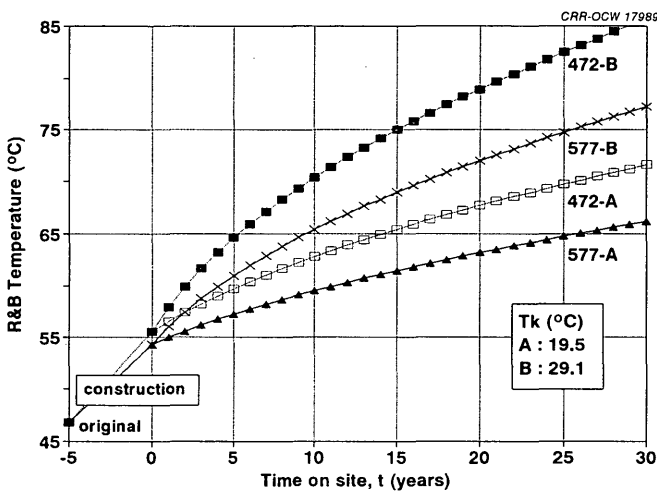


**FIGURE 2** Comparison of simulated field aging of bitumens 472 and 577 for a kinetic mean temperature of 19.5°C (Brussels) and 29.1°C (probably applying to Ontario, Pennsylvania, and Texas).

Bitumen 577 and in 5 or 14 years for Bitumen 472, according to whether the kinetic mean temperature is 19.5°C or 29.1°C. This means that with the latter temperature the rate of aging is 2.6 to 2.8 times higher.

By assuming a linear relationship between the annual values of kinetic mean temperature and mean air temperature, it is possible to evaluate annual kinetic mean temperature in different states and regions. The results are discussed further in this paper. The > or < signs in Table 4 indicate the trend to be expected on account of the greater or smaller amount of sun radiation in those regions. The case of 29.1°C (B), considered in Figure 3, could represent the situation in states or provinces such as Ontario, Pennsylvania, and Texas.

The long-term in-service behavior of different bitumens thus seems to be predictable, at least in a relative way, from kinetic data yielded by accelerated tests in the laboratory. The important parameters are the overall reaction constant

at various temperatures (between 70 and approximately 95°C) and the activation energy of the reactions.

### Comparison of Different Results Reported in the Literature

Two different ways to proceed may be adopted:

1. Confront the overall reaction constants estimated for the binder on site with the laboratory test results;
2. With due consideration of age in service, compare the variations in characteristics with those that can be estimated from the laboratory test results.

Ideally, the following data should be known on an in-service aged binder:

- $S_t$ : the value at time  $t$  of characteristic  $S$  of the binder recovered from the top slice (approximately 0.5 cm) of the pavement. The more there are different  $t$  values, the better;
- $S_i$ : the value of  $S$  at the beginning of in-service aging. This value is known if samples were taken during or the day after laying. If not, the value of  $S$  in the bulk of core samples (excluding the top slice) is a very good approximation of  $S_i$  in the case of a well-compacted dense mix (less than about 3 percent of voids); and
- $S_o$ : the  $S$  value of the original bitumen. If it is unknown, an estimation of R&B temperature and penetration can be made from the tender specifications for the binder.

### Comparison of Different Overall Reaction Constants $K_T$

From data found in the literature it is possible to evaluate the overall field reaction constant as previously described for the different indicators, and to compare it with laboratory test results. Examples of this are given in Figures 3, 4, and 5 for A7 content, R&B temperature, and 1/penetration, respec-

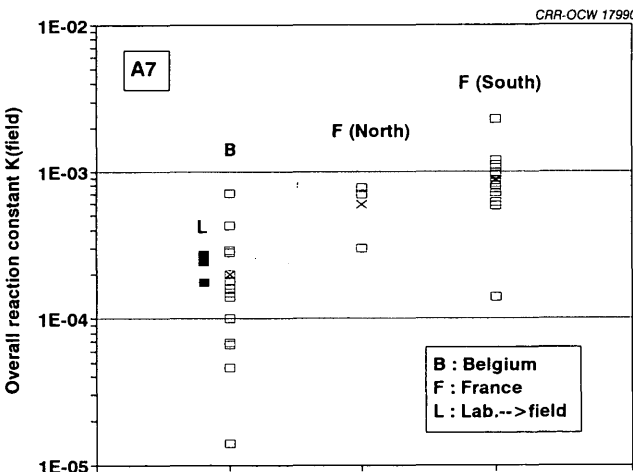


**FIGURE 3** Laboratory/field comparison for the overall reaction constant relating to development of asphaltenes content ( $x = \text{mean } K_T \text{ value}$ ).

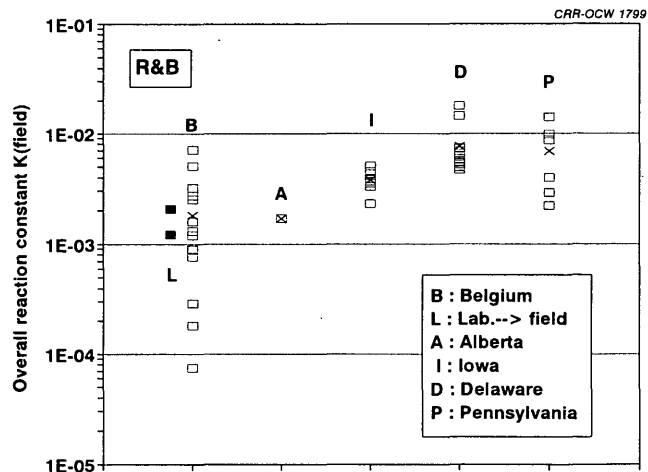


**FIGURE 4** Laboratory-field comparison for the overall reaction constant relating to development of R&B softening temperatures ( $x = \text{mean } K_T \text{ value}$ ).

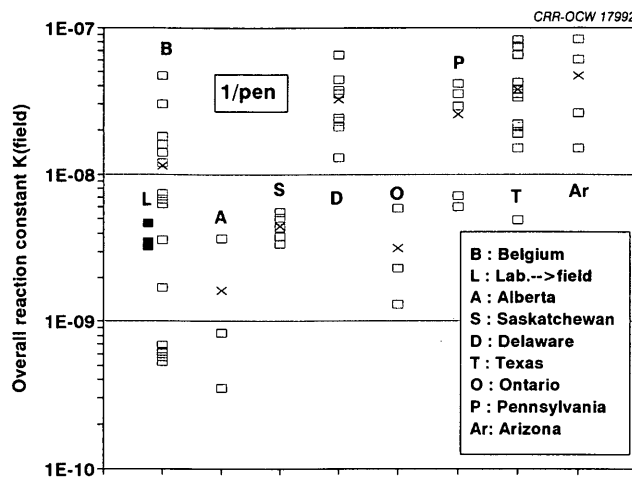


**FIGURE 5** Laboratory-field comparison for the overall reaction constant relating to development of penetration ( $x =$  mean  $K_T$  value).

tively. The processing of results, based on data, is presented for the different states, provinces, and regions as follows (8–11):

State, Province, or Region	A7 (%)	R & B (°C)	Penetration (1/10 mm)
Alberta (8)	—	A.52	A.52
Arizona (8)	—	—	B.13
Belgium (10,11)	(10,11)	(10,11)	(10,11)
Delaware (8)	—	A.36, 38	A.36, 38
France N (9)	(9)	—	—
France S (8)	A.14	—	—
Iowa (8)	—	A.34	—
Ontario (8)	—	—	A.48
Pennsylvania (8)	—	A.4a, 4b, 8	A.4a, 4b, 8
Saskatchewan (8)	—	—	A.26
Texas (8)	—	—	B.27

From these data it has been possible to calculate the overall reaction constant,  $K_T$ . Figure 3 represents the development of this constant for Belgium and the north and south of France, using A7 content as an indicator. The values of the overall reaction constant,  $K_T$ , for Belgium and various American and

Canadian States, respectively, based on R&B and the reciprocal of penetration, are given in Figures 4 and 5.

It can be seen in these three figures that the  $K_T$  values are different from one state, province, or region to another and that the shift to higher  $K_T$  values follows the trend of mean air temperature and sunshine in the different states, provinces, or regions, as mentioned in Table 4.

The calculated overall reaction constants,  $K_T$  is reviewed in Table 5 as follows:

1.  $K_T$  field: these are constants calculated from indicator values found in the literature for the bitumens used.

2.  $K_T$  extrapolated: from the  $K_T$  values calculated for three laboratory-aged Belgian 80/100 grade bitumens extrapolated  $K_T$  values have been calculated for the climatic conditions in the states, provinces, or regions considered, using the relevant presumed kinetic mean temperatures mentioned in Table 4.

Figure 6 represents mean overall reaction constants against the mean air temperatures in the states, provinces, or regions concerned, with 1/pen as an indicator.

#### Comments

The overall reaction constants  $K_T$  given in Table 5 and plotted on Figure 6 may be noted as follows:

1. Except for the state of Ontario, the values of the constants calculated for field aging and by extrapolation are more or less in agreement for the three indicators when these are available;

2. The value of  $K_T$  increases with mean air temperature and with kinetic temperature;

3. The  $K_T$  values for Ontario and Delaware apart, there is a good correlation between the logarithm of  $K_T$  (mean and field) and mean air temperature. The examples of Ontario (18°C) and Delaware (13°C) show that it is indeed the temperature of the pavement that should be considered. The results for Ontario actually concern the northern part (7);

4. Great differences can nevertheless be observed in the  $K_T$  values of a given state, province, or region. They suggest that the bitumen can play a major role by its properties and

**TABLE 5** Overall field reaction constants (different results from the literature)

State or region	T air (°C)	A7 ( $10^4 \cdot \% \cdot h^{-1}$ )		R&B ( $10^{-3} \cdot ^\circ C^2 \cdot h^{-1}$ )		1/pen [ $10^{-9} \cdot (10/mm)^2 \cdot h^{-1}$ ]	
		extrapol.	field	extrapol.	field	extrapol.	field
Alberta	0	-	-	$\leq 0.4$ -0.7	1.7	$\leq 1.1$ -1.7	0.35-3.7
Saskatchewan	3	-	-	-	-	$\leq 1.5$ -2.3	3.4-5.6
Belgium	10	1.7-2.7	0.14-7.1	1.2-2.1	0.07-7.1	3.2-4.7	0.53-30
Iowa	10.3	-	-	1.3-2.2	2.3-5.1	-	-
France (North)	(12)	2.2-3.2	3-8	-	-	-	-
Delaware	13	-	-	$\geq 1.6$ -2.7	4.7-18	$\geq 4.3$ -6.1	13-65
France (South)	(15)	3.4-5.4	1.4-23	-	-	-	-
Ontario	18	-	-	-	-	$> 7.5$ -10	1.3-5.9
Pennsylvania	18	-	-	$> 2.7$ -4.4	2.2-14	$> 7.5$ -10	6-41
Texas	17-23	-	-	-	-	$> 9.2$ -12	4.9-83
Arizona	21	-	-	-	-	$> 10$ -14	15-84

- : no results available

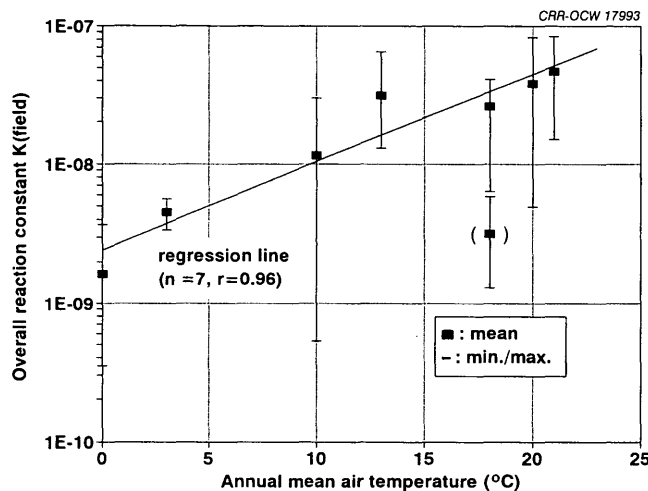


**FIGURE 6** Mean overall reaction constant relating to the development of penetration versus annual mean air temperature of the considered region.

characteristics and that it may behave differently, perhaps also as a result of widely varying susceptibility of aging.

#### Comparison of Simulated Indicator Development with Field Results

The second way to proceed is to monitor the development of indicators in service and to compare this with the field development calculated from laboratory-aged bitumens. In Figure 7 the increase of R&B temperature is plotted against the age of the asphalt pavement. The field development calculated for Bitumens 472 and 577 in the region of Brussels is represented by two dotted lines.

In both cases, a good agreement is found between aging observed on site and aging estimated from the accelerated laboratory tests on three 80/100-grade bitumens. As for the

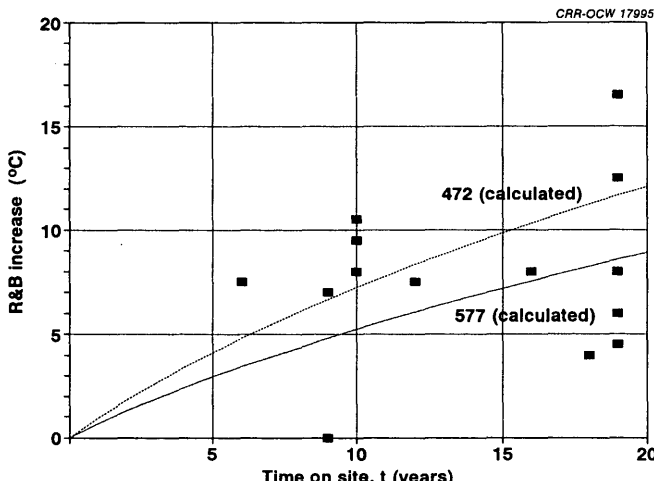


**FIGURE 7** Increase in R&B temperature with the years of service of the pavement (Belgium). Comparison with calculated development for Bitumens 472 and 577.

overall reaction constants (Figure 3), their values increase in ascending order in Belgium, the north of France and south of France. Such is also the case of mean air temperature and, consequently, kinetic mean temperature.

## CONCLUSIONS

1. Any binder for bituminous road pavements is subject to two types of aging during its life: rapid aging in construction and slow aging in service. The standard tests (RTFOT and DIN 52016) simulate in-construction aging adequately.

2. On the other hand, laboratory tests must be conducted at a temperature below 100°C to simulate the in-service aging of a bituminous binder; at higher temperatures the reaction mechanism is different from that which occurs on site.

3. The equipment developed at BRRC and the range of temperatures adopted (70 to maximum 95°C) seem appropriate for accelerated simulations of the field aging of bituminous binders.

4. The kinetic approach developed from the extent of reaction concept and involving technological characteristics of the bitumen as reaction indicators has proved feasible both in interpreting laboratory tests and in assessing field behavior. Below 100°C the kinetic model of diffusion most accurately fits the set of results obtained.

5. The characteristics used as indicators in the kinetic study are asphaltenes content, R&B-softening temperature and the reciprocal of penetration.

6. To pass on from laboratory data to field behavior, it is necessary to consider an annual value of kinetic mean temperature. This temperature can be evaluated:

- On the one hand, from the activation energy of the reactions investigated;

- On the other, from statical data on the distribution of temperatures at the surface of road structures. This distribution can be estimated from climatic data (air temperature, amplitude of daily variation, sun radiation, etc.) in the region concerned.

7. When overall reaction constants calculated from the results obtained on sites in regions with different climates are compared with those extrapolated from the results of accelerated laboratory aging tests and from the relevant presumed kinetic mean temperatures (which depend on mean air temperature and on sun radiation), the proposed kinetic approach is found to be valid for assessing the aging of bituminous binders in service.

8. The kinetic approach enables estimated constants for in-service aging to be related to the specific climate environment of the various countries or regions concerned.

## REFERENCES

1. A. F. Verhasselt. A Kinetic Approach of the Aging of Bitumens. *Asphaltenes and Asphalts*, Vol. II, T. F. Yen and G. V. Chillingarian, eds. Development in Petroleum Science Series, to be published by Elsevier Science Publishers, The Netherlands, 1993/94.

2. M. E. Brown and A. Galwey. Arrhenius Parameters for Solid-State Reactions from Isothermal Rate-Time Curves. *Analytical Chemistry*, No. 61, pp. 1136–1139, 1989.
3. A. F. Verhasselt and F. S. Choquet. A New Approach to Studying the Kinetics of Bitumen Aging. In *Proc., International Symposium on Chemistry of Bitumens*, Vol. II, Rome, 1991, pp. 686–705.
4. F. S. Choquet and A. F. Verhasselt. Natural and Accelerated Aging of Bitumens—Effects on the Asphaltenes. In *Symposium, Asphaltene Particles in Fossil Fuel Exploration, Recovery, Refining, and Production Processes*. Las Vegas, July 13–17, 1992.
5. C. De Backer. *Les températures dans les structures routières*. La Technique Routière, XXV/2, Brussels, 1980, pp. 1–29.
6. V. Veverka and C. De Backer. Aspects techniques du renforcement des chaussées. Ve Conférence routière africaine de l'IRF, *Formation technique et recherche*, Libreville, Gabon, 1983, pp. 151–160.
7. Institut Royal Météorologique de Belgique. *Bulletin mensuel, Observations climatologiques*, Bruxelles.
8. *Summary Report on Asphalt Properties and Relationship to Pavement Performance (SHRP Task 1.4)*, Strategic Highway Research Program, ARE Inc., Scotts Valley, Calif., May 1990.
9. F. Farcas and C. Such. Influence de la structure chimique des bitumes sur leur comportement rhéologique. Description des méthodes analytiques utilisées. *Journée d'études AFREM—Les Bitumes*, pp. 29–55, Saint-Rémy-lès-Chevreuse, 1991.
10. F. Choquet. The Development of Bituminous Binders in Pavements in Service. In *4th Eurobitume Symposium*, Vol. I, Summaries and Papers, Madrid, Spain, 1989, pp. 30–34.
11. F. S. Choquet. The Search for an Aging Test Based on Changes in the Generic Composition of Bitumens. In *Proc., International Symposium on Chemistry of Bitumens*, Vol. II, Rome, 1991, pp. 787–812.

# Some Aspects of the Effect of Asphalt Chemical Composition on Material Behavior and Pavement Performance

ILAN ISHAI, YAW A. TUFFOUR, AND JOSEPH CRAUS

The purpose of this paper is to look at some aspects of the effect of asphalt chemical composition on the properties and behavior of some fresh asphalt binders, as well as of plant-aged and field-aged samples, and the manner in which long-term aging may be affected by changes in material composition. The asphaltic binders involved are of the straight-run and propane-precipitated asphalt blend types, all of the 60/70 penetration grade. At this stage, data accumulated reflect construction conditions and the beginning of the service life of the test sections. No pavement distress has been reported so far that would warrant linkage to the type and characteristics of the asphalt binder used. However, definite relationships were found among the chemical composition of the asphalt and its physicorheological changes during short- and long-term aging. These relationships were also significant enough to distinguish among the behavior of straight-run asphalts and PPA asphalt blends. As more data become available with time, it is hoped that a more definite relationship can be established among the physicochemical properties of the asphalt and their effect on material behavior and longer-term pavement performance.

Asphalt cements have characteristics and properties significantly determined by the nature of their chemical composition. In general, the chemical character of an asphalt binder is derived from that of the parent crude, although process conditions during production from distillation of the crude may affect the chemistry of the material. Changes in chemical composition, which lead to changes in properties and behavior, may also occur during plant production of asphaltic mixtures, in which heating in the presence of air may cause a substantial level of oxidation of the asphalt binder, or during field service of the asphaltic pavement.

In spite of the link between asphalt chemistry and its behavior, the material is selected for application purposes on the basis of some standard physical rather than chemical tests. In some cases, such standard tests may even fail to differentiate one asphalt type from another, giving the impression of the existence of similarities in products and properties, although in effect, the asphalt materials could be quite different in their chemical composition and in the way they behave and age on production, application and service (1).

Examined in this paper are some aspects of the effect of asphalt chemical composition on the properties and behavior of some fresh asphalt binders, as well as of plant-aged and field-aged samples, and the manner in which long-term aging

may be affected by changes in material composition. The asphaltic binders involved are of the straight-run and propane-precipitated asphalt (PPA) blend types, all of the 60/70 penetration grade.

## ASPHALT CHEMISTRY BACKGROUND

The chemistry of asphalts is not as well defined as those of relatively simple chemical materials and compounds. The link between asphalt chemistry and its behavior has been established directly or indirectly through controlled chemical processes, by which asphalts may be made to acquire some required characteristics (2-4), and also through studies modeling aging and changes in asphalt properties by diffusion-controlled oxidation reactions in the material (5,6).

Because of lack of precise knowledge of asphalt chemistry, most methods for analyzing asphalts chemically are based on separating the material into broad chemical groups with distinct characteristics. Other methods break the various groups into further subgroups in order to improve understanding of the behavior of the material. Considering the complexity of asphalts, however, it is to some extent still doubtful whether the behavior of subgroups can confidently be said to relate to the global behavior of the material. Despite this shortcoming, the present level of knowledge of asphalt chemistry is being used in several ways, such as in supercritical extraction to engineer asphalt materials to have improved quality and better performance predictability.

The work reported here is based on the four-fraction method of chemical analysis of asphalts pioneered by Corbett (3,7). These fractions are the saturates, the asphaltenes, the naphthalene aromatics and the polar aromatics obtained by adsorption-desorption technique on a clay-silica-gel chromatographic column. Ishai et al. (8) have adopted the Gaestel Index ( $I_c$ ) to reflect the relationship between aging and the internal colloidal structure of asphalts. The interpretation of the chemical-group composition of the asphalt, which reflects its internal colloidal structure, was made by the Gaestel Index, as defined in the following equation.

$$I_c = \frac{\text{Asphaltenes} + \text{Saturates}}{\text{Naphthalene Aromatics} + \text{Polar Aromatics}} \quad (1)$$

In an earlier work (9), it was found that asphalt fractionation obtained by this method strongly correlated with ma-

terial properties, where the  $I_c$  as a single parameter was stronger in relating the asphalt chemical fractions to material rheology and aging than any single fraction, as will be discussed later in this paper.

## RESEARCH AND TECHNOLOGY BACKGROUND

In Israel, fresh paving-grade asphalt cements supplied to the asphalt industry may be a straight-run type or vacuum tower bottoms laced with PPA. PPA is a high consistency, high molecular weight asphalt product, obtained as the residue from the refinery production of lubricating oils by solvent (propane) precipitation. It may be blended with other soft asphalt residues (i.e., vacuum tower bottoms), to obtain paving-grade quality. Since their introduction a few years ago, the PPA blends have caused contradictory opinions, caused mainly by the phenomenon of tender mixes, causing construction problems, and to their unknown effects on long-term asphalt durability.

Consequently, a major effort has been devoted to investigate the effect of PPA asphalt cement blends on the chemistry, rheology, and long-term aging of asphalts and bituminous mixtures. The first phase of this work was dedicated to a preparatory laboratory study. Its results were well reported and published in the last five years (6 and 8, 9 through 13).

It was generally found that the PPA blends characteristically had lower viscosity and higher ductility, though better durability and moisture-damage resistance of their mixtures were noted than for the straight runs. No explanation has yet been found for the tenderness and sticky nature of the PPA mixtures, but it is suspected that the lower viscosity and higher ductility have a link with this character. It is also unclear to what extent this property would affect long-term performance.

A study of some asphalt samples by chemical analysis based on the Clay-Gel fractionation method also showed systematic differences between PPA blends and straight-run asphalt samples for same-penetration-grade bitumens. The PPA blends tended to have lower content of asphaltenes, higher polar aromatic fractions, and lower colloidal stability index (Gaestel Index) values than their straight-run counterparts. Unique relationships were established between material viscosity and the colloidal stability index for initial conditions and during aging. Typical examples are given in Figures 1 and 2. On the basis of these relationships, it appears that the relatively high polar aromatic fractions and low content of asphaltenes are a likely explanation for the low viscosity of PPA blends.

## FIELD TEST SECTIONS

The peculiar characteristics of the PPA blends and the merits of using one type of asphalt rather than another required field performance indicators. As a follow-up to the preparatory laboratory study, the Israel Public Works Department, in cooperation with the Technion Transportation Research Institute, in 1991 constructed a series of actual field-controlled test sections. These sections included separate stretches for straight-run asphalts and for PPA blends, with a view to obtaining firsthand information about material and pavement performance as related to basic rheological and chemical

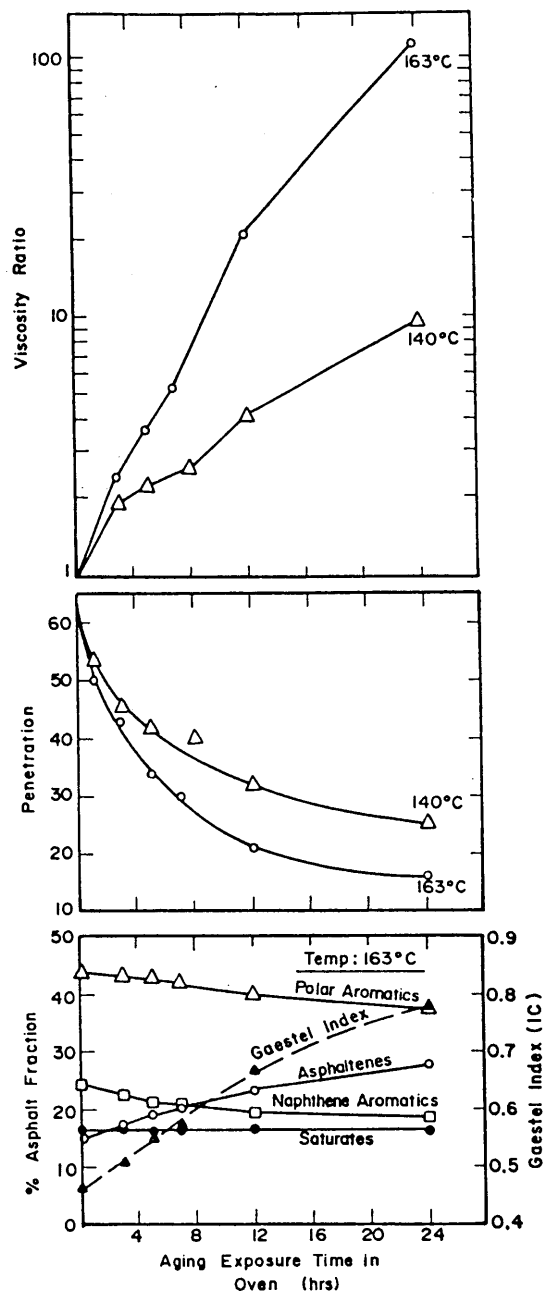


FIGURE 1 Relationship among the changes in asphalt chemical reactions and Gaestel Index and the changes in viscosity and penetration in the laboratory aging process (a straight-run asphalt) (9).

properties of the asphalts under field conditions (14). Among other parameters, pavement performance and material properties are monitored from time to time and correlated with chemical composition of cored samples taken at those instances.

To date, data accumulated so far reflect construction conditions and the beginning of the service life (up to 9 months) of the test sections. Data accumulated on properties of asphalts extracted from plant mixtures are found to tie in with those for fresh and oven-aged samples to show a clear correlation between asphalt properties and changes in chemical composition.

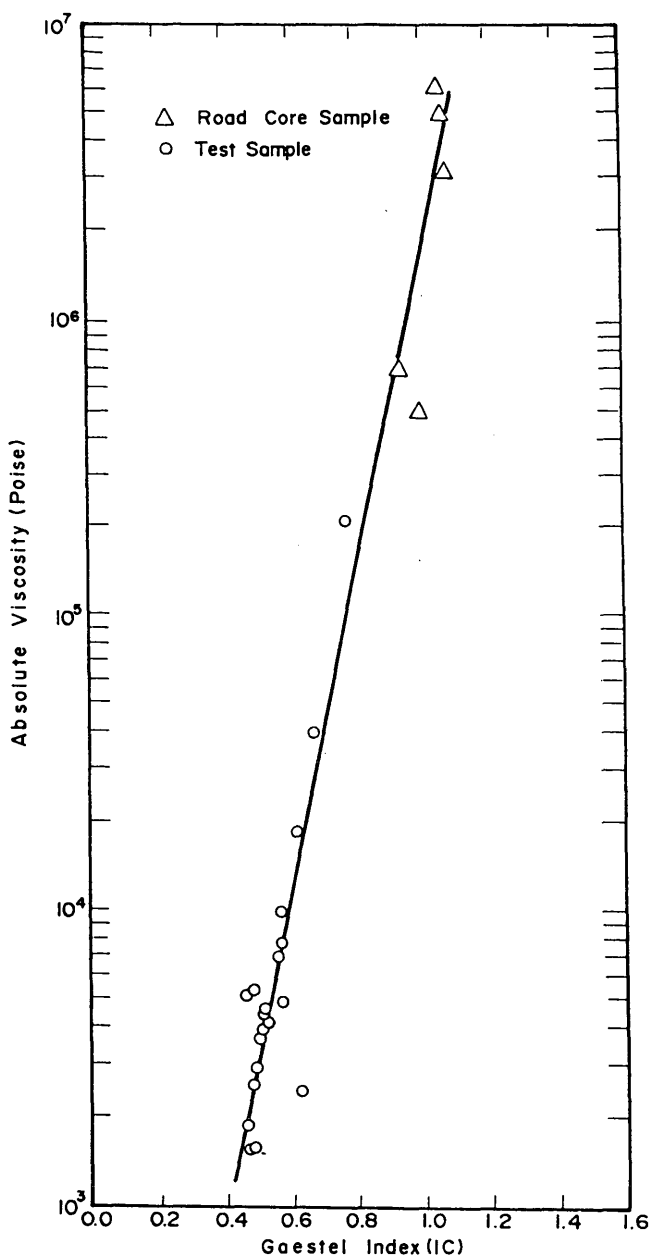


FIGURE 2 Relationship among viscosity and Gaestel Index at different laboratory and field aging levels for different types of asphalts (9).

## SITES, MATERIALS, AND TESTING PROGRAM

Controlled test sections were constructed at three sites in southern Israel in the vicinity of Ashdod and Beersheva. This construction was part of maintenance and rehabilitation activities on two major highways of the Israeli rural network. The sites were

1. Ramat Hovav (RH): Highway No. 40, 6 km south of Beersheva;
2. Beit-Kama (BK): Highway No. 40, 10 km north of Beersheva;
3. Nachshon (NA): Highway No. 32, 10 km west of Ashdod.

All bituminous mixtures were produced in a central asphalt plant located between Sites 2 and 3.

The experimental investigation that followed each construction site was based on a comprehensive testing system that included (see also Figure 3)

1. Tests on fresh asphalt cements;
2. Tests on recovered asphalt from plant produced mixtures;
3. Tests on aggregates and laboratory-produced bituminous mixtures;
4. Tests on plant-produced bituminous mixtures;
5. Tests on asphaltic concrete and recovered asphalt cement from samples cored soon after construction; and
6. Long-term followup on bituminous concrete and recovered asphalt under long service conditions.

Two types of asphalt cements were used: a straight-run and PPA blend, each obtained from a different producer. The fresh asphalt samples were monitored from production source to destination [i.e., samples were taken right after production (*A*), from delivery tanks before unloading at the site (*B*), and finally, from site storage facilities before entry into the asphalt plant (*C*)]. The idea behind sampling at those stages was to ascertain whether, during the transportation and storage stages, any variables were introduced into the material behavior. In the past, some contractors claimed (albeit without any tangible evidence) that asphalt cements arriving at their facilities had their properties somehow changed as a result of the transportation process from the production source. Tests carried out on these samples included comprehensive "fingerprinting" tests and clay-gel compositional analysis, as shown in Figure 3.

For plant-produced bituminous mixtures, samples were taken during each work day and for each bitumen type during laying of the test sections. The mixtures were used for recovering the asphalt binder for testing, as previously described. The blends were also used for preparing specimens for mechanical tests, which are not discussed in this paper. All materials belonging to this type of sample have been designated (*E*). Cores were also taken from the test sections at around 3 and 9 months after construction, the time periods representing the state of the test sections shortly after construction and 9 months of field aging. All asphalts recovered from the road core samples have been designated (*G3*) and (*G9*) for 3 and 9 months of field aging, respectively.

Two types of aggregates were used. For the sections at Ramat Hovav and Nachshon, the composition was totally dolomitic aggregates, whereas for Beit Kama it was + #4 sieve-basalt aggregates and - #4 sieve-dolomitic aggregates.

## RESULTS AND DISCUSSION

### Asphalt Cement Properties During Construction

#### Comparison Among Populations

Results of average physical and rheological properties of the asphalt cements during construction are summarized in Table 1. The table represents averages of 45 samples of fresh bitumen from the three sites and from A, B, and C groups, and

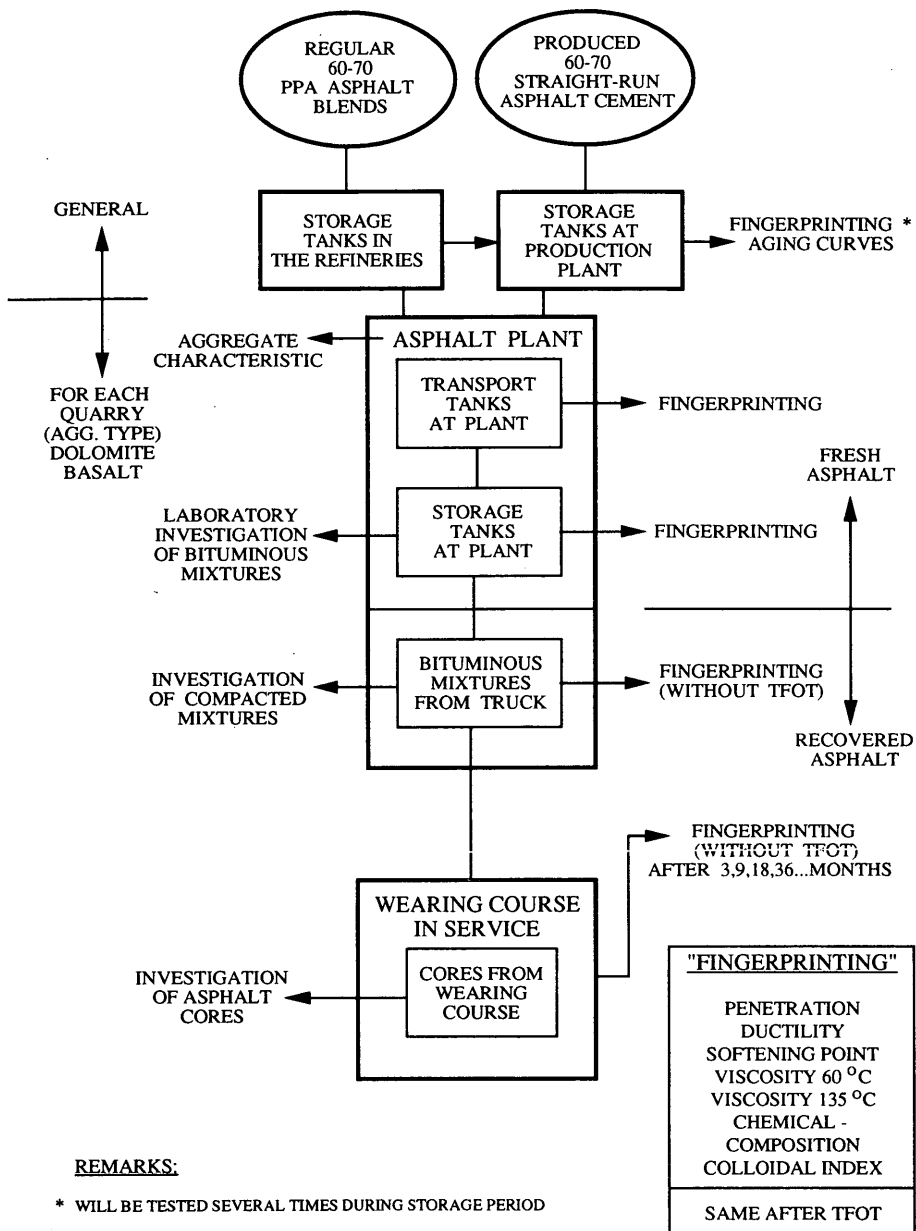


**FIGURE 3 Schematic description of experimental investigation that follows each construction site.**

31 samples of recovered asphalt from plant mixtures directed for the three sites. For the fresh asphalts, fingerprinting tests were made before and after thin-film oven testing (TFOT). In general, the tests included 54 straight-run samples and 21 PPA asphalt cement blends.

Before any conclusions can be reached about the effects of asphalt type and its chemical properties on material behavior, an examination should be made about the effect of the construction site (RH, BK, NA) and the asphalt group (A, B, and C). A statistical "Student-t" analysis was performed to check the significance of the differences among these various populations.

The results of the analysis showed that within the given sites there are no significant differences in asphalt properties among the various asphalt groups (A, B, C), and within each group there are no significant differences among the various sites (RH, BK, NA).

In general, it can be concluded that this comparative investigation is significant with respect to the comparison between the two types of asphalt (straight-run versus PPA blends), and with respect to the trends resulting from these comparisons, such as the effect of the chemical composition and behavior on aging. It is also evident that the properties of the asphalts did not change during the handling process (produc-

TABLE 1 General summary of average asphalt cement properties during construction (A, B, and C samples)

Asphalt condition	Type of asphalt Site	PPA blends				Straight-run			
		RH	BK	NA	General average	RH	BK	NA	General average
	No. of samples	5	3	5	Total 13	13	6	13	Total 32
Fresh Asphalt Cement (A, B, C)	Penetration (1/10mm)	65	63	61	63	66	66	68	67
	Ductility (cm)	104+	100+	100+	101+	100+	100+	100+	100+
	Softening Point ( $^{\circ}$ C)	47.5	50.1	49.9	49.0	49.0	50.3	50.3	50.0
	Absolute Viscosity (Poise)	1232	1291	1369	1298	1611	1552	1588	1591
	Kinematic Viscosity (Centistokes)	289	291	305	295	321	303	316	316
Fresh Asphalt Cement (A, B, C) After TFOT	Penetration (1/10mm)	38	38	40	39	43	44	45	44
	Ductility (cm)	80	100+	100+	92+	56	51	53	54
	Softening Point ( $^{\circ}$ C)	53.8	54.2	53.5	53.8	53.5	54.8	55.2	54.4
	Absolute Viscosity (Poise)	3675	3225	3375	3456	4901	4966	4572	4717
	Kinematic Viscosity (Centistokes)	426	406	424	421	450	453	443	448
	No. of Samples	3	1	5	Total 9	7	5	10	Total 22
Asphalt Recovered from Plant Mixtures (E)	Penetration (1/10mm)	38	40	43	41	41	48	43	44
	Ductility (cm)	81	100+	95+	91+	44	63	40	47
	Softening Point ( $^{\circ}$ C)	61.4	50.8	52.8	55.4	55.6	55.1	55.0	55.2
	Absolute Viscosity (Poise)	6677	3098	4058	4824	9247	4570	7791	7522
	Kinematic Viscosity (Centistokes)	542	423	459	483	553	472	535	526
	Mixing Temperature ( $^{\circ}$ C)	175	165	178	175	174	167	180	175

tion storage, transportation, and plant storage), and during the time gap (several months) between construction of the different testing sites.

#### Physical and Rheological Properties

In order to investigate the effect of asphalt chemical composition on material behavior and pavement performance, consideration should be given to the physicorheological behavior of the asphalts. The average value of the detailed data base is shown in Table 1. The correlative statistical analysis of this data base leads to the following trends in the relationship among major asphalt properties and the effect of the PPA on fresh and recovered asphalts during the construction process (see also Tables 2 and 3):

1. In most cases, almost no correlations exist among the different properties of fresh asphalts before and after TFOT. This is true for all relationship combinations of the straight-run asphalts. Only for the PPA asphalt blends were good

correlations obtained between the kinematic and absolute viscosity (Table 2).

2. The low correlations among penetration and viscosity (Table 2) indicated that the standard specified range of penetration does not ensure any well-defined values or ranges of viscosity. Despite the fact that the two types of asphalt are from the same penetration grade, they differ significantly in viscosity for a wide range of testing temperatures. The differences are especially significant for the asphalts recovered from the plant mixes (Table 1).

3. In contrast to the fresh asphalts, the correlations among properties of asphalts recovered from plant mixes are much higher (Table 3). Very high correlations were obtained among the viscosities, but good correlations were also obtained among the penetration and the two viscosities. The improvement in the correlation is mainly caused by the increasing range of asphalt parameter values of the recovered asphalt, because of different behavior under plant aging.

4. As for the comparison among the two types of asphalt, it can be seen that PPA asphalt blends possess lower pene-

TABLE 2 Statistical correlations among fresh asphalt properties (all sites and groups): (a) linear relationship  $Y = A + BX$  for PPA asphalt blends ( $N = 14$ ), and (b) linear relationship  $Y = A + BX$  for straight-run asphalt ( $N = 31$ )

X	Y	Before TFOT			After TFOT		
		Penetration	Softening Point	Absolute Viscosity at 60°C	Penetration	Softening Point	Absolute Viscosity at 60°C
Softening Point		$A = 119.88$ $B_2 = -1.147$ $R^2 = 0.18$	-	-	$A = 35.31$ $B_2 = 0.071$ $R^2 = 0.00$	-	-
Absolute Viscosity at 60°C		$A = 74.57$ $B_2 = -0.008$ $R^2 = 0.10$	$A = 41.04$ $B_2 = 0.06$ $R^2 = 0.40$	-	$A = 45.77$ $B_2 = -0.002$ $R^2 = 0.16$	$A = 53.00$ $B_2 = 0.000$ $R^2 = 0.01$	-
Kinematic Viscosity at 135°C		$A = 107.52$ $B_2 = -0.149$ $R^2 = 0.20$	$A = 30.27$ $B_2 = 0.064$ $R^2 = 0.27$	$A = -1792.15$ $B_2 = 10.509$ $R^2 = 0.69$	$A = 58.93$ $B_2 = -0.047$ $R^2 = 0.26$	$A = 52.26$ $B_2 = 0.004$ $R^2 = 0.01$	$A = -4213.99$ $B_2 = 18.348$ $R^2 = 0.87$

(a)

X	Y	Before TFOT			After TFOT		
		Penetration	Softening Point	Absolute Viscosity at 60°C	Penetration	Softening Point	Absolute Viscosity at 60°C
Softening Point		$A = 59.05$ $B_2 = 0.160$ $R^2 = 0.01$	-	-	$A = 41.39$ $B_2 = 0.044$ $R^2 = 0.00$	-	-
Absolute Viscosity at 60°C		$A = 66.79$ $B_2 = 0.000$ $R^2 = 0.00$	$A = 52.91$ $B_2 = -0.002$ $R^2 = 0.02$	-	$A = 52.12$ $B_2 = -0.002$ $R^2 = 0.21$	$A = 56.53$ $B_2 = -0.000$ $R^2 = 0.04$	-
Kinematic Viscosity at 135°C		$A = 84.82$ $B_2 = -0.056$ $R^2 = 0.04$	$A = 37.51$ $B_2 = 0.039$ $R^2 = 0.06$	$A = 275.18$ $B_2 = 4.104$ $R^2 = 0.11$	$A = 59.51$ $B_2 = -0.035$ $R^2 = 0.12$	$A = 58.00$ $B_2 = -0.007$ $R^2 = 0.02$	$A = -1672.78$ $B_2 = 14.415$ $R^2 = 0.29$

(b)

TABLE 3 Statistical correlation among recovered asphalt properties (all sites): (a) linear relationship  $Y = A + BX$  to PPA asphalt blends ( $N = 10$ ), and (b) linear relationship  $T = A + BX$  for straight-run asphalt ( $N = 21$ )

X	Y	Penetration	Softening Point	Absolute Viscosity at 60°C
Softening point		$A = 67.55$ $B_2 = -0.488$ $R^2 = 0.35$	-	-
Absolute Viscosity at 60°C		$A = 49.46$ $B_2 = -0.0017$ $R^2 = 0.72$	$A = 44.63$ $B_2 = 0.0022$ $R^2 = 0.71$	-
Kinematic Viscosity at 135°C		$A = 68.35$ $B_2 = -0.057$ $R^2 = 0.76$	$A = 26.45$ $B_2 = 0.059$ $R^2 = 0.56$	$A = -9635.50$ $B_2 = 29.880$ $R^2 = 0.94$

(a)

X	Y	Penetration	Softening Point	Absolute Viscosity at 60°C
Softening point		$A = 72.67$ $B_2 = -0.526$ $R^2 = 0.09$	-	-
Absolute Viscosity at 60°C		$A = 50.38$ $B_2 = -0.0008$ $R^2 = 0.73$	$A = 52.66$ $B_2 = 0.0003$ $R^2 = 0.32$	-
Kinematic Viscosity at 135°C		$A = 71.92$ $B_2 = -0.054$ $R^2 = 0.72$	$A = 44.24$ $B_2 = 0.021$ $R^2 = 0.33$	$A = -23090.94$ $B_2 = 58.323$ $R^2 = 0.93$

(b)

tration and lower viscosity values than straight-run asphalts. This is true for the fresh asphalt before and after TFOT and also for the recovered asphalts. It should be noted that this trend is contradictory for asphalt consistency because lower penetration indicates harder asphalt, whereas lower viscosity indicates softer asphalt. Again, attention should be given to the physical meaning of the viscosity and the realistic meaning of its testing temperature for construction and service conditions, as compared with the empirical character of the penetration test and its meaningless test temperature.

5. The difference between the two types of asphalt is also reflected in their ductility. Although adequate high values of ductility were obtained for the two types of fresh unaged asphalts, the difference among the straight-runs and the PPA blend asphalts is manifested in the aging process. The PPA blends maintain their high ductility values both after TFOT and plant mixing, whereas a severe drop in the ductility, down to values of less than 20 cm, characterizes the straight-run asphalts. This result stresses the inferiority of local straight-run asphalts in flexibility and adhesion.

#### Comparison with Other Populations

It will be interesting to compare the results of asphalt properties obtained during the construction of the test sections with properties of asphalt cement of other different and wider populations. During the preparatory laboratory research (6, 8, and 9 through 13), a daily sampling of asphalt cements was taken at the refineries. Within two years (1987–1989), more than 650 asphalt specimens were sampled and tested for a comprehensive fingerprinting (12,13). The second population represents asphalt cement fingerprinting taken during the quality control of overlaying jobs constructed in 1991 in northern Israel. This population includes 170 samples of fresh and recovered asphalt cements.

The comparison among the populations is summarized in Figures 4–6. These figures present the comparative variability in the different populations in the relationship between the penetration and absolute viscosity at 60°C. They also reflect the characteristics of the fresh asphalts before and after TFOT and asphalts recovered from plant mixes.

In the penetration-viscosity relationship, it can be seen that the PPA asphalt blends of the current investigation generally coincide with other wide-range practical populations tested between 1987–1991. On the other hand, the straight-run asphalts represent different populations characterized by a higher level of age hardening, as reflected in the absolute viscosity tested under realistic service temperature (60°C). This trend is more significant in the population of asphalts recovered from plant mixes (Figure 6).

### Long-Term Aging

The effect of temperature and time on changes in the physical and rheological properties of asphalt under accelerated conditions is commonly used to characterize the durability and aging potential of the asphalt. Long-term aging curves at different temperatures were used to differentiate among dissimilar asphalt types in the laboratory investigation (10,13). A typical long-term aging comparison among straight runs and different PPA blends is given in Figure 7 (11).

Similarly, about 50 aging curves were formed in this investigation, based on extensive accelerated long-term aging tests. The aging curves were based on penetration, two viscosities, and softening point. Typical test results for asphalt (A) from the BK site at two different exposure temperatures are presented in Table 4 and Figure 8.

On the basis of the comprehensive results, it was found that PPA asphalt blends are characterized by much lower viscosities in the long-term aging process as compared with straight-run asphalts. This is mainly reflected by the absolute viscosity, with up to three times difference, seen in Figure 8. This may indicate the higher aging sensitivity of the straight-run asphalt cements. It also conformed with the results obtained for the asphalts recovered from plant mixes.

### Chemical Composition

Summarized in Table 5 are the average values of the asphalt chemical composition during construction at all three sites. Also presented in the table are the values of the Gaestel Index ( $I_c$ ), which reflect the colloidal stability of the asphalt. Based on the detailed results and those of the table, the following trends are observed:

1. There is a significant difference in the chemical composition among the straight-run and the PPA blend asphalts. This difference lies mainly in the saturates and polar aromatic fractions. PPA asphalt blends contain less saturates (a difference of 3–4 percent) and more polar aromatics (a difference of 3–6 percent). The differences in the asphaltene and the naphthalene aromatic fractions are much smaller (1–2 percent).

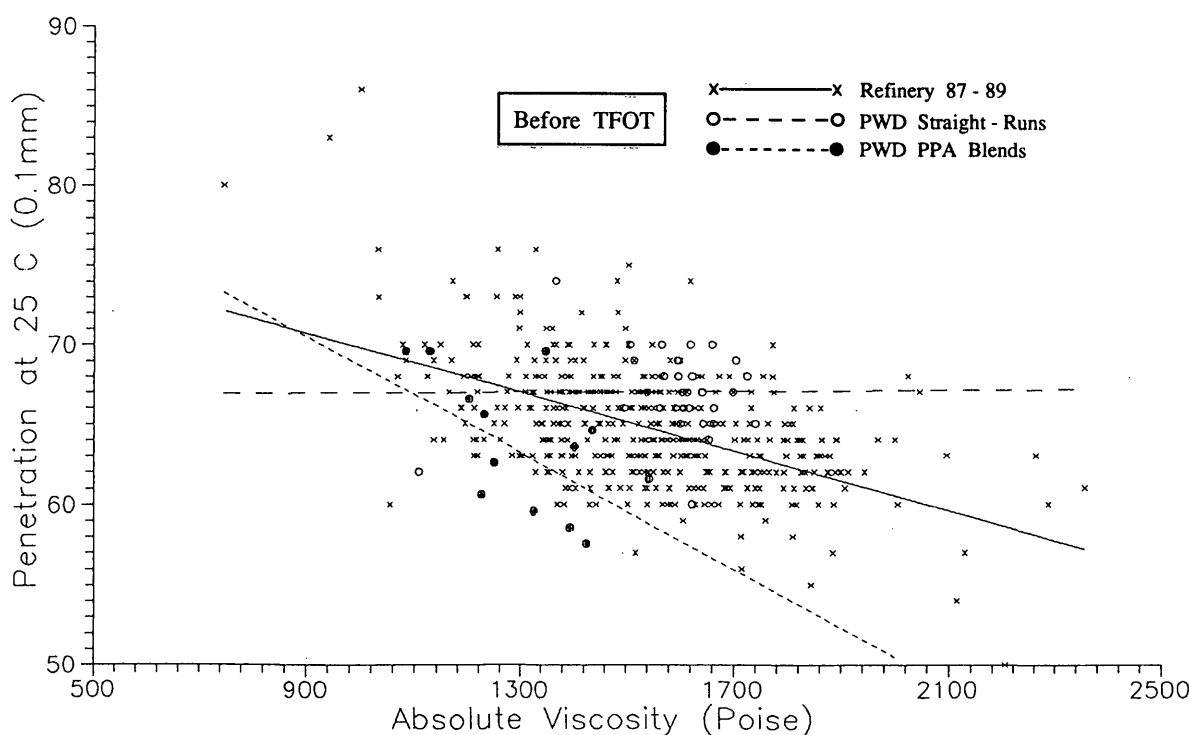


**FIGURE 4 Comparison among asphalt populations by relationship between penetration and absolute viscosity (at 60°C) for fresh asphalts.**

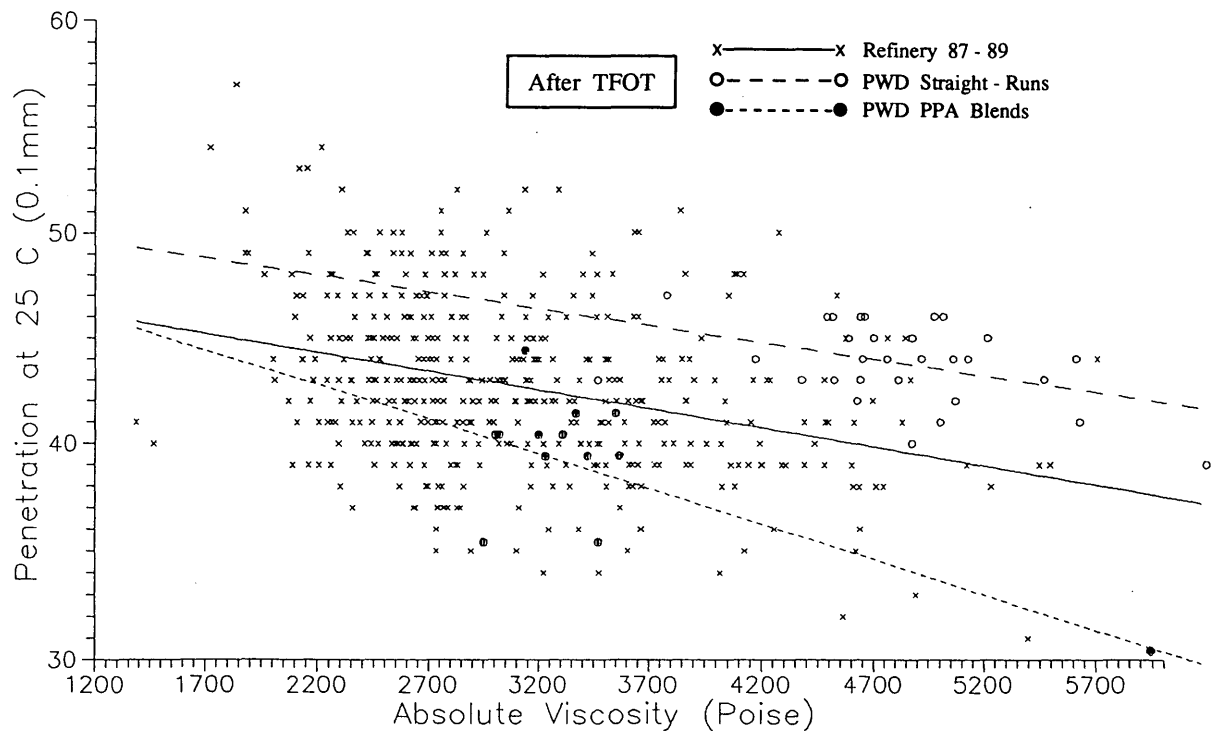


**FIGURE 5 Comparison among asphalt populations by the relationship between penetration and absolute viscosity (at 60°C) for fresh asphalts after TFOT.**

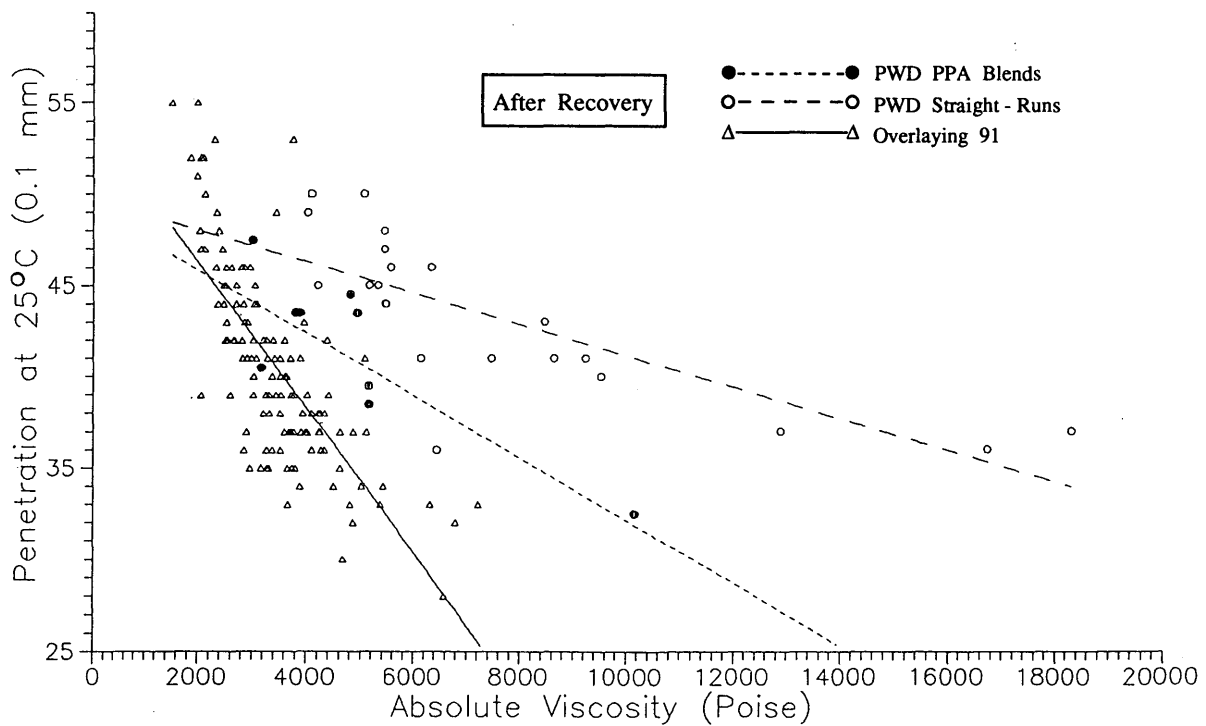


**FIGURE 6 Comparison among asphalt populations by the relationship between penetration and absolute viscosity (at 60°C) for recovered asphalts.**

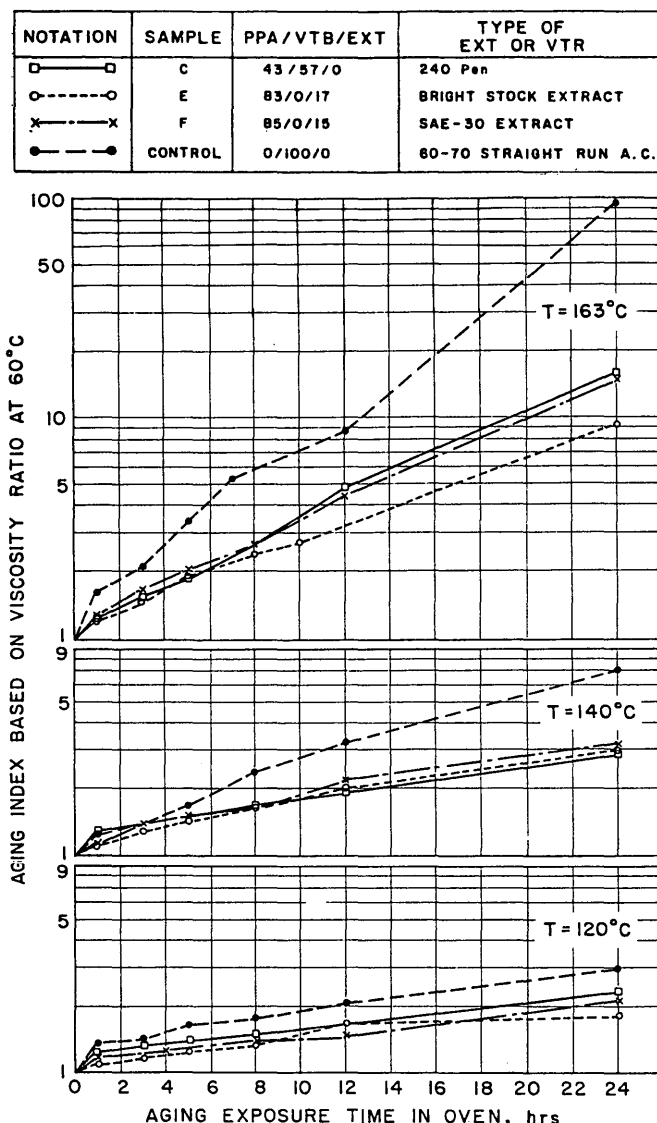


FIGURE 7 Typical long-term aging curves, based on absolute viscosity, for comparison among straight-run asphalts and different PPA asphalt blends (II).

cent), where the amount of asphaltenes in the PPA asphalts is less than in the straight runs. Accordingly, the value of the Colloidal Stability Index ( $I_c$ ) in PPA asphalt blends is smaller.

2. During the aging and hardening process, the following colloidal changes occur: In PPA asphalt blends, the polar aromatic fraction content is decreasing while transforming into asphaltenes with an increase in the latter's fraction content. This transformation is accompanied by minor changes in the content of the saturates and naphthalene aromatic fractions only. In straight-run asphalts, the increase of the asphaltenes fraction is probably caused by the transformation of both aromatic fractions, whereas the saturates fraction remains unchanged (as in the PPA blends), and does not contribute to the aging and hardening process. A similar trend

in chemical composition changes in the aging process is illustrated in Figure 1.

3. Because the colloidal changes in PPA asphalt blends occur mainly in the dissolvent phase (polar aromatics  $\rightarrow$  asphaltenes), and very seldom in the solvent phase, they are accompanied by smaller changes in the viscosity compared with straight asphalt, in which the colloidal changes are also caused by the transformation of solvent fractions into dissolvent ones (naphthalene aromatics  $\rightarrow$  asphaltenes). This leads to more significant increases in viscosity during the aging process.

4. An expression of the difference between the two types of asphalt with respect to their chemical composition-viscosity relationship, is presented in Figure 9 (based on Tables 1 and 5). This figure reflects again, in the given range, the significant relationship between asphalt aging and its chemical composition. It should be noted that asphalt aging is based on the realistic and physical viscosity parameter, which is measured at realistic service temperature. The figure stresses again the contrasts between the two types of asphalt and relates them to the chemical compositions. These differences are expressed either by the difference in the Colloidal Stability Index ( $I_c$ ) or by the higher sensitivity of the straight-run asphalt to aging and hardening in the weathering process; and

5. No significant relation whatever was found among the chemical composition of the asphalt and its changes and among the penetration values, either in the difference among the asphalts or the aging process.

#### Asphalt Cement Properties During Early Service Time

As mentioned previously, the changes in the asphalt cement from actual test-section wearing causes were monitored after construction. At this stage, cores were taken from the asphaltic surfaces 3 and 9 months after their construction (samples G3 and G9, respectively). Physical and rheological fingerprinting and also chemical composition analyses were performed on asphalt cements recovered from the pavement cores.

A summary of the physical, rheological and chemical composition changes that occurred in the asphalt cements during the early service time are presented in Tables 6 and 7. These results indicate the following trends:

#### The Aging Process

As can be observed from Table 7, and also expressed in Figure 10, the aging process of the asphalts continued even during the early service time immediately after construction. The process was reflected in all physico-rheological parameters tested. The evolution of these parameters during the beginning of service life (3 and 9 months) is described in Figure 10, and compared with the properties of the fresh asphalts and asphalt recovered from fresh plant mixes (0 months).

It can be seen that both asphalts age substantially during the short service time. This aging is more pronounced when

**TABLE 4 Typical table summarizing results of long-term aging tests (PPA asphalt blend, Beit Kama site)**

TFOT Exposure Temperature 163°C

Time (hrs.)	0	1	3	5	8	12	18	24
Penetration (25°C), 1/10mm)	68	59	52	45	40	35	28	25
Absolute Visc., (Poise)	1,623	2,340	3,395	4,698	8,870	20,470	50,980	203,350
Kinematic Visc., (cSt)	321	369	383	446	558	708	1053	1792
Softening Point, (°C)	50.1	52.0	54.1	54.0	56.2	60.5	64.3	69.6

TFOT Exposure Temperature 140°C

Time (hrs.)	0	1	3	5	8	12	18	24
Penetration (25°C), 1/10mm)	68	62	61	54	44	42	40	38
Absolute Visc., (Poise)	1,623	2,090	2,479	2,874	4,294	5,780	9,416	15,680
Kinematic Visc., (cSt)	321	355	368	388	437	481	547	662
Softening Point, (°C)	50.1	51.2	51.8	53.1	53.0	57.1	57.1	57.9

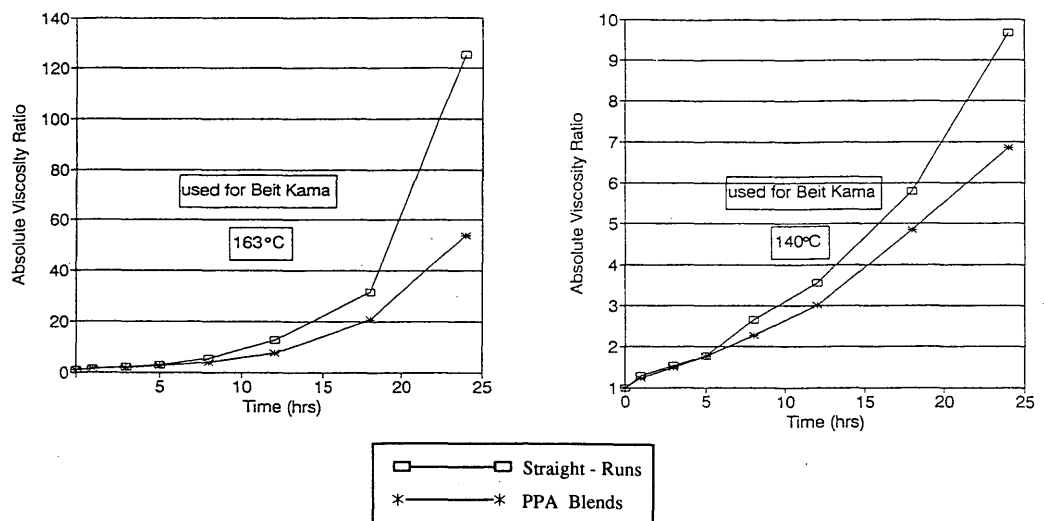


**FIGURE 8** Typical aging curves based on absolute viscosity that reflects the difference between the two types of asphalt for long-term durability (Asphalt A from Beit Kama site).

**TABLE 5** General summary of average values of asphalt cement chemical composition during construction

Asphalt Condition	Site	Straight-run					PPA Blends				
		AS	SA	NA	PA	$I_C$	AS	SA	NA	PA	$I_C$
Fresh Asphalt Cement (A)	RH	22.10	17.18	18.84	41.65	0.65	23.37	19.66	20.56	35.74	0.77
	BK	21.52	16.53	19.09	42.50	0.62	22.58	19.85	20.47	36.33	0.75
	NA	20.76	16.36	19.06	42.53	0.60	21.96	18.65	20.30	38.07	0.75
	Average	21.46	16.69	19.00	42.23	0.62	22.64	19.45	20.44	36.71	0.76
Fresh Asphalt Cement (A) After TFOT	RH	23.36	14.80	18.31	42.83	0.63	24.17	19.04	20.60	35.39	0.77
	BK	23.83	15.45	19.98	39.99	0.65	24.12	19.66	20.49	34.63	0.81
	NA	23.21	16.83	18.42	41.48	0.66	24.20	17.60	19.25	36.73	0.75
	Average	23.47	15.59	18.90	41.43	0.65	24.16	18.77	20.11	35.55	0.78
Asphalt Recovered from Plant Mixes (E)	RH	27.75	15.34	18.04	37.09	0.78	27.45	17.45	17.76	34.91	0.84
	BK	25.16	14.63	20.77	38.76	0.67	24.89	20.01	18.22	35.31	0.84
	NA	24.77	16.35	18.04	38.69	0.72	37.00	19.47	18.51	34.52	0.88
	Average	25.89	15.44	18.95	38.18	0.72	26.45	18.97	18.16	34.91	0.85

NA - Naphthalene Aromatics

AS - Asphaltenes

PA - Polar Aromatics

SA - Saturates

$$I_C = \text{Gaestel Index} = \frac{AS + SA}{NA + PA}$$

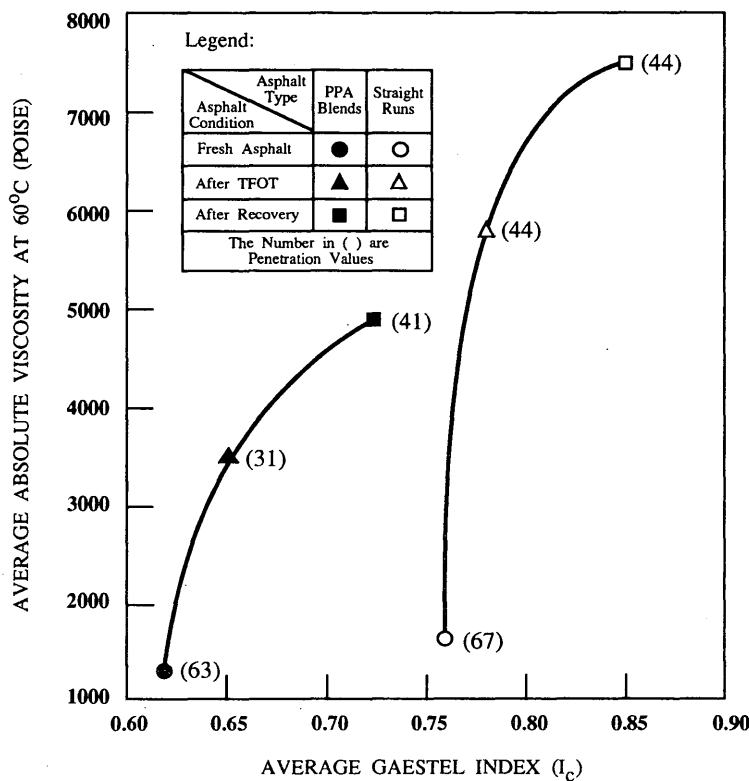


**FIGURE 9** Difference between two types of asphalt as expressed by viscosity-chemical composition relationship (fresh and recovered asphalts during construction).

expressed by the absolute viscosity and ductility, rather than by the penetration, softening-point or kinematic viscosity. The absolute viscosity increases up to 4.0–5.5 times its value after mixing, and the ductility decreases down to 5.8 times. Because the absolute viscosity is measured at critical service temperature (typical to the Israel Negev where the test sections are located), its aging trend seems to be most realistic to the hardening expected to occur during the longer service time. As related to flexibility and adhesion, the ductility could also be an important indicator of the expected pavement distress after long-term exposure to the specific semiarid climate.

The difference between the two types of asphalt still follows the same trends when the fresh asphalt and that recovered after mixing are compared. Here again, the rate of aging was much higher for the straight-run asphalts than for the PPA blends. This is reflected in all the aging parameters, as shown in Figure 10. On the basis of absolute viscosity, the straight-run asphalt aged about 25 times from the fresh state up to 9-month field service, whereas the PPA blends aged only 15 times. Also, on the basis of ductility, a drop of about 12 times from the fresh asphalt state up to 9 months' service was found for the straight runs, whereas the drop was only 6 times for the PPA blend. It should be noted that the ductility level of the straight-run asphalts reached a critical level of values less than 10 cm.

It would be interesting to compare the aging level in the standard TFOT exposure with the aging occurring under real mixing and service conditions. As shown in Table 1 and Figure

10, the hardening occurring in the standard TFOT is even less than that under routine plant mixing. In this sense, if the methodology suggested by Ishai (10) is used, together with the values of the aging curves in Figure 8 and similar ones, it can be seen that the aging level after 9 months' service is equivalent, on the average, to 16 hours of exposure in the TFOT (under 163°C). In this way, the laboratory aging curves can be calibrated to reflect and predict the aging under real service conditions.

#### Aspects of Chemical Composition

As shown in Table 8, and also expressed in Figure 11, the aging occurring during the early service time was also reflected by the changes in chemical composition. As distinct from the aging during the mixing process, in which the asphalt hardening was reflected mainly by the increase of asphaltene fraction with the saturates being constant, during the aging under service conditions, both the asphaltene and saturate fractions increased, whereas the polar aromatic fraction remained fairly constant.

Despite this difference in the relative changes in the chemical composition fractions, the Colloidal Stability Index ( $I_c$ ) continued to increase with the physical hardening (as expressed in Figure 10 by its relation to service time). A long-term relationship between  $I_c$  and absolute viscosity, similar to the short-term one expressed in Figure 9, is presented in

TABLE 6 General summary of asphalt cement property changes during early service time (G3 and G9 samples)

ASPHALT CONDITION	TYPE OF ASPHALT	STRAIGHT-RUN				PPA BLENDS			
		SITE	RH	BK	NA	General	RH	BK	NA
	No. of Samples	7	5	7	Total 19	3	1*	4	Total 7
Asphalt recovered from road cores after 3 months (G3)	Penetration (1/10mm)	30	33	32	32	26	-	24	25
	Ductility (cm)	11	15	12	12	27	-	26	26
	Softening Point ( $^{\circ}$ C)	59	57.6	58.5	58.4	57.5	-	59.0	58.4
	Absolute Viscosity (Poise)	21,117	14,348	15,517	17,272	11,737	-	10,488	11,023
	Kinematic Viscosity (Centistokes)	772	670	717	725	664	-	618	638
Asphalt recovered	No. of Samples	7	5	5	Total 17	3	1*	4	Total 7
Asphalt recovered from road cores after 9 months (G9)	Penetration (1/10mm)	26	25	28	26	24	-	24	24
	Ductility (cm)	8	7	8	8	14	-	18	16
	Softening Point ( $^{\circ}$ C)	61.8	61.7	63.2	62.2	58.0	-	60.5	59.4
	Absolute Viscosity (Poise)	42,130	43,859	35,706	40,749	17,425	-	21,948	20,010
	Kinematic Viscosity (Centistokes)	944	998	911	950	729	-	774	755

\* Tests on a single sample were omitted due to insufficient statistical verification

TABLE 7 General summary of average values of asphalt cement chemical composition changes during early service time (G3 and G9 samples)

ASPHALT CONDITION	TYPE OF ASPHALT	STRAIGHT-RUN					PPA BLENDS				
		FRACTION	SITE	AS	SA	NA	PA	I <sub>C</sub>	AS	SA	NA
Asphalt recovered from road cores after 3 months (G3)	RH		29.46	16.09	16.27	36.41	0.86		27.00	17.16	21.05
	BK		27.36	20.39	15.34	36.67	0.92		-	-	-
	NA		27.83	19.49	16.88	35.48	0.90		28.74	16.44	17.04
	Average		28.22	18.66	16.16	36.19	0.89		27.87	16.80	19.04
Asphalt recovered from road cores after 9 months (G9)	RH		30.27	20.89	14.44	33.29	1.07		28.59	19.05	13.81
	BK		28.61	21.50	14.64	35.13	1.01		-	-	-
	NA		30.02	19.21	16.02	34.72	0.97		28.77	16.44	15.33
	Average		29.63	20.53	15.05	34.38	1.02		28.68	17.74	14.57

NA - Naphthalene Aromatics

PA - Polar Aromatics

AS - Asphaltenes

SA - Saturates

$$I_C = \text{Gaestel Index} = \frac{AS + SA}{NA + PA}$$

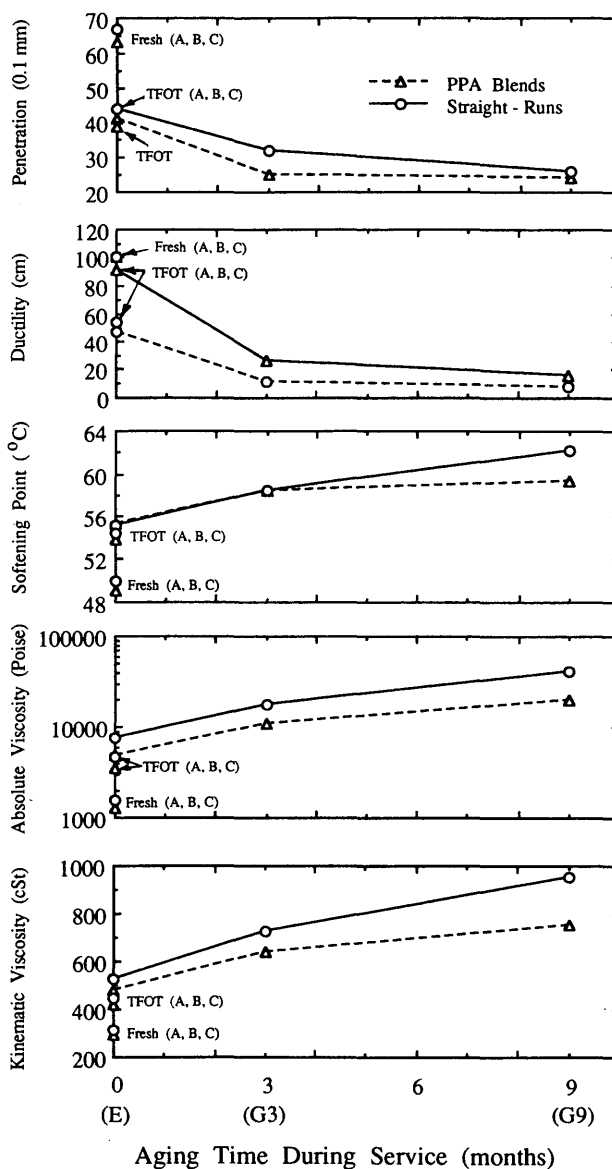


FIGURE 10 Evolution of physico-rheological asphalt parameters during early service aging.

Figure 12. As is also seen in Figure 2, the Colloidal Stability Index adequately reflected and correlated with long-term age hardening.

This quantitative relationship among physical hardening and changes in the chemical composition also reflected the difference between the two types of asphalt with respect to their sensitivity to aging and the relative advantage of the PPA asphalt blends.

## SUMMARY

Presented in this paper are some aspects of the effect of asphalt chemical composition on the properties and behavior of some fresh asphalt binders, as well as of plant-aged and field-aged samples, and the manner in which long-term aging

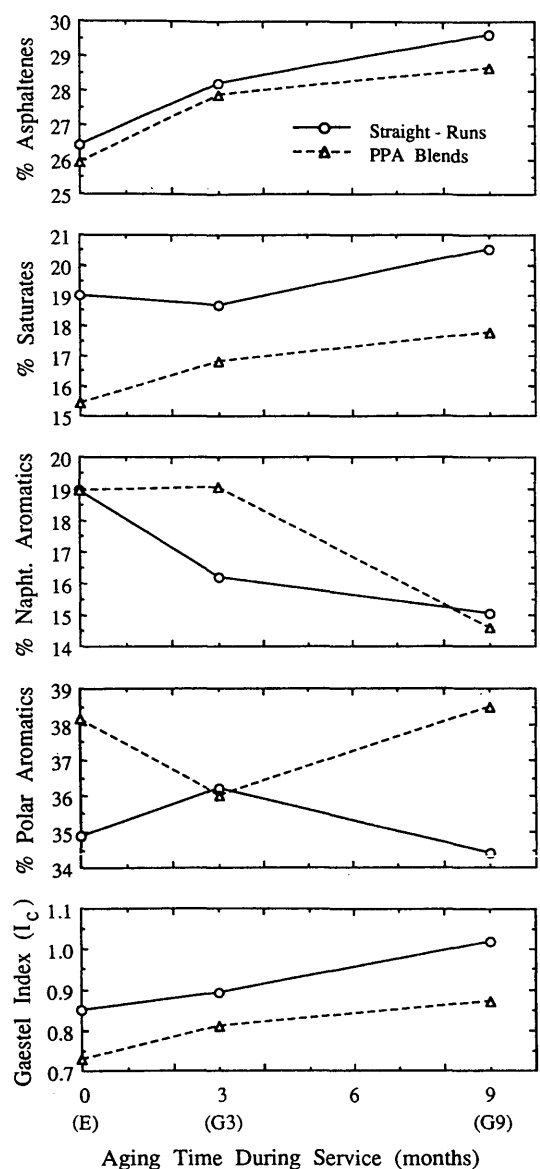
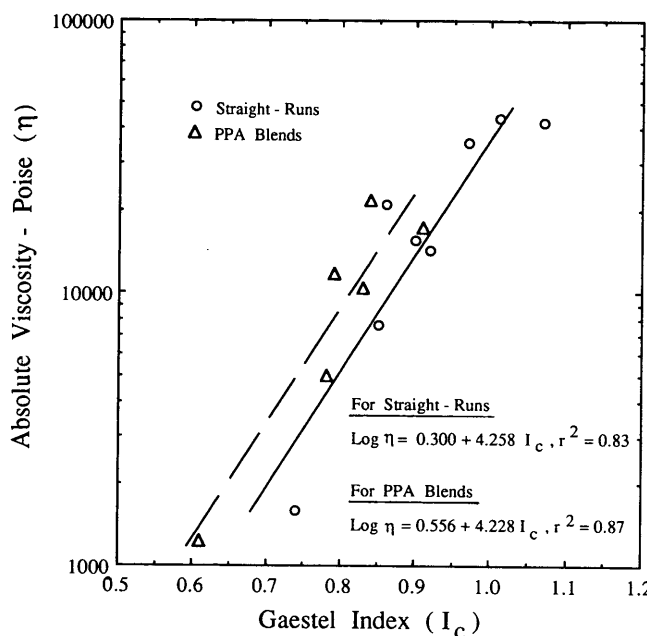


FIGURE 11 Chemical composition changes during early service time.

may be affected by changes in material composition. The asphalt binders involved were of the straight-run and PPA blend types, all of the 60/70 penetration grade.

At this stage, data accumulated reflect construction conditions and the beginning of the service life of the test sections. No pavement distress has been reported so far that would warrant linkage to the type and characteristics of the asphalt binder used. However, definite relationships were found among the chemical composition of the asphalt and its physicochemical changes during short- and long-term aging. These relationships were also significant enough to distinguish among the behavior of straight-run asphalt and PPA asphalt blends.

As more data become available with time, it is hoped that a more definite relationship can be established between the physicochemical properties of the asphalt and their effect on material behavior and longer-term pavement performance.



**FIGURE 12 Long-term relationship between Colloidal Stability Index and asphalt viscosity during aging in mixing and in early service.**

#### ACKNOWLEDGMENTS

This research was financed by the Israel Oil Industry (Paz Oil Co., Delek Oil Co., Sonol Oil Co., Haifa Refineries, and Haifa Basic Oils), and by the Israel Public Works Department, Research and Materials Section. The authors wish to thank these organizations for their sponsorship and help. Thanks are also due to R. Yovel, A. Altberg, A. Aines, F. Hirosh, and S. Yechiel for their technical and administrative assistance.

#### REFERENCES

- C. Giavarini and P. De Filippis. Relationship Between the Production Process and Chemical Structure of Bitumens. In *Proc., International Symposium on the Chemistry of Bitumens*, Vol. 1, 1991.
- Bituminous Materials*, Vol. 3. (Arnold J. Hoiberg, ed.), 1965.
- L. M. Corbett. Relationship Between Composition and Physical Properties of Asphalt. *Asphalt Paving Technology*, Vol. 39, 1970.
- B. Brûlé, G. Raymond, and C. Such. Relationship Between Composition, Structure, and Properties of Road Asphalts: State of Research at the French Public Works Central Laboratory. In *Transportation Research Record 1096*, TRB, National Research Council, Washington, D.C., 1986.
- E. J. Dickinson. The Diffusion-Controlled Reaction of Oxygen with Films of Bituminous Binder. *Journal of Australian Road Research*, Vol. 14(3), Sept. 1984.
- Y. A. Tuffour and I. Ishai. The Diffusion Model and Asphalt Age-Hardening. *Asphalt Paving Technology*, Vol. 59, 1990.
- L. W. Corbett. Composition of Asphalt Based on Generic Fractions, Using Solvent Deasphalting, Elution-Adsorption, Chromatography and Densimetric Characterization. *Analytical Chemistry*, Vol. 41, 1969.
- I. Ishai, B. Brûlé, J. C. Vaniscote, and G. Ramond. Some Rheological and Physico-Chemical Aspects of Long-Term Asphalt Durability. *Asphalt Paving Technology*, Vol. 57, 1988, pp. 65–93.
- Y. A. Tuffour, I. Ishai, and J. Craus. Relating Asphalt Aging and Durability to its Compositional Changes. *Asphalt Paving Technology*, Vol. 58, 1989.
- I. Ishai. A Suggested Methodology for the Analysis of Asphalt Age-Hardening. *ASTM Journal of Testing and Evaluation*, Vol. 15, No. 3, May 1987, pp. 127–132.
- I. Ishai and Y. A. Tuffour. The Use of Propane Precipitated Asphalt (PPA) in Bituminous Paving Mixtures. *Asphalt Paving Technology*, Vol. 56, 1987, pp. 599–631.
- I. Ishai and S. A. Asante. *Interrelationship Between Asphalt Properties as Sampled in the Refineries During Two Years*. Technion, Transportation Research Institute, Research Report 90-153, Haifa, Israel, Feb. 1990.
- Y. A. Tuffour and I. Ishai. *Durability and Aging of Asphalt Cement for Paving*. Technion, Transportation Research Institute, Research Report 90-152, Haifa, Israel, Feb. 1990.
- I. Ishai, J. Craus, and Y. A. Tuffour. *A Comparative Investigation of Asphalt Cements for Paving*. Part 1—General Background, Experiment Description and Asphalt Properties. Technion, Transportation Research Institute, Project 115–123, Haifa, Israel, Dec. 1991 (in Hebrew).

# Preparation and Characterization of Asphalt-Modified Polyethylene Blends

WILLIAM H. DALY, ZHAOYAO QUI (CHIU), AND IOAN NEGULESCU

Eight asphalt samples from four manufacturers with grades from AC-10 to AC-30 were characterized by  $^{13}\text{C}$  nuclear magnetic resonance, dynamic mechanical analysis (DMA) and differential scanning calorimetry (DSC). Glass transition temperatures ( $T_g$ ) and activation energies for the relaxation process of the asphalt were determined with DMA experiments. Polyethylene, a recyclable waste that is abundantly available either as virgin material not included in specifications or from solid waste classification processes, was slightly chlorinated to improve its compatibility with asphalt. High-density polyethylene (HDPE), chlorinated polyethylene (CPE), and maleated polyethylene (MGPAs)-modified asphalts were studied with DMA in both bending and shear modes. DSC, fluorescence reflection microscopy, and Fourier transform infrared were also employed to characterize the polymer-modified asphalts. Creep resistance and low-temperature crack resistance of the asphalt and the polymer-modified asphalts were evaluated. The results confirm that CPEs with low chlorine contents (< 15 weight percent) are more compatible with asphalt than is HDPE. Marked improvements in blend properties are also observed with MGPAs, provided that the degree of maleation does not exceed 3 percent.

Blends of polymeric materials with asphalt are complex and characteristically unique paving material systems. For any specific asphalt cement (AC), the physical properties of the asphalt-polymer blend are affected by the amount of polymeric material added, its composition, its molecular weight, and so on, but the most important variable may be the compatibility of the AC with the admixed polymer. The ability to enhance polymer-asphalt compatibility is complicated further by the variations in asphalt compositions within a given grade (1). Our research efforts are directed toward developing a simple method to estimate the compatibility of polymer additives with asphalt, to assess the phase structure of the asphalt-additive mixture, and to compare blended polymer-asphalt performances with those of the pure asphalt matrix. Chemical modification of polymers facilitates the preparation of polymer additives with varying degrees of crystallinity and polarity, factors that influence the compatibility of polymers in a matrix. Using dynamic testing techniques, we have assessed the performance of ACs modified with polyethylene that have been subjected to various degrees of chlorination and maleation.

Polymer additives should reduce the temperature sensitivity of ACs by increasing the high-temperature viscosity. Ideally, the resultant binder should have a very low thermal sensitivity throughout the range of use, but a low viscosity at mixing

temperatures (2). Resistance to permanent deformation as well as tensile and fatigue strength should be enhanced relative to the properties of the unmodified asphalt. However, the binder must maintain good adhesive properties and exhibit high aging resistance. A suitably modified binder should exhibit reduced plastic deformation at high temperatures, better low temperature resiliency, and better performance in service under heavy oscillatory loads.

The most important parameter governing the success of a polymer modifier in asphalts is its compatibility. The asphaltenes are suspended in the oils by the resins, making asphalt a colloidal system. The introduction of any incompatible polymer under agitation into such a system at high temperature generally results in asphaltene flocculation and oil bleeding, leading to a binder having no cohesion (2). Polymers must improve not only AC properties, but the performance of binder-aggregate combination as well (3).

Plastics give strength to the asphalt, but the ability to recover from extension is lost (4). Thermoplastics that are partially crystalline, such as polyethylene (PE) and polypropylene (PP), have attracted increasing attention because this class of polymer combines the advantages of rubber and fibers. The crystalline segments of polyolefins serve as high-strength fillers in the asphalt-polymer blend and improve the blend properties over all service conditions. However, the polyolefins are only slightly compatible with asphalt; thus, the blends tend to separate at high temperatures. Ethylene-vinyl acetate copolymers (EVA) are more compatible and improve resistance to permanent deformation and increase modulus (3). The presence of vinyl acetate comonomers decreases the crystallinity of the PE blocks, leading to increased flexibility and toughness. In one study on surface dressings, the EVA-modified asphalt ranked among the best of the asphalts tested in the areas of fatigue resistance and field performance (5).

PE is a potentially useful modifier for increasing the low-temperature fracture toughness of asphalt concrete (6), and it may confer additional pavement stability at elevated temperatures, which would minimize rutting and distortion caused by creep. Further, because polyolefins make up approximately 60 percent of plastic solid wastes, a reliable source of PE, either from virgin material or from recycled waste, is assured. HDPE is highly crystalline, but the amorphous domain exhibits a low glass transition temperature. This allows PE to contribute additional toughness and ductility at low temperatures to PE-asphalt blends, particularly those prepared from soft asphalts. However, it is known that asphalt-PE mixtures have a tendency toward gross phase separation (i.e., gross incompatibility) when standing at an elevated tem-

perature for long periods (7). Therefore, modification of PE is needed to enhance its compatibility with asphalt. Chlorination of PE is a simple technique to change the polarity, reduce the crystallinity, and increase the density of the polymer to match the density of asphalt. If the density of the polymeric additive is comparable with that of the asphalt matrix, the driving force for gross phase separation is minimized. Partially chlorinated polyolefin waxes are known to improve stability of asphalt-polymer blends (8,9), so we elected to prepare and characterize PEs with various degrees of chlorination to improve the polymer interaction with polar components of asphalt. The extent of chlorination can be used to vary the crystallinity of the polymer additive.

## EXPERIMENTAL WORK

### Nuclear Magnetic Resonance and Fourier Transform

#### Infrared Characterization of Asphalt

The application of nuclear magnetic resonance (NMR) to the analysis of asphalt samples is well established (10–12). Samples were dissolved in deuterated chloroform at a concentration of 10 percent [weight/volume (w/v)]; spectra were measured using Bruker 200 MHz Fourier transform nuclear magnetic resonance. A relaxation agent, Cr(acac)<sub>3</sub>, 12 mg/ml, was added to the <sup>13</sup>C NMR samples. Using an interpulse time of 6 sec and more than 8,000 scans, reliable quantitative spectra can be obtained (13). The observations on eight samples of Louisiana asphalts are summarized in Table 1. Asphalt samples, 5 percent (w/v) chloroform solution in a 1-mm cell were examined by quantitative Fourier transform infrared

(FTIR) using a Perkin Elmer 1700 FTIR. The overlapped peaks in 1550–1800 cm<sup>-1</sup> were resolved by a curve fitting program based on the work of Petersen and his colleagues (14). The results (Table 1) show significant differences in composition among asphalt samples of the same grade.

### Crystallinity of Asphalt

Linear paraffins present in asphalt readily crystallize. The relative crystallinity of a given asphalt can be measured by DSC (15,16). A Seiko DSC 220C calibrated for temperature and enthalpy with indium was employed to estimate the relative volume of the crystalline phase in each of the asphalt samples. The DSC was conducted on ≈ 10 mg samples sealed in an aluminum sample pan using an empty aluminum sample pan with cap as a reference. Initially each sample was cooled at 3°C/min to –45°C and then heated at 3°C/min. The heats of fusion ( $\Delta H_f$ ) observed are listed in Table 1. The percent crystallinity was estimated from this data by assuming that completely crystallized hydrocarbons in an asphalt matrix exhibit an average enthalpy of 200 Joules/gram (J/g).

### Chlorination of Polyethylene

HDPE was supplied by Paxon Polymer Co. The polymer had weight and number average molecular weights of  $8.5 \times 10^4$  and  $1.9 \times 10^4$ , respectively; M.I. = 25, m.p. 131°C,  $\Delta H_f$ , 343 J/g. Solution chlorination was performed in 1,1,2,2-tetrachloroethane (TCE); the polymer was dissolved at 130°C to a concentration of 7 percent (w/v) under nitrogen flow. The

TABLE 1 NMR and DSC characterization of asphalt composition

Sample	ACA	ACB	ACC	ACD	ACE	ACF	ACG	ACH
Grade	AC-10	AC-20	AC-10	AC-20	AC-10	AC-20	AC-20	AC-30
Arom H%	5.5	6.1	6.9	6.0	6.3	6.8	7.1	5.7
Arom C%	28.2	30.4	37.3	34.1	33.4	33.7	34.0	24.5
Linear Aliph%	41.8	41.6	22.5	21.8	19.5	21.2	22.3	23.2
Phenolics <sup>a</sup>	0.0086	0.0058	0.0069	0.003	0.012	0.0093	0.0036	0.004
Pyrrolics <sup>a</sup> Carboxylic Acid <sup>a</sup>	0.0142	0.0112	0.0225	0.0135	0.0137	0.014	0.0145	0.0137
	0.109	0.0828	0.0318	0.021	0.0220	0.0311	0.0242	0.0324
Ketone <sup>a</sup>	0.133	0.13	0.0275	0.0195	0.0796	0.043	0.027	0.0362
Quinolone <sup>a</sup>	0.0412	0.0298	0.0269	0.027	0.023	0.0238	0.0175	0.0109
Sulfoxide <sup>a</sup>	0.0022	0.001	0.0014	0.0036	0.0043	0.004	0.0008	0.0015
$\Delta H_f$ , (J/g)	7.7	7.8	8.5	9.2	5.8	8.6	11.3	9.6
% cryst. <sup>b</sup>	3.9	3.9	4.3	4.6	2.9	4.3	5.7	4.8
Cracking Temp Tc, (°C)	-12	-9	-3	-5	-20	-10	0	-3

<sup>a</sup> in mmol/g asphalt.

<sup>b</sup>Average entropy for 100% crystallinity = 200 J/g [14]

solution was then maintained at 110°C under a constant flow of chlorine gas, and the reaction was initiated with 2,2-azobis(2-methylpropionitrile) (AIBN), 0.02 g/l g of HDPE. After the desired reaction time, the reaction mixture was quenched in a large volume of methanol. The product was separated by filtration, washed several times with methanol, and vacuum dried at 55°C for a week. The properties of the CPEs prepared for this study are as follows: CPEA, 2.7 weight percent Cl, mp 125°C,  $\Delta H_f$ , 301 J/g; CPEB, 8.9 weight percent Cl, mp 114°C,  $\Delta H_f$ , 206 J/g; CPEC, 15.2 weight percent Cl, mp 106°C,  $\Delta H_f$ , 99 J/g; and CPED, 2.7 weight percent Cl, amorphous. The microstructure and morphology of chlorinated PEs have been reported (17,18), and the factors controlling these parameters are documented. Asphalt polymer blends (APBs) were prepared by melting the desired quantity of polymer (PE or CPE) in asphalt at 150°C while stirring at a rate of 200–500 rpm for 2 hr under N<sub>2</sub> atmosphere. All APBs contain 5 percent by weight of polymer unless otherwise mentioned.

#### Preparation of Maleated PE

The maleation was conducted using conditions described by Gaylord (19). Low-density polyethylene (LDPE), 20 g, MI = 0.22, was dissolved in 150 ml dichlorobenzene (DCB) at 130°C, and a mixture of 4 g of maleic anhydride (MAH) and 0.68 g triethyl phosphate (TEPA) was added. After raising the reaction temperature to 150°C, the maleation was initiated by adding 1 ml dicumyl peroxide (DCP) solution (0.5 g DCP in 15 ml DCB); further 1 ml aliquots of DCP solution were injected every 15 min. The MAH content was controlled by reaction time. The polymer used in this study was allowed to react for 1 hr; the resultant maleic anhydride content was 2.8 weight percent. At the end of the reaction, the solution was allowed to cool to room temperature and poured into 750–1000 ml methanol; the precipitate was washed several times with methanol and dried in vacuo at room temperature for more than 72 hr.

The maleated polymers were mixed with asphalts at 180°C under N<sub>2</sub> for 4 hr. The polymer contents are 5 weight percent unless otherwise mentioned.

#### DMA Bending Mode Measurements

In a typical DMA experiment, an asphalt sample was heated to 150°C in a sand bath. The asphalt sample was then poured into a brass mold and kept at room temperature for at least an hour. The sample size was 50 mm long, 10 mm wide and 1.68 mm thick. The sample was run in bending mode at cooling rate of 1°C/min using 0.1 percent strain at the desired frequency. The T<sub>g</sub> was identified as the temperature corresponding to the maxima of loss modular E'' at each frequency. Imposition of a larger strain (1 percent) on the asphalt samples at 50 Hz in DMA experiments will induce cracking at a specific temperature during the cooling. The temperature, called cracking temperature (T<sub>c</sub>), can be used to estimate the low-temperature cracking resistance of asphalt or asphalt/polymer blends.

#### DMA Shearing Mode Measurements

The shearing mode measurements were conducted at temperatures well above the glass transition temperature of asphalts and polymers employed. The samples were "sandwiched" between two parallel plates with a size of 10 × 10 mm. Sample thickness was held to about 1.5 mm, measured with a deviation of ±0.05 mm. Master curves were used with reference frequency of 20 Hz.

### DISCUSSION OF RESULTS

#### Compatibility Analysis by Differential Scanning Calorimetry

The thermal behavior of asphalts is complex, and depends on their sources, methods by which they are manufactured, and thermal history. In a typical asphalt there are three transition temperatures (Tr) at -42°C (Tr1), -10°C (Tr2) and 43°C (Tr3), and one melting peak at 28°C. A thermogram of a chlorinated PE containing 15.2 percent chlorine (CPEC) exhibits two transition temperatures at -15°C and 80°C, Figure 1, curve E. Because of the high-scale expansion required to illustrate the low temperature transition, the melting peak at 106°C is completely off scale.

The DSC curves of AC10-CPEC blends of various concentrations are compiled in Figure 1. In Curve C, obtained with a blend of CPEC with AC10 (20/80, w/w), the following changes are observed: a new Tr is observed at -13°C instead of Tr2s at -10°C and -15°C for AC10 and CPEC respectively, the melting peak for AC10 and Tr at 80°C of CPEC disappear, leaving an intermediate Tr of 42°C, and the melting peak for CPEC is lowered to 95°C. The melting peak of AC10 cannot be seen in all blends, but the Tr3 transition becomes stronger when polymer concentration is increased. The melting peak of CPEC was shifted downward a maximum of 12° at a CPEC concentration of 10 weight percent. Figure 2 is a compilation of thermograms of AC10-HDPE blends at various concentrations. Note that Tr1 broadens as the concentration of HDPE is increased, Tr2 disappears at 30 percent HDPE, and the melting peak of AC10 disappears in all blends.

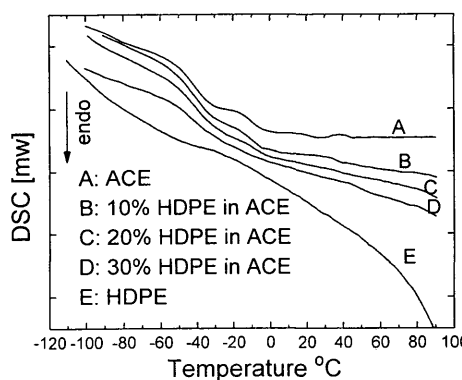
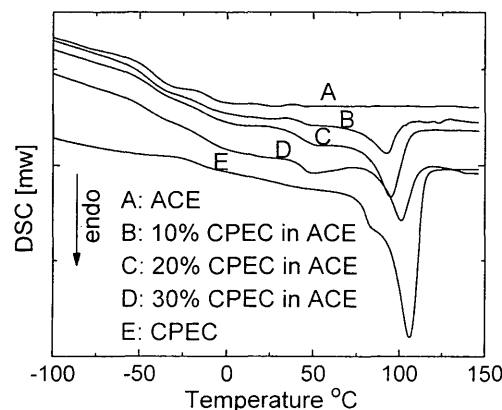


FIGURE 1 DSC thermogram of AC10/CPEC blends at various weight ratios.



**FIGURE 2** Partial DSC thermogram of AC10/HDPE blends at various weight ratios.

The multiple transitions observed in DSC thermogram of AC10 (Figure 1) shows that AC10, like most asphalts, is a heterogeneous rather than a homogeneous system. It has been found that saturates and aromatics make the main contributions to thermal effects observed in DSC thermogram of asphalts (16). After the maltenes were removed from AC10 by solvent extraction, all three of transition temperatures decreased, and no crystalline fraction was detected. The transitions of AC10 become broad or weak as the concentration of HDPE increases, and no asphalt melting point is observed. Clearly, HDPE interacts with the saturates fraction and extracts them from the asphalt. In contrast, the transitions of AC10 become stronger when concentration of CPEC increases; blends of CPEA and CPEB exhibit intermediate properties. Apparently, introduction of chlorine atoms onto the polymer chain adjusts the interaction parameters to reduce single component extraction.

All melting peaks from polymers move toward low temperatures as polymer concentration decreases. The magnitude of the melting point depression indicates the extent of the interactions between the polymers and AC10. There are sufficient quantities of saturates in AC-10 to plasticize low concentrations of polymer; however, as the concentration of polymer is increased beyond 10 percent, the saturates are completely extracted and the relative concentration of the plasticizer decreases. Thus, the reduction in the melting point depression as the polymer concentration increases confirms the complete extraction of asphalt components into the polymer phase. These results suggest that high concentrations of any polymer additive will disrupt the compatibility of the asphalt mixture.

#### Fluorescence Reflection Microscopy

The macrostructure of the asphalt-polymer mixtures was examined using fluorescence reflection microscopy (FRM). Our observations (Figure 3) confirm previous reports (2,20) that there are basically two phases existent in asphalt-polymer blends, a continuous asphalt-rich phase and a polymer-rich phase. The dispersed polymer-rich phases are expected to improve the toughness of brittle asphalt at low temperature and reinforce asphalt at high temperatures (21,22). The CPE-rich phase is larger than the HDPE-rich phase in asphalt

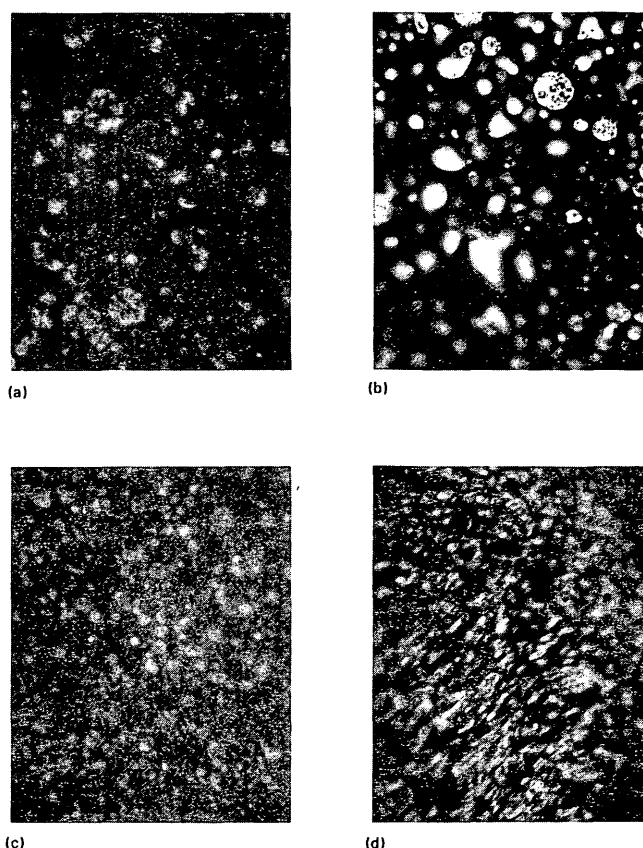


**FIGURE 3** Fluorescence reflection microscopy images: (a) 5 percent HDPE in AC-10, (b) 5 percent CPEC in AC-10, (c) 10 percent HDPE in AC-10, and (d) 10 percent CPEC in AC-10.

blends prepared under comparable conditions, indicating that a higher percentage of the asphalt components have been absorbed in the polymer phase. Samples containing 10 weight percent CPEC exhibit bicontinuous phase morphology; the phase transformation is accompanied by a marked increase in viscosity. Blends with 10 weight percent HDPE retain the polymer droplets in an asphalt-continuous phase.

The enhanced compatibility of CPE in asphalt can be attributed to a change in the polymer polarity as well as to changes in morphology stemming from the reduced crystallinity. In crystalline polymers like HDPE, interaction with solvents and reagents is limited to the readily accessible amorphous regions. Selective extraction of the saturates from the asphalt matrix by HDPE would be expected; this process would disrupt the balance of components in asphalt mixtures and promote phase separation. Although chlorination of HDPE was conducted in solution, analysis of the chlorine distribution in the chains indicates that chlorination is not perfectly random. Runs of unreacted methylene groups that can crystallize remain. Chlorinated methylene groups do not enter the crystallites, so the amorphous region contains a higher chlorine content than that measured in bulk samples. Thus the amorphous regions are substantially more polar, and the presence of chlorine atoms on the polyolefin chain will improve the compatibility of the polymer with aromatic components and functional groups containing heteroatoms, such as, N, S, O, in asphalt. The polar components of asphalt would have a

greater affinity for the amorphous regions of CPE and a corresponding increase in the compatibility of these polymers with asphalt would be expected. Introduction of chlorine adjusts the interaction parameters to reduce single component extraction; thus the delicate equilibrium among the asphalt components is maintained.

### Low-Temperature Cracking

The low-temperature cracking test is quite sensitive to polymer-asphalt interactions. Because asphalt is a rather low molecular weight material compared with the polymer additives, it becomes quite brittle at temperatures below its glass transition. The amorphous regions of the polymer additives remain flexible at low temperatures, whereas the crystalline phases provide tie points to limit chain reptation. Thus these polymers should be effective impact modifiers. However, the extent of polymer contribution to blend properties depends on the degree of compatibility with the asphalt matrix.

As can be seen in Table 2, the blends do indeed exhibit  $T_{cs}$  below the  $T_g$  of pure asphalt measured at the same frequency. We have shown that the  $T_c$  of pure asphalt falls above the corresponding  $T_g$  (Table 1), so the polymer component has improved the low temperature properties of the blends. Furthermore, CPE-modified asphalts have lower  $T_{cs}$  than HDPE-modified asphalts, as might be expected from a more amorphous polymer with a higher degree of interaction with asphalt.

### Dynamic Rheology

Rheological measurements under oscillating conditions yield the dynamic mechanical properties of polymers (i.e., the storage modulus,  $G'$ , the loss modulus,  $G''$ , and a mechanical damping or internal friction,  $\tan \delta$ ). In studies of the response of a material to vibrational forces, stress, strain, frequency, and temperature are the key variables. When a material is subjected to cyclical stress under conditions analogous to those encountered in the intended applications, the data reflect both short- and long-term responses to the stress conditions. If time-temperature superposition can be applied, dynamic data

obtained at short-time intervals at high temperature can be transformed to yield long loading time data relevant to thermal cracking (23).

On a molecular basis, the magnitude of  $G'$  depends on the nature of the conformation rearrangements that can take place within the period of the deformation (24). Examination of plots of  $\log G'$  versus either temperature or frequency (Figure 4) reveals that the slope of the curve for ACE-HDPE is close to that for ACE. In other words, adding HDPE to ACE simply induces a parallel shift of the  $\log G'$  curves toward high temperature or low frequency. The presence of HDPE particles results in the development of partially separated regions in the asphalt matrix, which are characterized by a higher rigidity than in the bulk asphalt. A contributing factor to both the parallel shift and the slight difference between slopes of the two curves is the selective adsorption of asphalt components by HDPE. Adsorption of the saturates by HDPE enriches the asphalt phase with aromatics resins and asphaltenes and creates a more rigid continuous phase. The dynamic mechanical response of ACE-HDPE is mainly from the continuous asphalt phase that is indirectly affected by the presence of HDPE.

Compared with that of ACE-HDPE, slopes of  $\log G'$  curves of ACE-CPE blends decrease and become more linear (Figure 5). Asphalt is much more temperature sensitive or frequency sensitive than the polymer additives employed. The decrease in temperature sensitivity exhibited by the blends may imply that the polymer rich phase is increasingly directly involved in responding to the dynamic mechanical load. The effect is particularly pronounced in the higher temperature regimes. Introduction of chlorine atoms enhances compatibility among the polymer additives and asphalt; thus the volume of the polymer-rich phase will be increased because of the improved "solubility" in the asphalt.

### Creep Testing

A constant stress creep test was run at 5, 15, 25, and 35°C, respectively, with a Bohlin CS rheometer using a cone and plate mode; the stress applied was 590 Pa. The tests (Figures 6,7) illustrate a pronounced difference among HDPE and CPE blends. Two different asphalt samples, AC-10 and AC-

TABLE 2 Glass transition temperature ( $T_g$ ) from  $E''$  and cracking temperature ( $T_c$ ) of concerned asphalts, polymers, and asphalt-polymer blends

Sample	Tg, (°C)			$T_c$ , (°C)
	1 Hz	10 Hz	50 Hz	
ACE	-32.2	-26.6	-22.5	-20
ACD	-14.9	-9.9	-4.1	-5
CPEB	-12.7	-7.9	-5.7	- <sup>a</sup>
CPEC	-15.2	-12.4	-9.4	- <sup>a</sup>
ACE-HDPE	-30.3	-25.0	-20.5	-23
ACE-CPEB	-31.9	-26.3	-21.6	-28
ACE-CPEC	-31.8	-25.7	-21.4	-31
ACD-HDPE	-14.3	-8.5	-3.7	-7
ACD-CPEB	-16.9	-10.8	-6.0	-8
ACD-CPEC	-16.6	-10.4	-6.7	-10

<sup>a</sup> the test was not conducted.

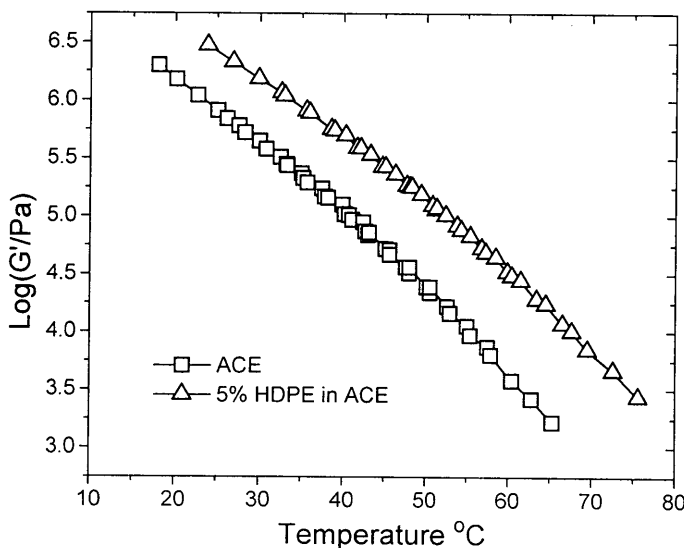


FIGURE 4 Plot of  $\log G'$  versus temperature for Curve A, AC-10 (ACE), and Curve B, 5 percent HDPE in ACE.

20, were blended with HDPE, semicrystalline CPEB (8.9 weight percent Cl) and amorphous CPEC (15.2 weight percent Cl). With the exception of the AC-10 blend at 15°C, the presence of HDPE did not change the creep behavior significantly. The compliance curves observed for the HDPE blends parallel those obtained with pure asphalt. However a significant difference in the compliance of CPE blends was observed; further it is possible to distinguish among the degrees of chlorination in the two CPE samples.

#### Creep Recovery

The resiliency of the asphalt blends was evaluated with the constant stress rheometer by imposing a stress for a given

period of time, then releasing the stress and allowing the sample to relax to an equilibrium deformation. This test is intended to be analogous to the Resiliency Test (ASTM D3883), but it can be run on relatively small samples without requiring special sample preparation. The samples were examined under two conditions: long-term (1,000-sec strain imposition) and short-term (10-sec strain imposition). The results are summarized in Table 3. The creep gives an indication of the resistance of the binder to deformation and the recovery percentage gives an indication of the elastic resilience of the binder. The short-term tests probe the sample response under conditions of elastic strain; higher recovery values indicate a more durable binder. The long-term tests examine the resistance of the samples to creep and the interaction of the polymer matrix

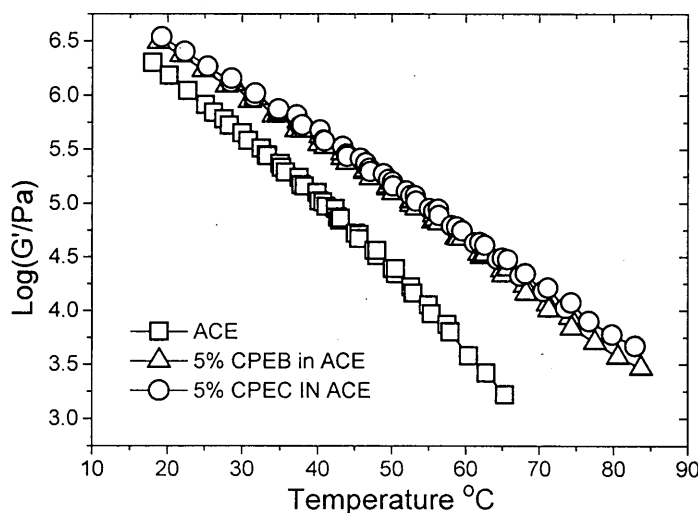
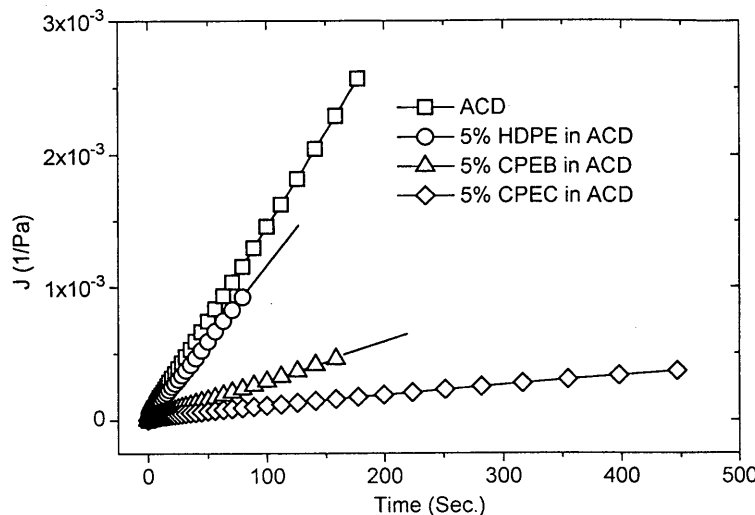


FIGURE 5 Plot of  $\log G'$  versus temperature for Curve A, ACE-10 (ACE); Curve B, 5 percent CPEB in ACE; and Curve C, 5 percent CPEC in ACE.



**FIGURE 6** Constant stress creep curves at 35°C. Curve A, AC-20 (ACD); Curve B, 5 percent HDPE in ACD; Curve C, 5 percent CPEB in ACD; and Curve D, 5 percent CPEC in ACD.

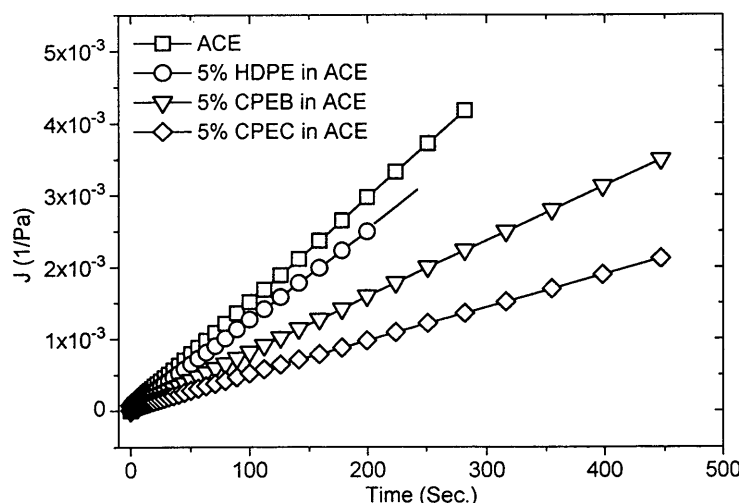
with the asphalt; pure asphalt samples do not exhibit any recovery under these conditions.

Typical plots for long-term recovery of polymer asphalt blends are shown in Figure 8. Note that high-density PE exhibits very low resistance to creep and very little recovery; thus the interaction between HDPE and the asphalt matrix is limited. Modification of the PE by either chlorination or maleation reduces the extent of creep significantly and a notable recovery is observed.

Typical results of short-term tests are shown in Figure 9. The elastic recovery of modified PE blends is quantitative; pure PE blends develop a permanent set.

## CONCLUSIONS

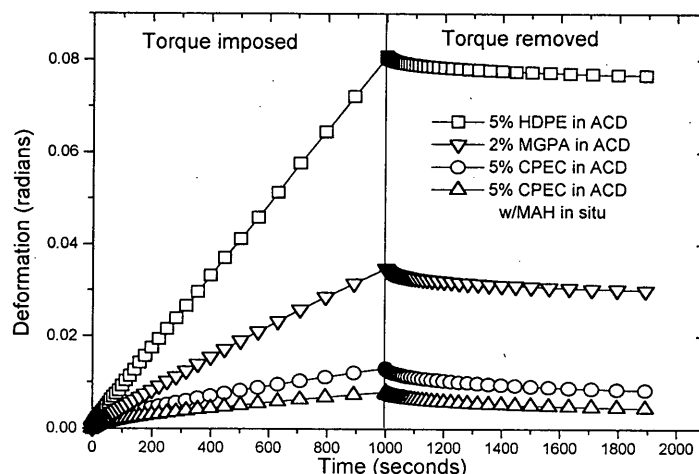
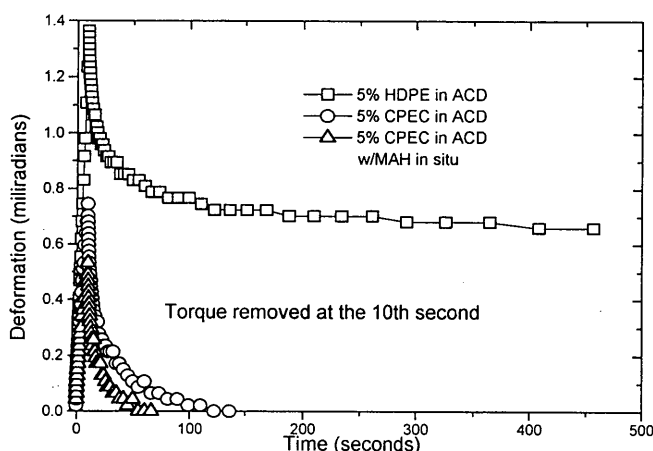
1. Low-level chlorination of PE can be controlled to produce semicrystalline polymeric additives. Chlorinated PEs containing less than 15 weight percent chlorine interact more extensively with an asphalt matrix than with PE. The interaction is substantiated by changes in the DSC, creep resistance, and blend rheology.
2. Maleation of PE must be controlled to low levels (< 4 percent) to maintain compatibility of the asphalt blends. However, the interaction of slightly modified samples is clearly improved.



**FIGURE 7** Constant stress creep curves at 35°C. Curve A, AC-10 (ACE); Curve B, 5 percent HDPE in ACE; Curve C, 5 percent CPEB in ACE, and Curve D, 5 percent CPEC in ACE.

**TABLE 3** Summary of creep-recovery tests on polymer-modified asphalts at 35°C

Sample	Creep @ 10 sec. (milliradians)	Recovery (%)	Creep @ 1000 sec. (milliradians)	Recovery (%) @ 1000 sec.
ACB	13	25 @ 500 sec.	119	0
ACD	21	13 @ 500 sec.	207	0
5% LDPE in ACB	6.9	71 @ 500 sec.	481.0	2
5% CPEC in ACB	2.7	100 @ 112 sec	45.9	48
5% MGPA in ACB	0.4	100 @ 28 sec.	5.4	44
5% HDPE in ACD	1.4	51 @ 500 sec.	80.7	5
5% CPEC in ACD	0.7	100 @ 112 sec.	13.7	34
5% CPEC in ACD w/MAH in situ	0.53	100 @ 45 sec.	7.9	43
5% LDPE in ACD	0.92	74 @ 500 sec.	47.3	8
2% MGPA in ACD	0.90	83 @ 500 sec.	26.0	16

**FIGURE 8** Long-term creep recovery at 35°C for polymer-asphalt blends.**FIGURE 9** Short-term creep recovery of polymer-asphalt blends at 35°C.

3. DSC can be used to ascertain the asphalt crystallinity and the distribution of asphalt components among phases in asphalt-polymer blends.

4. The low-temperature cracking properties of asphalts closely parallel the  $T_g$ s measured at 50 Hz (Table 2). Both the  $T_g$  and low-temperature cracking temperatures increase when the crystalline asphalt component increases.

5. Asphalt-PE blends are more rigid than asphalt but the temperature sensitivities are parallel (Figure 5). Asphalt-CPE blends are less temperature sensitive and the temperature sensitivity varies inversely with the CPE chlorine content (Figure 6). The decrease in temperature sensitivity observed implies that the polymer-rich phase is responding more directly in CPE blends.

6. Constant stress creep tests and creep recovery tests are very sensitive methods for detecting asphalt-polymer interaction.

## ACKNOWLEDGMENTS

This work is supported by a contract from the Louisiana Transportation Research Center. Special appreciation is extended to Harold Paul, who served as the contract technical representative and provided helpful and incisive comments and suggestions. We wish to thank Seiko Instruments, USA, for their generous support to enable us to purchase Seiko Thermoanalysis Stations and LEQSF for the funds to purchase a Bohlin Rheometer.

## REFERENCES

1. *The Asphalt Handbook*. Manual Series No. 4 (MS-4), Asphalt Institute, College Park, Md., 1989.
2. B. Brule, Y. Brion, and A. Tanguy. Paving Asphalt Polymer Blends: Relationships Between Composition, Structure and Properties. *Asphalt Paving Technology*, Vol. 57, 1988, pp. 41-64.
3. G. N. King, H. W. Muncy, and J. B. Prudhomme. Polymer Modification: Binder's Effect on Mix Properties. *Asphalt Paving Technology*, Vol. 55, 1986, pp. 519-540.
4. J. H. Collins and W. J. Mikols. Block Copolymer Modification of Asphalt Intended for Surface Dressing. *Asphalt Paving Technology*, Vol. 54, 1985, pp. 1-17.
5. L. D. Coyne. Evaluation of Polymer Modified Chip Seal Coats. *Asphalt Paving Technology*, Vol. 57, 1988, pp. 545-575.
6. P. Jew and R. T. Woodhams. Polyethylene-Modified Bitumen for Paving Applications. *Asphalt Paving Technology*, Vol. 55, 1986, pp. 541-563.
7. S. A. Hesp and R. T. Woodhams. *Polyolefin-Asphalt Emulsions*. ASTM STP 1108 (K. R. Wardlaw and S. Schuler, eds.), Philadelphia, Pa., 1991.
8. A. C. Pitchford and H. J. Sarret. *Paving Asphalt Containing Chlorinated Polyethylene*. U.S. Patent No. 3,312,649, April 1967, 5pp.
9. S. G. Fogg and P. H. Westerman. *Bituminous Compositions Containing a Chlorinated Polymer*. British Patent No. 1,475,924, June 1977, 5pp.
10. L. Petrakis, D. T. Allen, G. R. Gavalas, and B. C. Gates. Analysis of Synthetic Fuels for Functional Group Determination. *Analytical Chemistry*, Vol. 55, Aug. 1983, pp. 1557-1564.
11. I. Gawel. Structure Investigation of Asphalts Produced from Paraffin-Base Crude Oil by Different Method. *Fuel*, Vol. 66, No. 5, May 1987, pp. 618-621.
12. A. P. Hagen, M. P. Johnson, and B. B. Tandolf. <sup>13</sup>C NMR Studies of Roadway Asphalts. *Fuel Science and Technology International*, Vol. 7, No. 9, Dec. 1989, pp. 1289-1326.
13. D. J. Cookson and B. Smith. Optimal Conditions for Obtaining Quantitative <sup>13</sup>C NMR Data. *Journal of Magnetic Resonance*, Vol. 57, No. 3, May 1984, pp. 355-368.
14. J. C. Petersen, Quantitative Functional Group Analysis of Asphalts Using Differential Infrared Spectrometry and Selective Chemical Reactions—Theory and Application. In *Transportation Research Record 1096*, TRB, National Research Council, Washington, D.C., 1986, pp. 111.
15. F. Noel and L. W. Corbett. A Study of the Crystalline Phases on Asphalt. *Journal of the Institute of Petroleum*, Vol. 56, No. 551, 1970, pp. 261-265.
16. B. Brule, J. P. Planche, G. P. King, P. Claudy, and J. M. Lettoff. *Relationships Between Characterization of Asphalt Cements by Differential Scanning Calorimetry and Their Physical Properties*. American Chemical Society, Division of Petroleum Chemistry, Vol. 35, No. 3, July 1990, pp. 330-337.
17. Z. Chai, L. Shi, and R. N. Sheppard. Microstructure of Solution-Chlorinated Polyethylene by <sup>13</sup>C Nuclear Magnetic Resonance. *Polymer*, Vol. 25, March 1984, pp. 369-374.
18. B. H. Chang, R. Zeigler, and A. Hiltner. Chlorinated High-Density Polyethylene, II. Solid State Structure. *Polymer Engineering Science*, Vol. 28, No. 18, 1988, pp. 116-781.
19. N. G. Gaylord. *Maleic Anhydride-Modified Polymers*. U.S. Patent No. 4,506,056, March 19, 1985.
20. C. Lenoble. *Performance/Microstructure Relationship of Blends of Asphalts with Two Incompatible Polymers*. American Chemical Society, Division of Petroleum Chemistry, Vol. 35, No. 3, July 1990, pp. 541-549.
21. C. B. Bucknall and W. W. Stevens. Rubber Toughening of Plastics. Parts 5. Fatigue Damage Mechanism in ABS and HiPs. *Journal of Materials Science*, Vol. 15, 1980, pp. 2950-2985.
22. C. B. Bucknall and C. J. Page. Rubber Toughening of Plastics. Parts 6. Effect of Rubber Particles on the Kinetics of Creep in Polypropylene. *Journal of Materials Science*, Vol. 17, 1982, pp. 808-816.
23. H. S. Pink, R. E. Merz, and D. S. Bosniack. Asphalt Rheology: Experimental Determination of Dynamic Moduli at Low Temperature. *Asphalt Paving Technology*, Vol. 49, 1980, pp. 64-94.
24. R. B. Bird, R. C. Armstrong and O. Hassager. *Dynamics of Polymeric Liquids*. Vol. 1, Fluid Mechanics, 2nd Ed., John Wiley & Sons, Inc., New York, 1987.